

# Molecular Remodelling during Atrial Fibrillation

© 2002 V.L.J.L. Thijssen

ISBN : 90-5278-358-6

Druk : Datawyse | Universitaire Pers Maastricht

# Molecular Remodelling during Atrial Fibrillation

## PROEFSCHRIFT

ter verkrijging van de graad van doctor aan de Universiteit Maastricht, op gezag van de Rector Magnificus,  
Prof.Dr. A.C. Nieuwenhuijzen Kruseman, volgens het besluit  
van het College van Dekanen, in het openbaar te verdedigen op vrijdag 1 november 2002 om 12.00 uur

door

**Victor L.J.L. Thijssen**  
geboren te Tegelen op 8 maart 1972.



Promotor

*Prof. Dr. M. Borgers*

Co-promotores

*Dr. J. Ausma*

*Dr. G.J.J.M. van Eys*

Beoordelingscommissie

*Prof. Dr. R. Reneman (Voorzitter)*

*Prof. Dr. H.J.G.M. Crijns*

*Prof. Dr. M.H. Hofker*

*Prof. Dr. F.C.S. Ramakers*

*Prof. Dr. B. Wieringa (Katholieke Universiteit Nijmegen)*

*Financial support by the Netherlands Heart Foundation for  
the publication of this thesis is gratefully acknowledged.*

*Additional financial support for the publication of this thesis  
was provided by **Vitatron Medical BV** (Arnhem, The  
Netherlands).*

*The great tragedy of Science - the slaying of a beautiful hypothesis by an ugly fact.*

Thomas Henry Huxley, 1825 - 1895

# Contents

Chapter 1   Introduction	9
Structural Changes of Atrial Myocardium during Chronic Atrial Fibrillation	
<i>Aim of this Thesis</i>	21
Chapter 2	23
Structural Remodelling of Atrial Myocardium in Patients with Cardiac Valve Disease and Atrial Fibrillation	
Chapter 3	35
Altered Expression of Troponin I Isoforms in Patients with Atrial Fibrillation	

Chapter 4 | 49

Analysis of troponin I isoform expression during chronic atrial fibrillation in the goat

Chapter 5 | 65

Analysis of altered gene expression during sustained atrial fibrillation in the goat

Chapter 6 | Discussion 83

Structural remodelling during chronic atrial fibrillation: act of programmed cell survival

<i>Summary</i>	101
<i>Samenvatting</i>	105
<i>Curriculum Vitae</i>	109
<i>List of Publications</i>	111
<i>Dankwoord</i>	115
<i>References</i>	117



# Chapter 1

## | *Introduction* |

adapted from

### STRUCTURAL CHANGES OF ATRIAL MYOCARDIUM DURING CHRONIC ATRIAL FIBRILLATION

V. Thijssen, J. Ausma, G-S. Liu, M. Allessie, G. van Eys, M. Borgers

Cardiovasc Pathol 2000; 9: 17-28

| 9

*Concepts without factual content are empty; sense data without concepts are blind. The understanding cannot see. The senses cannot think. By their union only can knowledge be produced.*

Immanuel Kant, 1724 - 1804

## 1 | Introduction

Atrial fibrillation (AF) is a cardiac arrhythmia that is electrocardiographically characterised by irregular and disorganised atrial activity with respect to both rate and rhythm<sup>1</sup>. At present, AF is one of the most frequently detected arrhythmia's in the clinical setting. In the western population, AF occurs with a prevalence of 0.9% and AF is strongly related to increasing age. In people over 40 years, prevalence already is 2.3%, rising up to 5.9% for those older than 65 years<sup>2</sup>. Apart from advanced age, risk factors for AF include diabetes, hypertension, congestive heart failure, rheumatic and non-rheumatic valve disease, myocardial infarction, and ischemic heart disease<sup>2-5</sup>. Furthermore, AF is not only an independent risk factor for stroke, but AF by itself is also associated with a 1.5- to 1.9-fold increase in mortality risk<sup>5-7</sup>.

The mechanism(s) by which AF is sustained have been a great puzzle for many decades and several theories were proposed<sup>8-11</sup>. Nowadays, Gordon K. Moe's 'multiple wavelet' hypothesis is generally accepted to describe the cause and maintenance of AF<sup>12,13</sup>. In the development of this hypothesis as well as in the understanding and knowledge of the various mechanisms and behaviour of different cardiac arrhythmia's, experimental models have played an important role<sup>14-16</sup>. The last 20 years, animal models on AF have been mainly used to study anti-arrhythmic therapeutic interventions<sup>17-20</sup>. The last decade research more and more shifted towards cellular aspects of AF, concentrating on possible mechanism(s) and underlying cellular changes<sup>21-24</sup>.

## 2 | Structural remodelling in patients with AF

In patients suffering from AF, atrial contractile function gets disturbed and the time and extent of recovery of function following cardioversion is related to the duration of AF<sup>25-27</sup>. It was observed that immediately after cardioversion, atrial contraction was usually weak, but its strength increased progressively during the initial weeks of regained sinus rhythm<sup>25,28</sup>. Whether the delayed recovery after longer periods of AF was caused by calcium overload or due to changes in atrial function and/or structure remained unknown. In 1983, Mary-Rabine *et al.* described the presence of cellular degeneration in the atrial cardiomyocytes of patients suffering

from atrial arrhythmia's. This degeneration consisted of focal accumulation of sarcoplasmic reticulum, mitochondrial aggregation, widening of the undifferentiated portions of the intercalated discs, and replacement of myofibrils by glycogen granules<sup>29</sup>. Similar observations were made in patients with lone atrial fibrillation by Frustaci *et al.*<sup>30</sup>, in patients with combined valvular disease and atrial fibrillation by Thiedemann *et al.*<sup>31</sup>, and in our group<sup>88</sup>. In the latter group of patients, a clear differentiation could be made between adaptive and maladaptive remodelling of atrial structure (Fig. 1)<sup>88</sup>. From these human studies it was not clear whether there was a causal relationship between observed changes and arrhythmia. In order to elucidate this issue, animal models in which time related events of AF could be studied had to be developed.

### 3 | Structural remodelling in animal models on AF

In 1997, two papers were published, which addressed the structural changes in atrial myocardium of goats after prolonged periods of sustained AF<sup>32,33</sup>. In atrial myocytes from such animals, the following structural changes were observed using light- and electron microscopy (Fig. 2): i) Cardiomyocytes gradually disposed of their contractile material, starting from the perinuclear region towards the periphery of the cell. Remnants of the sarcomeres, especially clumps of Z-band material, were frequently observed; ii) Glycogen had accumulated in sarcomere depleted areas; iii) A network of disorganised membranes, probably altered profiles of sarcoplasmic reticulum, were present in myolytic areas; iv) Mitochondria took on an elongated shape with longitudinal orientated cristae which appeared in cross sections as small, doughnut-like structures; v) Nuclear heterochromatin showed a homogenous distribution throughout the nucleoplasm<sup>32</sup>. In 1982 Boyden *et al.* described that in the enlarged atria of dogs suffering from mitral valve fibrosis, a condition often accompanied by arrhythmia's, a small number of altered cells, characterised by sarcomere disruption, myolysis and glycogen accumulation, the presence of collapsed tubules of sarcoplasmic reticulum, and aggregates of abnormally shaped mitochondria, were present<sup>34</sup>. These observations in dogs as well as those described by Mary-Rabine in humans, showed several similarities to the findings after prolonged sustained atrial fibrillation in goats (Table 1)<sup>32</sup>. However, the structural chan-

## Figure 1 |

Electron microscopy of adaptive and maladaptive ultrastructural changes in atrial myocardium of patients with cardiac valve disease and atrial fibrillation.

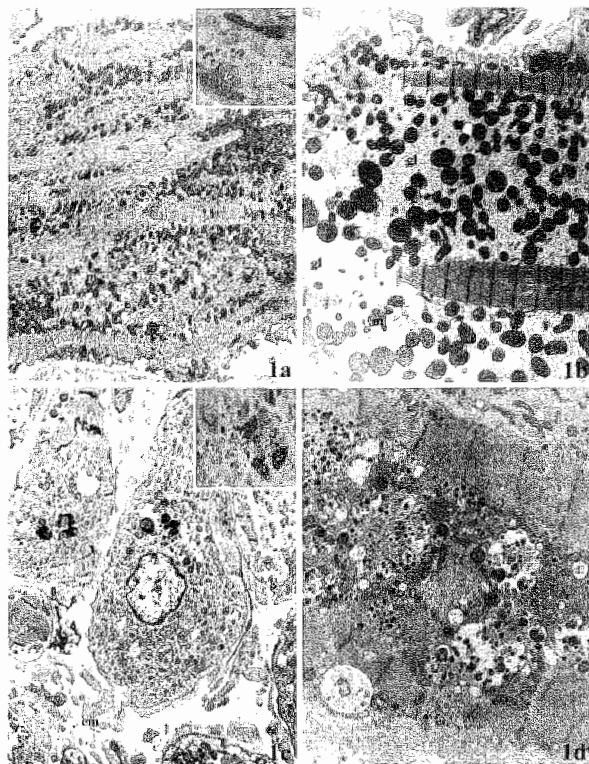
a) A hypertrophied atrial cardiomyocyte in which adaptive structural remodelling, i.e. myolysis, glycogen storage (gl) and numerous small and abnormally shaped mitochondria (m), are visible (Original magn.: x 1425). Inset: light microscopy of atrial myocardium from patient, stained with PAS/toluidine blue, in which large amount of glycogen is visible as darkly stained material (Original magn.: x 400).

b) Detail of an adaptive atrial cardiomyocyte showing extensive myolysis and storage of huge amounts of glycogen (gl) in which numerous small and abnormally shaped mitochondria (m) are visible (Original magn.: x 2940).

c) Maladaptive atrial cardiomyocyte showing typical degenerative features such as numerous secondary lysosome-like bodies, most probably of autophagic origin.

Also an increase in extracellular matrix (em) can be seen (Original magn.: x1760). Inset: light microscopy of atrial myocardium from patient with degenerated cells in which vacuoles (v) are visible within the cytosol. PAS-stained glycogen is visible as darkly stained material (Original magn.: x 250).

d) Detail of a maladaptive atrial cardiomyocyte showing cytosolic blebs filled with membrane-bound vesicles and amorphous bodies of unknown origin (Original magn.: x5280).



12 |

ges in the goat study were not interpreted as 'degenerative', because typical degenerative changes, such as cytoplasmic vacuolisation and oedema, mitochondrial swelling, loss of membrane structure and organisation, accumulation of secondary lysosomes, and lipid droplets appeared to be virtually absent<sup>32</sup>. Moreover, morphological changes specific for apoptosis, such as increased cytoplasmic density occurring with cell cytoplasm shrinking, the appearance of apoptotic bodies or condensation of nuclear chromatin were not present after chronic atrial fibrillation in the goat<sup>35</sup>. In addition, neither altered expression of Bcl-2, P53 or proliferating cell nuclear antigen nor an increase in TUNEL reactivity could be demonstrated<sup>35</sup>, suggesting that apoptosis does not play an important role in the observed remodelling of cardiomyocyte structure during AF. The lack of increase in extracellular space (fibrosis) suggested that prominent cell death, resulting either from apoptosis or necrosis, had not taken place. However, Mongeon *et al.* (unpublished) observed that after extensive periods of AF in dogs (up to 18 months), more severe changes do occur, including an increase of extracellular space, eluding to the fact that cell

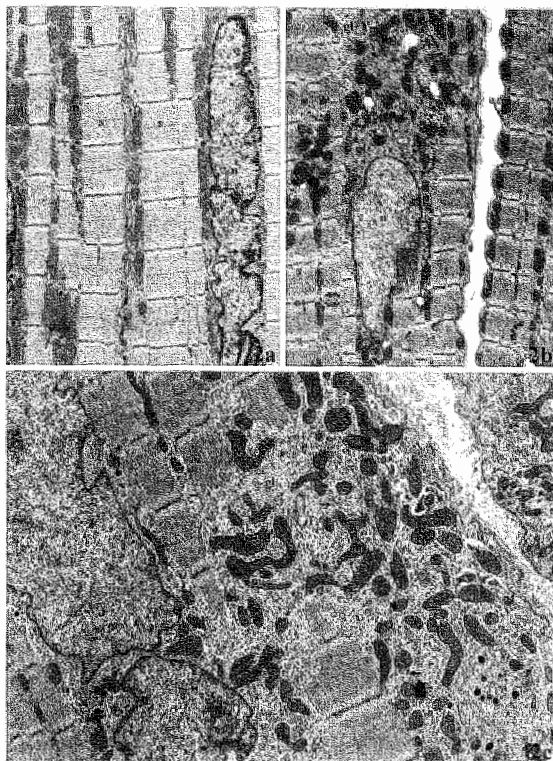


**Figure 2 |**

Electron microscopy of atrial myocardium from goats in sinus rhythm and after prolonged sustained atrial fibrillation.

a) Detail of an atrial myocyte from a goat in sinus rhythm. Sarcomeres (s) are regularly structured and surrounded by rows of mitochondria (m). In the nucleus (n), clustered heterochromatin (arrows) is visible at the nuclear membrane (Original magn.: x 3400).

b) Detail of an atrial myocyte from a goat after 4 weeks of sustained AF. Although normally structured sarcomeres (s) are still present, myolysis has occurred in the vicinity of the nucleus (n). In the myolytic area, glycogen (gl) is present together with odd shaped mitochondria (m). Instead of a clustered pattern, heterochromatin is evenly distributed throughout the nucleoplasm (Original magn.: x 2000).

c) Detail of an atrial myocyte from a goat after 16 weeks of sustained AF, showing a myolytic area with glycogen (gl) accumulation, numerous abnormally shaped mitochondria (m), and remnants of sarcoplasmic reticulum (arrows). Also, the nucleus (n) with dispersed chromatin is visible (Original magn.: x 4600).

death might have occurred (Fig. 3).

Ausma *et al.*<sup>32</sup> hypothesised that the perceived structural alterations represented an adaptive response of dedifferentiation rather than cardiomyocyte degeneration, because many of the features seen in the atrial myocytes during sustained AF were also present during myocyte development. To determine whether chronic atrial fibrillation incited atrial myocytes to adopt a dedifferentiated state, the expression and organisation of proteins that are characteristic of cardiomyocyte development were examined<sup>33</sup>. A number of observations were made supporting the hypothesis that chronic AF induced myocardial dedifferentiation (Fig. 4): i)  $\alpha$ -Smooth muscle actin, of which the expression in normal cardiomyocytes is gradually lost during cardiac development, was re-expressed during AF; ii) Titin epitopes gradually disappeared in a pattern reverse to the pattern seen during cardiac development, resulting in a molecular organisation similar to that in the fetal stage; iii) Cardiotin, a sarcoplasmic reticulum related protein, of which the expression has not been seen during fetal development, disappeared during chronic AF; iv) Desmin co-localisation with desmoplakin and

**Table 1 |**

Structural changes in atrial cardiomyocytes after AF

H=human, D=dog, G=goat,  
SR=sarcoplasmic reticulum  
a (Wouters et al.  
unpublished); b (29); c  
(32); d (Mongeon et al.,  
unpublished); e (34); f  
(31). Features that appear  
in italic are also present in  
fetal cardiomyocytes.

	adaptive	structural changes
		maladaptive
<i>diminished amounts of sarcomeres</i>	$(H^{a,b,f}, G^c, D^{d,e})$	increased extracellular matrix $(H^{a,f}, D^d)$
<i>accumulated glycogen</i>	$(H^{a,b,f}, G^c, D^{d,e})$	cytosolic blebbing $(H^a)$
<i>small, elongated mitochondria</i>	$(H^{a,f}, G^c, D^d)$	mitochondrial disruption $(H^{a,b,f}, D^d)$
<i>disorganised SR</i>	$(H^f, G^c, D^{d,e})$	focal accumulation of SR $(H^{b,f})$
<i>increased cell size (hypertrophy)</i>	$(H^f, G^c)$	increased cell size (hypertrophy) $(H^{b,f}, D^{d,e})$
<i>homogenous distribution of heterochromatin</i> ( $H^a, G^c, D^d$ )		secondary lysosomes $(H^{a,f})$

desmoglein, which play a role in the myofibril attachment to the junctional membrane, was lost. This detachment of desmin from the intercalated disc resembled its organisation in certain stages of cardiomyocyte development<sup>33</sup>. All the observed structural changes as well as the changes in expression and organisation of muscle cell specific proteins, were indicative of a fetal-like phenotype. However, the cardiomyocyte dedifferentiation was limited because markers of early myocardial development could not be detected (vimentin, cytokeratin 8 and 18) and in cardiac myocytes in which normal sarcomeres were present, the expression of sarcoplasmic proteins also appeared to be normal<sup>33</sup>.

To evaluate the time course of the process of dedifferentiation, the structural changes in cardiomyocytes were analysed after 1, 2, 4, 8, and 16 weeks of burst pacing induced AF in goats and compared to normal cardiomyocytes. The first change to be observed was a redistribution of chromatin in the nucleus. Progressive increase in myolysis and subsequent glycogen storage was seen till 8-16 weeks, simultaneously with depletion of sarcoplasmic reticulum and gradually increasing numbers of

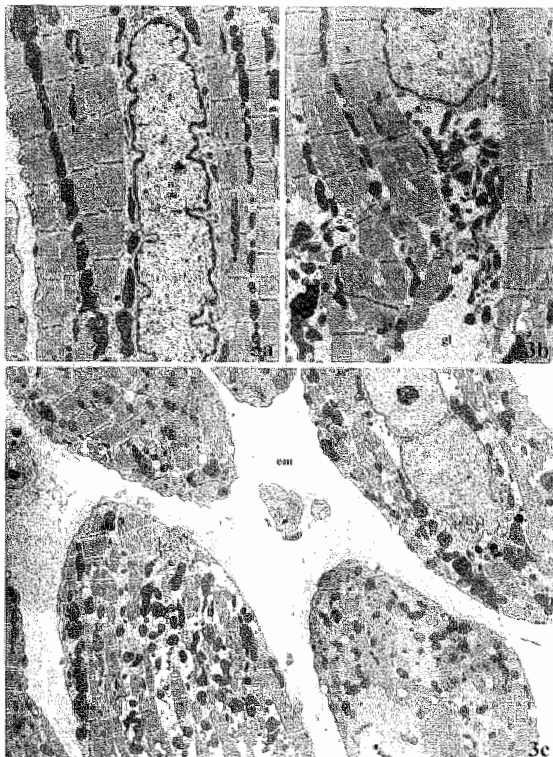


**Figure 3 |**

Electron microscopy of atrial myocardium from dogs in sinus rhythm and after prolonged sustained atrial fibrillation.

- a) Detail of an atrial myocyte from a dog in sinus rhythm, showing normally structured sarcomeres (s) bordered by rows of mitochondria (m) and heterochromatin clustering (arrows) at the membrane of the nucleus (n) (Original magn.: x3400).
- b) Detail of an atrial myocyte from a dog with sustained AF for 18 months. Sarcomeres (s) are depleted and replaced by glycogen (gl). Numerous oddly shaped mitochondria (m) are present and nuclear (n) chromatin is dispersed (Original magn.: x2720).
- c) Atrial myocardium from a dog with sustained AF for 18 months. Apart from typical changes, i.e. myolysis, glycogen accumulation and the presence of oddly shaped mitochondria, also a clear increase in extracellular matrix (em) is visible (Original magn.: x1320).

| 15

small mitochondria<sup>36</sup>. Immunohistochemical studies showed changes in the presence of structural proteins. Proteins normally present in differentiated cardiomyocytes, i.e. cardiotin, titin and desmin, gradually disappeared whereas  $\alpha$ -smooth muscle actin, a fetal protein, reappeared<sup>37</sup>.

#### 4 | Mechanisms of structural remodelling

The cause and mechanisms underlying the structural changes during AF are not well understood, and several factors may be involved in the onset of dedifferentiation of cardiomyocytes.

##### 4.1 | Ischemia

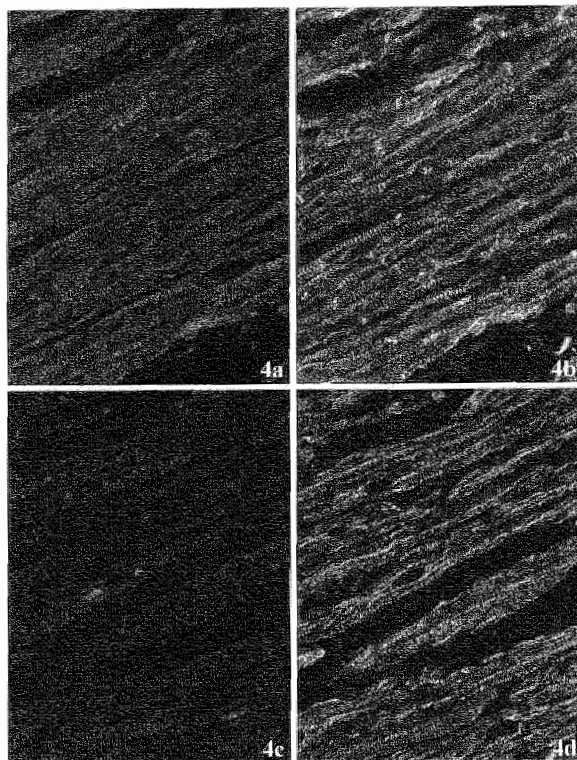
In 1982, White *et al.* showed that induction of AF resulted in a more than twofold increase of blood flow and oxygen consumption in the atrial tissue<sup>38</sup>. As a result, the flow reserve during AF will be markedly reduced and a further increase in metabolic demand might lead to atrial ischemia. Opposite to this, Jayachandran *et al.* reported a reduced atrial blood flow in

## Figure 4 |

Immunohistochemistry on atrial myocardium from goats in sinus rhythm and after 16 weeks of sustained atrial fibrillation

a,c) In cardiomyocytes from a goat in sinus rhythm a clear titin double-band cross striation is visible (a; original magn.: x 400). After 16 weeks of sustained atrial fibrillation, the cross-striations are interrupted and a only a dotted pattern remains visible at the periphery of the cardiomyocyte (c; original magn.: x 400).

b,d) In cardiomyocytes from a goat in sinus rhythm a single-banded cross-striation pattern together with intercalated disc staining can be seen for desmin (b; original magn.: x 400). Sixteen weeks of sustained atrial fibrillation results in a less apparent staining of the cross-striations as well as the intercalated disc (d; original magn.: x 200).



16 |

dogs with rapid pacing induced AF, but again the result would be atrial ischemia<sup>39</sup>. In chronic hibernating myocardium, a condition occurring in patients as a result of low-flow ischemia, the ventricular cardiomyocytes display structural changes that are similar to the changes seen in chronic AF<sup>40,41</sup>. These changes have been suggested to be an adaptive response of the cardiomyocytes to a lowered oxygen supply, to resist the ischemic environment present in chronic hibernating myocardium<sup>42</sup>. In contradiction to the previous studies, it has been suggested that in the goat model of AF ischemia was absent because neither changes in cytochrome c oxidase, NADH oxidase and proton-translocating ATPase activities, nor changes in adenine nucleotides and their degradation products have been found<sup>43</sup>. A decrease in creatine phosphate which has been observed in goats and pigs after AF was probably the result of increased metabolism rather than an effect of ischemia<sup>43,44</sup>. Whether ischemia actually occurs during AF, giving rise to cardiomyocyte remodelling, is unknown.

## 4.2 | Stretch

Early after the induction of atrial fibrillation a diminished contractility occurs<sup>44</sup>, and a decrease or absence of regular contractile activity results in increased passive stretch, due to volume overload. Stretch has been shown to influence atrial protein expression<sup>45-48</sup>. Furthermore, passive stretch might explain the observed increase in cell size of the cardiomyocytes<sup>49-51</sup>. Mary-Rabine *et al.* and Ausma *et al.* found a clear correlation between the degree of myolysis and cell size, with an almost 2 fold increase in size of severely affected cells<sup>29,32</sup>. This increase in cell size of the cardiomyocytes after AF might therefore reflect stretch induced hypertrophy.

Apart from these direct effects on atrial myocytes, atrial stretch has also been shown to facilitate the development of sustained AF by heterogeneously prolonging the atrial effective refractory period within the atrial tissue<sup>52,53</sup>. Therefore, atrial stretch might not only be a result of atrial fibrillation but it may also be held responsible for the maintenance of both electrical and structural atrial remodelling.

## 4.3 | Calcium homeostasis

| 17

There are several major differences between calcium handling in the fetal and adult heart, as reviewed by Nijjar *et al.* and Vornanen<sup>54,55</sup>, and it is beyond the scope of this introduction to describe them in detail. However, one of the possibly important changes in calcium homeostasis which occurs at the onset of AF is calcium overload<sup>44,56-58</sup>. In goats with AF there was clear evidence of calcium overload, but it appeared that after two weeks of AF, cardiomyocytes were able to adapt to the new calcium homeostasis and after 16 weeks of AF, no more signs of calcium overload could be found<sup>59</sup>. This adaptation of the calcium homeostasis coincided with the structural remodelling of cardiomyocytes during AF, and it was proposed that cardiomyocyte dedifferentiation served as a protective mechanism against calcium overload<sup>59</sup>.

In dogs, a reduction in the transient L-type calcium current ( $I_{CaL}$ ) has been described after rapid atrial pacing for 1 or 6 weeks<sup>24</sup>. In these dogs, the amplitude of calcium release was reduced and the kinetics of calcium release and re-uptake was slowed down, indicating an impaired calcium homeostasis and

depressed contractility<sup>60</sup>. Although short term inhibition of L-type calcium channels might be the result of high intracellular calcium concentration, i.e. calcium overload<sup>61</sup>, it was suggested that regulation of expression of L-type calcium channels might be involved in the long term changes of  $I_{Cal}$  as observed in dogs<sup>60</sup>. Studies in rat and rabbit cardiomyocytes have demonstrated that there is an increase in peak  $I_{Cal}$  density during development and after birth<sup>62,63</sup>. Therefore, the observed decrease of  $I_{Cal}$  during AF might reflect a return to a less differentiated state.

## 5 | Future perspectives

### 5.1 | Reversibility

As already mentioned, it has been observed that patients suffering from AF show a delay in recovery after cardioversion<sup>25-28</sup>. A delay in the restoration of contraction after treatment of cardiomyocytes *in vitro* with verapamil, was also reported by Sharp *et al.*<sup>64</sup>. Ausma *et al.* hypothesised that the delayed contractile recovery might be due to the time needed by atrial cardiomyocytes to undo the structural changes that occur during extended periods of AF<sup>32</sup>. Furthermore, the time course of structural changes indicated that longer episodes of AF resulted in increased severity of structural alterations<sup>36</sup>. Whether the cardiomyocytes were able to return to their normal phenotype after induction of normal sinus rhythm or if there was a point of no return, remained unknown. Studies on the possible reversibility of structural remodelling after AF might answer these questions and provide leads to improve efficacy of clinical interventions.

### 5.2 | Molecular mechanisms

The molecular mechanisms leading to the adaptive phenotype of cardiomyocytes during AF are largely unknown. In fact, little is known about the molecular response of cardiomyocytes to AF. Van Wagoner *et al.* found that in patients with chronic AF, the outward potassium current densities were reduced together with a 50-60% decrease of Kv1.5  $\alpha$  subunit expression<sup>65</sup>. They implied calcium overload as a possible trigger responsible for this observation.

Calcium overload was also suggested to cause a reduced sodium

current density in atrial myocytes of dogs after 7 days of rapid atrial pacing, possibly by downregulation of sodium channel expression level<sup>66</sup>. Previously, increased calcium concentration had been shown to downregulate sodium channel expression in rats<sup>67</sup>. Although the changes in potassium and sodium current densities were associated with a shortening of atrial effective refractory period, thereby serving as possible substrates for sustaining AF, their involvement in the observed dedifferentiation of cardiomyocytes is unknown.

To investigate the molecular mechanisms that are involved in cardiomyocyte adaptation to chronic AF, expression screening techniques like differential display as described by Liang and Pardee<sup>68</sup> can be applied. This technique has already been used to identify or confirm altered expression of genes that are involved in several cardiac diseases<sup>69-74</sup>. Studies in which differential display has been used on cardiomyocytes after AF have not been presented so far, probably because differential display is a rather new technique and animal models on AF only recently became available. Comparing expression patterns in the atria of goats at different time intervals of AF might identify not only unknown genes that are upregulated or downregulated but also genes which are transiently expressed during AF. These genes might be important in expression regulation and control of structural remodelling, and they might provide information about the underlying pathways. A better understanding of the causes and triggers for structural remodelling could offer leads for better treatment of patients suffering from chronic AF by slowing down, blocking or even reversing the structural remodelling, thereby improving atrial conduction and contractile function.

## 6 | Concluding remarks

Atrial fibrillation has fascinated numerous investigators from various scientific fields ever since it was described. Almost the entire twentieth century efforts to elucidate the mechanisms of this intriguing arrhythmia have been made by anatomists, morphologists, electrophysiologists, and since the last decade also by molecular biologists. All have provided information on the changes during AF, but essential questions remain to be answered. What triggers the atrium to end normal sinus rhythm and start fibrillating? Does structural remodelling precede,

coincide or follow electrical remodelling? To what extent are the consequences of AF, i.e. electrical and structural remodelling, reversible? Is structural remodelling really a protective adaptation or merely a delayed degeneration? Which molecular mechanisms are involved in AF? Is susceptibility to AF genetically imprinted? All these aspects, and more have to be studied to fully comprehend how atrial rhythm gets disturbed and how this irregularity persists and eventually results in atrial dysfunction or even death.

Experimental models are essential tools for investigating AF and it is important that such models mimic the *in vivo* situation in humans as much as possible. However, most models available at present represent ‘lone’ fibrillation, i.e. fibrillation in the absence of other cardiac complaints, whereas in general, AF patients suffer from an underlying heart disease. Hence, in models of lone AF, the influence of a heart disease on AF and their relationship remains unknown. Furthermore, in humans, AF often occurs at a later age and lasts for many years, a situation which is difficult to simulate in animal models. Thus, age related and long term effects of AF can not be easily studied using animal models. Despite these limitations, experimental models have proven to contribute considerably in the study of AF and refinement of these models will only increase their value.

Up to now, experimental models of AF have predominantly been used to elucidate the electrical and structural aspects. Electrical remodelling has been found to occur at the onset of AF and appears to be completed after two weeks. The first obvious signs of structural remodelling become apparent after 2 to 4 weeks of AF and reach a steady state between 8 to 16 weeks. However, little is known about the molecular mechanisms that underlie both electrical and structural remodelling. Changes in the expression levels of channels appear to be involved in electrical remodelling whereas in structural remodelling expression of structural proteins appears to be altered.

During AF, cells have to translate changes in activation patterns, stretch, and/or oxygen availability into new cellular structures by inducing/suppressing different sets of genes. One of the first changes seen in cardiomyocytes after AF is the redistribution of heterochromatin within the nucleus, which indicates that the cell is actually reorganizing its genetic material to cope with the new situation. Our lack of knowledge about such a shift in gene expression, which might be considered as molecular

remodelling, emphasises the increased demand for molecular biological input. The development of new molecular techniques to screen differences in gene expression, e.g. differential display, serial analysis of gene expression, and DNA arrays, together with the advancement of knowledge in functional genomics, will help to answer questions related to the nature of molecular remodelling and its role in electrical and structural remodelling during AF. A combined implementation of (electro)physiological, morphological, and molecular biological techniques, will enable scientists to unravel the nature of this fascinating arrhythmia.

## 7 | Aim of this thesis

The main goal of this study was to establish the role of altered gene expression (molecular remodelling) on the induction and maintenance of atrial remodelling during AF. The first part of the study focussed on structural remodelling in the atria of patients with AF. Subsequently, the changes in the composition of Troponin I isoforms in patients with AF were studied. Due to the complex etiology in patients, the Troponin I expression was further analysed in the goat model of AF. Finally, the goat model was used to analyse the changes in atrial gene expression during AF. Differential display was performed to identify unknown genes involved in atrial remodelling during atrial fibrillation in order to unravel the molecular mechanisms underlying the pathophysiology of AF.



# Chapter 2

## STRUCTURAL REMODELLING OF ATRIAL MYOCARDIUM IN PATIENTS WITH CARDIAC VALVE DISEASE AND ATRIAL FIBRILLATION

L. Wouters, G-S. Liu, W. Flameng, V. Thijssen, F. Thoné, M. Borgers

Exp Clin Cardiol 2000; 5:158-163

| 23

**Objectives:** The aim of this study was to assess both qualitatively and quantitatively the structural alterations in atrial myocardium associated with cardiac valve disease with or without atrial fibrillation (AF).

**Methods:** Of sixty-two consecutive patients from two hospital centres that underwent surgery for mitral, tricuspid, or aortic valve repair, a biopsy was obtained from the right atrium appendage. Light microscopic morphometry was carried out and the percentage of myocytes with either myolytic or degenerative changes, the amount of connective tissue, and the average cell surface area were scored.

**Results:** Irrespective of AF, a high degree of myolysis was present in the atrial cardiomyocytes. Atrial myocytes in patients with AF were significantly larger than in patients without AF. There was a significant positive correlation between cardiomyocyte size and structural changes. Electron microscopy showed that the majority of altered cardiomyocytes displayed the structural characteristics of foetal heart cells such as a decreased amount of myofibrils, large increase in glycogen, unorganised sarcoplasmic reticulum, mitochondria of varying size and shape, and nuclei with dispersed heterochromatin.

**Conclusions:** Atrial myocytes of patients with valvular heart disease and AF show structural changes similar to those seen in ventricular myocytes from chronic hibernating myocardium and atrial myocytes in a goat model of sustained chronic AF. These structural changes may explain the depressed contractile behaviour of the atrial myocardium during AF and the delay in recovery of contractility after cardioversion.

## 1 | Introduction

24 |

Atrial fibrillation (AF) occurs quite commonly in various types of valvular heart disease and it may be reverted to normal sinus rhythm by means of pharmacological or electrical cardioversion. However, a delay in recovery of atrial contractile function after cardioversion of atrial fibrillation is often noticed. Usually, after cardioversion, contractile strength increases progressively to reach normal values<sup>25,28,75</sup>. It has been shown that the time course of recovery of atrial function is related to the duration of AF<sup>25-27</sup>. Up to now, it is still not clear whether this delay in recovery is due to functional or structural changes of the atrium.

Structural changes, such as cell hypertrophy and degenerative changes in the right atrium of patients with valvular heart disease were already reported in the 1970s<sup>31,76</sup>. Complex structural changes were also described by Mary-Rabine *et al.* in atrial myocytes of patients with heart disease of various causes<sup>29</sup>. In about 30% of the patients these authors observed degenerative changes accompanied by changes in cellular substructures, such as loss of myofibrils, presence of glycogen granules, accumulation of sarcoplasmic reticulum-like material and aggregates of mitochondria. In the majority of patients with degenerative changes, the changes were accompanied by the presence of hypertrophied cells with an increased number of myofilaments, lobulated nuclei, and focal widening of Z-bands<sup>29</sup>. Furthermore, a relationship between these degenerative changes and the occurrence of atrial arrhythmias could be established. However, at that time, the concept of dedifferentiation of cardiomyocytes, as observed in the left ventricle of patients with coronary artery stenosis, had not been put forward<sup>40</sup>. This idea of cardiomyocyte dedifferentiation raised the question whether the ultrastructural changes, originally described as degenerative could correspond to dedifferentiation rather than to degeneration and if so, is the dedifferentiation a cause rather than a consequence of atrial arrhythmias?

Recently, in a goat model of sustained AF, structural changes were observed which resemble dedifferentiation, more than degeneration<sup>32</sup>. After 9-23 weeks of sustained AF, most of the atrial myocytes showed a number of cellular changes including myolysis, accumulation of glycogen, changes in mitochondrial shape and size, and dispersion of nuclear chromatin. The dedifferentiation of the atrial myocytes was accompanied by an

increase in cellular size and reorganisation of protein expression to a more foetal like pattern<sup>33</sup>. Degenerative changes were present only to a small extent and there were no obvious signs of apoptosis<sup>32,35</sup>. Myolysis, glycogen accumulation, dispersion of nuclear chromatin and increased cardiomyocyte size were also reported by Aimé-Sempé et al in patients with dilated right atria and AF<sup>77</sup>. However, in addition to these adaptive changes and in contrast to the study in goats, a number of cardiomyocytes in these patients also showed signs of degeneration/apoptosis. The purpose of the present study was to establish whether dedifferentiation rather than degenerative changes were involved in cardiac valve disease with or without chronic AF.

## 2 | Methods

### 2.1 | Patients

The study included sixty-two consecutive patients from two hospital centres located in Belgium (n=32) and China (n=30), who underwent surgery for mitral, tricuspid, or aortic valve repair. The study was approved by the local ethical committees for research. The diagnostic characteristics of the patients are listed in Table 1. In addition, atrial samples of 5 patients undergoing coronary bypass surgery without valvular involvement were taken as controls. In the Belgian study, there were 17 women and 15 men with age ranging from 43 to 83 years (median 69). The Chinese patients consisted of 17 women and 13 men, ranging in age between 20 and 59 years (median 42). The majority of the patients suffered from AF (Belgium 17/32, China 25/30).

**Table 1 |**  
Clinical diagnosis of patients.

	Belgium	China
Mitral valve involvement	23	28
Tricuspid valve involvement	7	14
Aortic valve involvement	14	15
Rheumatic heart disease	0	28
Coronary heart disease	14	0

## 2.2 | Microscopic examination

Small biopsies, measuring 2 mm in diameter, were obtained from the right atrium during valvular and/or coronary surgery. The tissue samples were fixed in 3% glutaraldehyde buffered to pH 7.4 with 90 mM  $\text{KH}_2\text{PO}_4$ , adjusted with 0.1 N KOH. After fixation for at least 24 hours at room temperature, the samples were washed in the same buffer for 24 hours and postfixed for 1 hour in 1%  $\text{OsO}_4$  buffered to pH 7.4 with 0.05 M veronal acetate. Next, the samples were rapidly dehydrated through a graded ethanol series, and routinely embedded in the epoxy resin Epon. Light microscopic morphometry was performed on 2  $\mu\text{m}$  thick Epon sections. To quantify the degree of myolysis and to identify myolytic cells with accumulation of glycogen, sections were stained with periodic acid-Schiff (PAS) and counterstained with toluidine blue. In order to quantify the extent of myolysis in the cardiomyocytes, a minimum of 100 myocardial cells (107-1277) per sample was evaluated. The extent of cellular changes was evaluated only in cells in which the nucleus was present in the plane of the section. Cells were identified by morphometry as myolytic if myolysis involved at least 10% of the cytosol. Cells were considered to be degenerative when secondary lysosomal structures (large inclusion bodies) were abundantly present.

To assess the amount of connective tissue in the myocardium, morphometry was carried out using a special grid with vertical and horizontal lines providing 121 intersections (points). This technique has been used in a previous study<sup>78</sup>. In accordance with the principles of morphometry, counting the number of points overlying a certain structure results in the quantitative determination of the volume of the structure under investigation in relation to the volume of the entire tissue under the square grid. The total number of points (121) was regarded as 100%, and the points counted in the connective tissue were expressed as the percentage of the entire tissue within the limits of the grid. The axis of the grid was then rotated approximately 45 degrees and the points were counted again. The same procedure was performed on a different area of the same section. Longitudinal sections at magnification x250 were evaluated. Blood vessels and perivascular interstitial cells were excluded from the connective tissue.

Average cell surface area ( $\mu\text{m}^2$ ) was evaluated by counting the number of cells in a 1  $\text{cm}^2$  grid with corrections for the amount

of connective tissue<sup>32</sup>.

Ultrastructural examination of the subcellular and extracellular composition was performed on 50 nm thin sections. These were examined, either unstained or counterstained with uranium acetate and lead citrate, in a Philips CM 100 electron microscope.

## 2.3 | Statistical Analysis

Data on myolytic cell changes are summarised as median values and range. Differences between groups were tested for statistical significance by means of stratified Wilcoxon-Mann-Whitney rank sum test with the two hospital centres as the different strata. The relation between different morphometric measurements was evaluated using the partial Spearman rank-order correlation. In this particular application, the partial rank order correlation corresponds to a Pearson correlation on the ranked data, from which the average rank of the corresponding hospital centres is subtracted. This avoids bias due to differences in baseline. Exact two-sided P-values and 95% confidence intervals for the Spearman rank correlation were obtained by Mont-Carlo sampling. In the decision making process, exact two-sided P-values less than or equal to 0.05 were considered to indicate statistical significance. Statistical computations were carried out in StatXact 4.0 and SAS6.12.

## 3 | Results

### 3.1 | Qualitative structural changes

Light microscopy: As expected, atrial tissue samples derived from non-fibrillating / non-valvular diseased patients showed uniformly well preserved cardiomyocytes surrounded by normal connective tissue (figure 1a). In all valvular diseased patients, irrespective of concomitant atrial fibrillation, changes were noticed which varied in number and extent from patient to patient (vide infra). These changes comprised depletion of sarcomeres (myolysis), accumulation of glycogen, and in general cell surface enlargement (figure 1b). In addition to these alterations, a number of clearly degenerative changes occurred in a limited number of patients. Cells were classified as degenerative when the cytosol became filled with huge secondary lysosomal structures (inclusion bodies) and/or vacuoles containing amorphous

## Figure 1 |

Light microscopic pictures of 2 µm thin sections from atrial myocardium.

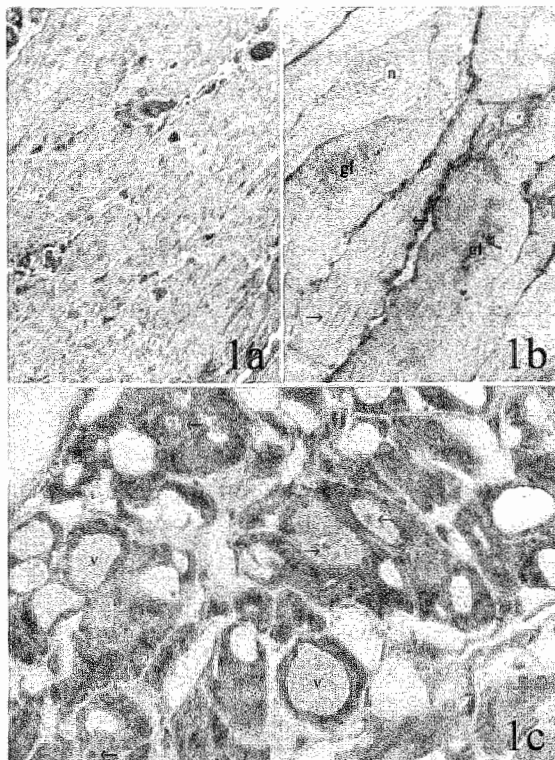
a) Control tissue with normally structured cardiomyocytes.

Sarcomeres, stained with toluidine blue, are present throughout the cytoplasm of the cardiomyocytes whereas glycogen (dark areas) is virtually absent (Original magn.: x 400).

b) Section from a patient showing myolytic areas in which the sarcomeres are replaced by glycogen (gl).

Some remnants of sarcomeres are still visible (arrows). n = nucleus (Original magn.: x 800).

c) Section from a patient showing a severely affected area with cells containing huge glycogen filled vacuoles (v) and vesicles containing amorphous structures of unknown origin (arrows; original magn.: x 800).



structures (figure 1c). A remarkable difference between the Belgian and Chinese patients was the presence of glycogen filled vacuoles in the latter group.

Electron microscopy: Depletion of sarcomeres and the huge storage of glycogen, as observed by light microscopy, were confirmed by ultrastructural examination. In addition, other changes of a non-degenerative nature were seen in all samples of valvular diseased patients. Characteristic observations in such affected cells were (figure 2a-c): i) The presence of a large number of small, abnormally shaped mitochondria, embedded in a matrix of glycogen granules. ii) The depletion of smooth sarcoplasmic reticulum. iii) The frequent occurrence of strands of rough endoplasmic reticulum. iv) Golgi fields producing huge numbers of ANF containing granules. v) Nuclei with dispersed heterochromatin. As for the degenerative changes, cytosolic blebs filled with membrane-bound vesicles and amorphous bodies of unknown but most probably autophagic origin, were seen (figure 3a). In some samples, ultrastructural features were observed that might be related to the presence of apoptosis. These occurred in the most severely affected areas and presented

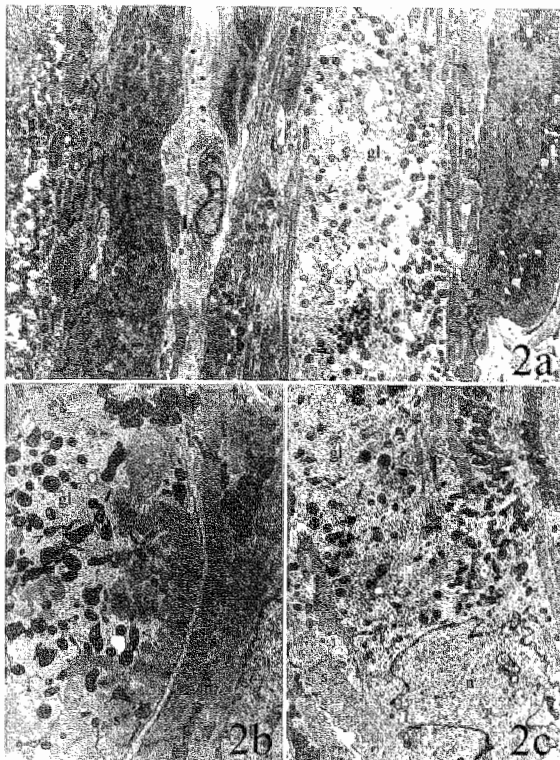


**Figure 2 |**

Electron microscopic pictures of 50 nm thin sections from atrial myocardium.

a) Overview of cardiomyocytes with different degrees of ultrastructural changes. The middle cell shows extensive myolysis and sarcomeres (s) are only present at the cell border. The myolytic area is filled with glycogen (gl) and many oddly shaped mitochondria (arrow heads) are visible. The darkly stained vesicles represent atrial granules. Both neighbouring cells also show signs of myolysis, although less extensive. Again numerous small and oddly shaped mitochondria are present in the myolytic areas (Original magn.: x 1800).

b) Detail of a myolytic cardiomyocyte adjacent to a normal cardiomyocyte. In the normal cardiomyocyte (right), regularly structured sarcomeres (s) are visible with rows of mitochondria (m) in between. In the nucleus (n), clumped heterochromatin (arrows) is present at the nuclear membrane. The myolytic cardiomyocyte (left) is filled with glycogen (gl) and sarcomeres are only present at the border of the cell. Note the oddly shaped mitochondria (arrow head; original magn.: x 3400).

c) Detail of a severely affected cell containing huge amounts of glycogen (gl) and only remnants of sarcomeres (s). Note the evenly distributed chromatin in the nucleus (n; original magn.: x 2100).

'horse-shoe' shaped nuclei with marked clumping of heterochromatin, and condensation of cytosolic compartments. These cells, in contrast to the above mentioned myolytic cells, were not hypertrophied and showed no signs of sarcomere loss (figure 3b).

### 3.2 | Quantitative structural changes

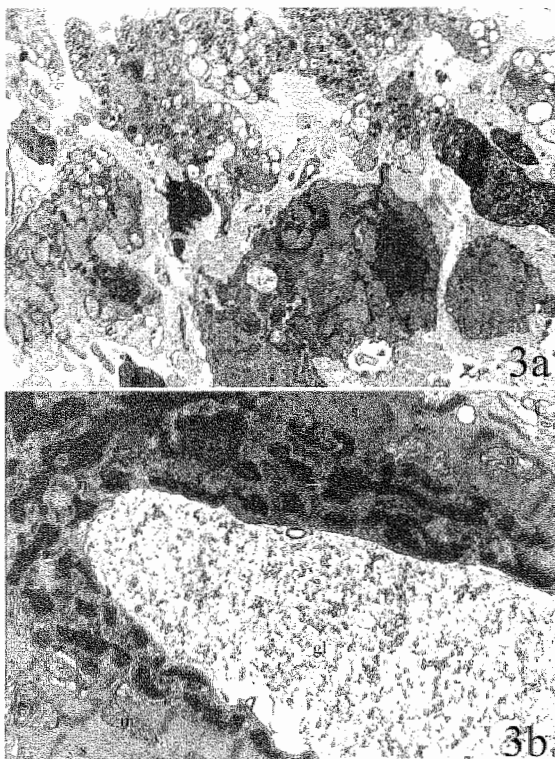
Structural changes in patients with or without AF from the two hospital centres are summarised in Table 2. In patients, both with and without AF, a considerable but highly variable proportion of the atrial myocytes (up to 97%) was affected. The structural changes could be attributed mostly to myolytic changes, while more severe, degenerative changes were present only to a minor extent. Myolytic and degenerative changes did not differ significantly among patients with and without AF. Median values for cell surface area of atrial myocytes in patients without chronic AF corresponded to a shortest axis diameter of 10-12 µm, values considered as normal by other authors<sup>29,77</sup>. However, a significant increase of cellular size was noted in

### Figure 3 |

Electron microscopic pictures of cardiomyocyte degeneration.

a) Detail of severe degeneration comprising necrotic remnants, cytosolic blebs filled with vesicles, and the presence of indefinable bodies of unknown origin (Original magn.: x 2500).

b) Detail of a possibly apoptotic cardiomyocyte. A huge vacuole containing glycogen (gl) is surrounded by normally structured sarcomeres (s) and mitochondria (m), while the 'horse-shoe' shaped nucleus (n) shows marked clumping of the heterochromatin (arrows; original magn.: x 7700).



30 |

chronic AF patients. Median values for cell surface area of atrial myocytes in these patients were 37-44% larger compared to patients without chronic AF. No significant difference between the two groups was found regarding the amount of connective tissue.

Table 3 contains the partial Spearman rank correlation coefficients between cell surface area and the other morphometric measurements, adjusted for the hospital centre. The size of the atrial myocytes correlated significantly with the total number of affected atrial myocytes. A significant correlation was also found for the amount of connective tissue and the percentage of myocytes with degenerative changes.

### 4 | Discussion

A variety of ultrastructural degenerative changes in atrial myocytes has been reported by several authors in patients with atrial disease<sup>29-31,77</sup>. Mary-Rabine *et al.* observed myolysis and degeneration of atrial cardiomyocytes and suggested, however without substantial quantification, the changes were most

**Table 2 |**  
Summary of Morphological data.

Median values (Ranges).

† = Hospital centre:  
Belgium (B) or China (C)

	Stratum <sup>†</sup>	No AF	AF	P-Value
% Total changes	B	64 (11-97)	70 (18 - 90)	0.430
	C	58 (41 - 94)	77 (11 - 100)	
% Myolytic changes	B	42 (9 - 76)	51 (18 - 83)	0.175
	C	55 (29 - 60)	65 (11 - 97)	
% Degenerative changes	B	10 (2 - 58)	9 (0 - 55)	0.292
	C	12 (0 - 35)	5 (0 - 52)	
Cell surface area (mm <sup>2</sup> ) (hypertrophy)	B	426 (352 - 755)	613 (266 - 1190)	0.001
	C	372 (327 - 423)	509 (355 - 982)	
% connective tissue (fibrosis)	B	11 (3 - 28)	15 (3 - 28)	1.000
	C	10 (7 - 45)	7 (2 - 23)	

pronounced in patients with atrial fibrillation<sup>29</sup>. The majority of the ultrastructural alterations seen in patients with atrial disease, were similar to those reported in patients with chronic hibernating myocardium<sup>40,41</sup> and in goats with 'lone' atrial fibrillation, i.e. atrial fibrillation without any underlying cardiac disease<sup>32</sup>. In these latter studies, the ultrastructural changes seen in the ventricular and atrial cardiomyocytes have been suggested to be of an adaptive nature rather than degenerative (reviewed by Thijssen *et al.*<sup>79</sup>). Although the present study predominantly shows structural changes that appear to be of adaptive nature, degenerative changes are also observed, mainly in the severely affected areas. This is different from what has been observed in 'lone' AF in the goat, but in accordance with findings of other authors<sup>29-31,77</sup>. Ultrastructural analysis, still the hallmark method to identify apoptosis<sup>80</sup>, shows that the observed degenerative changes resemble apoptotic degeneration. No involvement of cardiomyocyte apoptosis was found in patients with chronic hibernating myocardium and goats with sustained atrial fibrillation<sup>35</sup>, although it has been shown that apoptosis occurs in several cardiac diseases (reviewed by Anversa *et al.*<sup>81</sup>)<sup>82-85</sup>. It

**Table 3 |**

Partial Spearman rank correlation (95% confidence interval) of structural changes with cell surface area and interstitial space

	Cell surface area		Connective tissue	
	r	P-value	r	P-Value
% Total changes	0.520 (0.315, 0.725)	< 0.001	0.285 (0.076, 0.494)	0.025
% Myolytic changes	0.491 (0.306, 0.676)	< 0.001	-0.027 (-0.237, 0.183)	0.834
% Degenerative changes	0.226 (-0.025, 0.477)	0.080	0.378 (0.167, 0.589)	0.002
Connective tissue	0.154 (-0.112, 0.420)	0.233	-	-

has been proposed that cardiomyocyte apoptosis occurs if already dedifferentiated cells are unable to adapt to a further decrease in oxygen supply<sup>82</sup>. However, apoptotic cells in this study did not show signs of accompanying dedifferentiation. In fact, there appeared to be a clear distinction between dedifferentiated, necrotic and apoptotic cardiomyocytes. This might indicate that cell degeneration and apoptosis are not the end-stage of ongoing dedifferentiation, but result from other underlying factors.

Morphometric data show remarkable differences between Belgian and Chinese patients, such as the appearance of large glycogen filled vacuoles in the latter group. Vacuolisation has been shown to occur during reversible myocardial damage<sup>86</sup> and has been proposed to be a predictor of vulnerability to the development of atrial fibrillation following cardiac surgery<sup>87</sup>. Most of the differences can be explained by the difference in pathology, i.e. 28 out of 30 Chinese patients had a history of rheumatic heart disease. Despite these differences, our findings that the atrial myocytes of these patients show predominantly myolytic changes and that the occurrence of AF is accompanied by an increase in cellular size, were consistent in both groups of patients.

The present study shows that patients with different forms of valvular disease develop profound structural changes in their atrial myocytes, including a severe loss of contractile material. Presumably, this depletion of contractile material has reached such an extent that it is impossible for AF, as an extra contributing

factor, to induce more myolysis. Occurrence of AF is associated with a markedly enlarged cell size. This is in agreement with the results obtained in goats with sustained AF<sup>32</sup>. It is still not clear whether the changes observed in the present study as well as in the goat can be classified as reversible or irreversible. To address this question, time-related experiments in the goat have been set up to study the course of progression of the changes as well as the potential of reversibility.



# Chapter 3

## EXPRESSION OF TROPONIN I ISOFORMS IN PATIENTS WITH ATRIAL FIBRILLATION.

V. Thijssen, J. Ausma, L. Gorza, I. Van Gelder,  
M. Borgers, G. van Eys

In preparation

| 35

**Background:** Cardiomyocyte differentiation is accompanied by a switch in expression from slow skeletal Troponin I (ssTnI) to cardiac Troponin I (cTnI). Both atrial fibrillation (AF) and mitral valve disease (MVD) are characterised by structural remodelling that is indicative of cardiomyocyte dedifferentiation. We investigated whether TnI isoform composition was affected in the atria of patients with AF and MVD. **Methods:** The following groups were included in this study: 1) patients undergoing coronary artery bypass grafting with no previous AF, 2) patients with SR and MVD, 3) patients with chronic AF and MVD, 4) patients with lone paroxysmal AF (PAF), and 5) patients with lone chronic AF (CAF). Western blotting was performed to detect alterations in the TnI isoform expression. Quantitative RT-PCR (QRT-PCR) was used to establish changes in the mRNA composition of ssTnI and cTnI as well as the ratio between ssTnI/cTnI. **Results:** Western blot analysis with a TnI antibody revealed the presence of an additional lower band beside the expected cTnI band. This additional band was identified as ssTnI because it moved at the same electrophoretic mobility as ssTnI and could not be detected with a cTnI specific antibody. The band was present in approximately 60% of the patients in each group, except for patients with CAF with or without MVD. QRT-PCR showed that the ssTnI/cTnI mRNA ratio in patients with an additional band was in favour of a shift towards ssTnI expression. In patients with sinus rhythm the absolute amount of cTnI mRNA was 600-fold higher as compared to ssTnI mRNA. In the presence of either MVD, PAF, or CAF, the amount of cTnI mRNA over ssTnI mRNA increased significantly, up to 3,500-fold in patients with both MVD and CAF. **Conclusions:** Atrial expression of ssTnI protein does occur in patients, irrespective of the presence of PAF or MVD. The expression of ssTnI is not the result of ongoing cardiomyocyte dedifferentiation because patients with CAF do not display ssTnI expression. Rather than ssTnI, the expression of cTnI increases both as a result of MVD, PAF, and CAF. The alterations in TnI isoform composition during MVD and AF could be involved in the contractile dysfunction of the atrium during AF following cardioversion.

## 1 | Introduction

Atrial fibrillation (AF) is accompanied by electrical and structural remodelling of the atrium which results in reduced atrial function. Both in patients and in animal models it has been shown that the structural alterations are indicative of cardiomyocyte dedifferentiation<sup>32,79,88</sup>. The most prominent changes consist of extensive myolysis, increased glycogen storage, cardiomyocyte hypertrophy, mitochondrial shape changes and redistribution of heterochromatin<sup>32,88,89</sup>. Furthermore, the morphological changes are accompanied by protein expression and cellular organisation patterns that are reminiscent of foetal cardiomyocytes<sup>33,90</sup>. Morphological changes, similar to those found during AF, are found in the atria of patients with mitral valve disease (MVD) even in the absence of AF<sup>88</sup>.

Different TnI isoforms have been described for fast-twitch skeletal muscle (fsTnI), slow-twitch skeletal muscle (ssTnI), and cardiac muscle (cTnI)<sup>91,92</sup>. In the foetal human heart ssTnI is the predominant isoform, which is gradually replaced by cTnI during cardiac development<sup>93,94</sup>. In the adult heart, only the cTnI isoform is expressed, except for cells of the conductive tissues (e.g. AV node)<sup>93-96</sup>. The isoform-switch during heart development has been described for several species<sup>97-100</sup>.

Apart from a shift during heart development, TnI status is influenced by cardiac disease. Regulation of TnI activity has been suggested to be involved in altered Ca<sup>2+</sup> sensitivity of the myocardium<sup>101-103</sup>, and changes in TnI activity appear to be mainly regulated by protein phosphorylation<sup>103-106</sup> and/or protein degradation<sup>107-109</sup>. Alterations in the expression level of the cTnI isoform during cardiac disease have not been found<sup>93</sup>, and re-expression of the ssTnI isoform has also not been detected<sup>93,104,105</sup>. Recently, it was shown that activation of calpains was responsible for elevated TnI degradation during increased preload or hypoxia<sup>110,111</sup>. Activation of calpains has also been found during atrial fibrillation<sup>112,113</sup>. As a consequence, AF might result in degradation of cTnI which could explain the decreased contractile function of the atrium. To determine the role of TnI isoform expression in cardiomyocyte dedifferentiation and contractile dysfunction during AF and MVD, we have analysed the composition of TnI isoforms at the protein and mRNA level in patients suffering from MVD with or without AF.

## 2 | Materials and Methods

### 2.1 | Human atrial tissue

Human material consisted of right atrial appendages obtained from patients as described elsewhere<sup>114,115</sup>. A total of 27 patients divided over 5 different groups were used in this study: 1) Control patients with normal sinus rhythm (SR, n=5) undergoing coronary bypass surgery, 2) patients with mitral valve disease and normal sinus rhythm (MVDSR, n=4), 3) patients with mitral valve disease and chronic atrial fibrillation (MVDAT, n=4), 4) patients with lone paroxysmal atrial fibrillation (PAF, n=6), 5) patients with lone chronic atrial fibrillation (CAF, n=8). Atrial tissue was obtained during surgery, snap-frozen in liquid nitrogen and stored at -80°C. Patients characteristics have been described previously<sup>114,115</sup>. All the patients gave their written consent and the study was approved by the Institutional Review Board.

### 2.2 | Western blotting and antibodies

Two monoclonal antibodies reacting with cardiac and/or skeletal Troponin I were used to detect cTnI degradation and re-expression of ssTnI. Monoclonal antibody Ti-54 recognises both cTnI and the ssTnI, whereas Ti-1 reacts specifically with the cardiac TnI isoform<sup>98</sup>. Cryostat sections from tissue samples were homogenised in electrophoresis sample buffer, boiled for 10 min, and equal protein amounts of each sample, together with molecular weight standards (Biorad), were run at 100 mA on a 13% polyacrylamide gel. Subsequently, protein was transferred onto a nitro-cellulose filter, saturated for 1 hour with ovalbumin in TBST (10 mM Tris-HCl pH 8.0, 150 mM NaCl, 0.5% Tween20) and incubated with the primary antibody (Ti-54, 1:3000; Ti-1, 1:1000) for 1 hour at RT in TBST. After washing 3x10 min in TBST, filters were incubated for 1 hour with peroxidase conjugated secondary antibody (1:5000). Following 3x10 min washing in TBST, peroxidase activity was detected by the ECL method. All experiments were performed in triplicate.

**Table 1 |**  
Primers and probes used for quantitative real-time RT-PCR

Target	Primers probe	Sequence/modification
human cTnI	Forward	5' GCCCACCTCAAGCAGGTG 3'
	Reverse	5' TTGCGCCAGTCTCCCACCTC 3' <u>TAMRA</u>
	Probe	5' AGAAGGAGGACACGGAGAAGGAAACCG 3' <u>DABCYL</u>
human ssTnI	Forward	5' GCCCACCTCAAGCAGGTG 3'
	Reverse	5' CATCAGGCTTTAGCAAGAG 3' <u>FAM</u>
	Probe	5' CCCAAGATCACTGCCTCCCGCA 3' <u>DABCYL</u>

### 2.3 | Primers and probe design

Primers and probes used for PCR are listed in table 1. The overall homology between the coding regions of cTnI and ssTnI is approximately 60%. To avoid cross-reactivity the primer/probe combinations were confined to regions of poor homology between cTnI and ssTnI. The primers and probes were specific for cTnI or ssTnI, and designed using Primer Express software (PE Applied Biosystems). This software sets several requirements concerning GC-content, annealing temperature and amplicon length, which the primers and probe have to meet to ensure optimal primer/probe combinations. The probes for cTnI and ssTnI were labelled with the reporter dyes TAMRA and 6-FAM respectively, in combination with DABCYL as quencher. Primers as well as probes were synthesised by Eurogentec.

### 2.4 | Quantitative real-time RT-PCR

Total RNA from 30 mg human atrial appendage tissue was isolated using the RNeasy mini kit (Qiagen) according to the manufacturer's instructions. During the procedure, possible genomic DNA contamination was removed by on-column DNase treatment with the RNase-free DNase set (Qiagen). Total amount of isolated RNA was incubated at 65°C for 5 minutes and reverse transcription was performed for 1.5 hours at 37°C with 600 U of M-MLV reverse transcriptase (GibcoBRL) in 50 µL of 50 mM Tris-HCl, pH 8.3, 75 mM KCl, 3 mM MgCl<sub>2</sub>, 10

mM DTT, 1mM dNTPs in the presence of 40 U RNase inhibitor RNasin® (Promega) and 0.5 µg oligo(dT) primer (GibcoBRL). Subsequently, reverse transcriptase was inactivated by incubation at 95°C for 5 minutes and cDNAs were stored at -20°C. Real-time PCR, as described elsewhere<sup>116,117</sup>, was performed with the ABI PRISM 7700® Sequence Detection System apparatus and software (PE Applied Biosystems) using the Real-time PCR Taqman Kit (Eurogentec). The PCR reaction was performed in a 50 µl volume containing 3 µl cDNA, 1x PCR buffer, 200 µM dATP, dGTP, dCTP, dTTP, and dUTP, 0.025 U/µl Hot Goldstar DNA polymerase, 100 nM probe, and 150 nM of each primer. Cycling conditions consisted of a Hot Goldstar activation step of 10 minutes at 95°C, followed by 50 cycles of 15 seconds at 95°C and 1 minute at 60°C. Data were analysed with the Sequence Detection System software (PE Applied Biosystems). The parameter Ct (threshold cycle) was defined as the cycle number at which the fluorescent signal passed a fixed value (threshold) above baseline. Thus, there is an inverse relation between the Ct value and the level of expression. High levels of expression are represented by low Ct values because high levels of mRNA result in a rapid increase in the fluorescent signal and subsequently, the threshold value is reached earlier during PCR as compared to low amounts of mRNA.

## 2.5 | Statistical analysis

Data are displayed as mean values ± SEM of three independent experiments. For statistical analysis the mean values of the ssTnI/cTnI ratio were used. Significant differences between the groups were analysed by means of the Wilcoxon-Mann-Whitney rank sum test. All p-values are two-sided and p-values < 0.05 were considered to be statistically significant. Statistical computations were performed in SPSS 10.0.5.

# 3 | Results

## 3.1 | Patients

A total of 27 patients was included in this study, with a mean age of 58 years (range 37 - 74). Nineteen patients were male and 8 patients were female. The patients could be divided in 3

groups when atrial rhythmic activity was used as the sole selection criteria: sinus rhythm (SR, n=9), paroxysmal AF (PAF, n=6), and chronic AF (CAF, n=12). When also the underlying disease was taken into account, 5 different groups could be distinguished: normal sinus rhythm (SR, n=5), SR + mitral valve disease (MVDSR, n=4), CAF + mitral valve disease (MVDAF, n=4), lone paroxysmal AF (lone PAF, n=6), and lone chronic AF (lone CAF, n=8). The characteristics of the patients, subdivided over either 3 or 5 groups are given in table 2.

### 3.2 | Degradation of cTnI

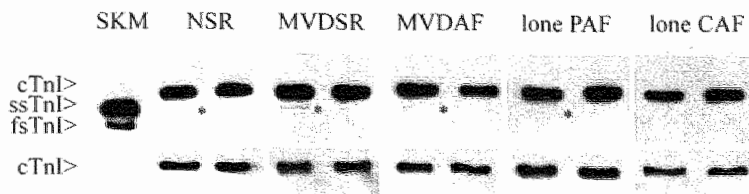
Western blotting was used to detect degradation of cTnI and to determine whether or not expression of ssTnI could be found in any of the patient groups. Figure 1 shows a typical example of a Western blot with atrial tissue from several patients stained with Ti-54 (upper panel), an antibody that recognises both

**Table 2 |**  
40 | Patients characteristics

Values are presented as mean  $\pm$  SD or number of patients, except where indicated different. SR = sinus rhythm; PAF is paroxysmal AF; CAF = chronic AF; SR is normal sinus rhythm; MVDSR is mitral valve disease combined with SR; lone PAF = lone paroxysmal AF; MVDAF = mitral valve disease combined with AF; lone CAF = lone chronic AF;  
<sup>\*</sup>p<0.05, PAF vs. CAF;

<sup>†</sup>p<0.05, lone PAF vs. SR;  
 NYHA = New York Heart Association Class for exercise tolerance.

	SR		PAF		CAF	
male/female (n)	6/3		6/0		7/5	
age (yrs)	61 $\pm$ 10		48 $\pm$ 8*		61 $\pm$ 12	
duration PAF (median, range (hours))	-		9 (0.2-14.4)		-	
duration CAF (median, range (months))	-		-		8.6 (0.5-20)	
NYHA						
Class I	5		3		3	
Class II	4		3		1	
Class III	0		0		8	
	NSR	MVDSR	lone PAF	MVDAF	lone CAF	
n	5	4	6	4	8	
male/female (n)	2/3	4/0	6/0	2/2	5/3	
age (yrs)	67 $\pm$ 9	52 $\pm$ 12	48 $\pm$ 8 <sup>†</sup>	62 $\pm$ 8	60 $\pm$ 12	
duration PAF (median, range (hours))	-	-	9 (0.2-14.4)	-	-	
duration CAF (median, range (months))	-	-	-	4.5 (0.5-13)	10.6 (6-20)	
NYHA						
Class I	4	1	3	0	3	
Class II	1	3	3	0	1	
Class III	0	0	0	4	4	



cardiac and skeletal TnI. In human skeletal muscle, two bands were visible representing ssTnI and fsTnI. In human cardiac tissue one prominent band was found that represents cTnI. In addition to this cTnI band, several patients displayed a faint band at the same electromobility shift as the ssTnI band in skeletal muscle. To distinguish between cTnI degradation and ssTnI expression, Western blotting was performed with Ti-1, a cTnI specific antibody (figure 1, lower panel). Using this antibody, no additional bands could be found, even when Ti-1 antibody was used at 10-fold concentration or after extensive detection time following ECL (up to 45 minutes). This indicates that the faint bands represent ssTnI expression rather than cTnI degradation. The overall results of the Western blot analysis are shown in table 3. In the SR and PAF group, an additional band could be observed in approximately 60% of the patients, whereas in the CAF group only 1 out of 12 patients (8%) displayed an additional band.

**Figure 1 |**  
Western blot analysis of TnI isoform expression

The upper panel shows a representative Western blot on two patients from each group with Ti-54 which recognises both cTnI and ssTnI. The asterisk indicates the additional band which moves with the same electromobility as ssTnI. The lower panel shows a representative Western blot on the same patients with a cTnI specific antibody (Ti-1). Note that in none of these samples an additional band is visible. ECL detection time was ~10 min. SKM = skeletal muscle; SR = sinus rhythm; MVDSR = mitral valve disease with sinus rhythm; MVDAF = mitral valve disease with atrial fibrillation; PAF = paroxysmal atrial fibrillation; CAF = chronic atrial fibrillation; cTnI = cardiac Troponin I; ssTnI = slow-twitch skeletal Troponin I; fsTnI = fast-twitch skeletal Troponin I.

| 41

patient group	Ti-54 additional band	Ti-1 additional band
NSR	3/5	SR 5/9 (56%)
MVDSR	2/4	0/4
LPAF	4/6	PAF 4/6 (67%)
MVDAF	1/4	0/4
LCAF	0/8	CAF 0/12 (0%)

**Table 3 |**

TnI isoform composition during AF.

SR = sinus rhythm; PAF = paroxysmal AF; CAF = chronic AF; MVDSR is mitral valve disease combined with SR; lone PAF = lone paroxysmal AF; MVDAF = mitral valve disease combined with AF; lone CAF = lone chronic AF.

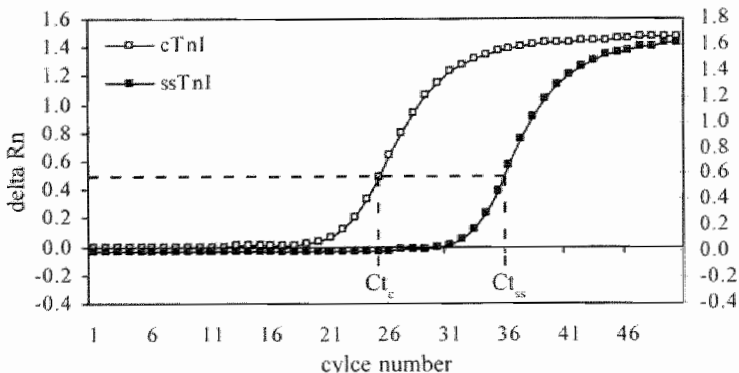
### 3.3 | Expression of TnI isoforms

To determine the mRNA expression levels of cTnI and ssTnI we performed quantitative real-time RT-PCR. With this technique, the time course of a PCR can be followed by measuring the release of a fluorescent dye. The Ct-value, which

**Figure 2 |**

Quantitative RT-PCR

Two representative amplification curves generated during quantitative RT-PCR on a patient with SR. QRT-PCR was performed with primers specific for cTnI (open squares) or ssTnI (closed squares). Determination of the Ct-values is indicated by the dotted lines.

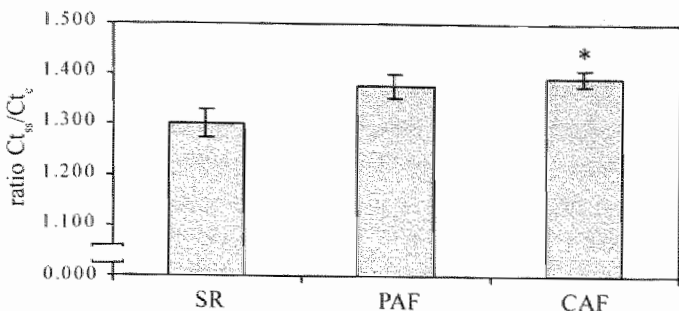


42 |

indicates the cycle number at which the generated fluorescence passes a given threshold, is a direct representation of the amount of mRNA present in the sample<sup>117</sup>. It is important to note that low Ct-values represent high levels of expression, because it takes less cycles to reach the threshold value. Within the range of 100 ng to 10 pg template DNA, a linear relationship between the Ct and the logarithm of DNA could be observed for both cTnI and ssTnI (data not shown). Figure 2 shows an example of the amplification plots of cTnI and ssTnI generated during PCR on atrial tissue from a patient with sinus rhythm. The derived Ct values, Ct<sub>c</sub> and Ct<sub>ss</sub> respectively, are also indicated.

Because changes in the absolute Ct values between different samples might also be influenced by differences in tissue integrity or the efficiency of RNA isolation and subsequent reactions, we determined the ratio between the Ct<sub>ss</sub> and Ct<sub>c</sub>. Changes in the Ct<sub>ss</sub>/Ct<sub>c</sub> ratio thus indicate a shift in expression towards either cTnI or ssTnI. In figure 3A the different ratios are shown for the different patient groups. Compared to SR, CAF resulted in a statistically significant increase in Ct<sub>ss</sub>/Ct<sub>c</sub> ratio which suggests higher expression of cTnI. However, when also the underlying mitral valve disease was taken into account, all patient groups with PAF or CAF displayed a statistically significant increase in their Ct<sub>ss</sub>/Ct<sub>c</sub> ratio as compared to patients with sinus rhythm (Figure 3B). To determine whether a change in the Ct<sub>ss</sub>/Ct<sub>c</sub> ratio reflected the changes at the protein level we compared the Ct<sub>ss</sub>/Ct<sub>c</sub> values of patients in which no ssTnI could be observed and patients which displayed a ssTnI band on a Western blot. The latter group showed a significant lower Ct<sub>ss</sub>/

A

**figure 3 |**

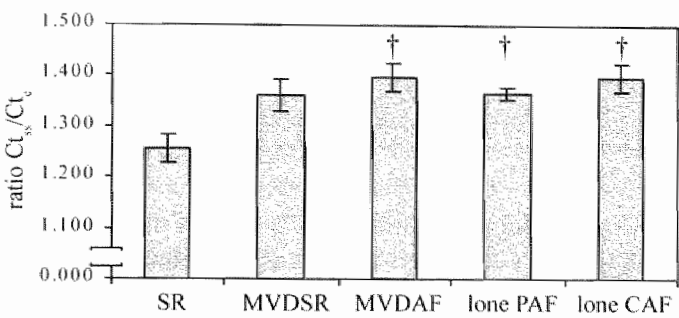
Quantitative analysis of  $Ct_{ss}/Ct_c$  ratio's between different patient groups

A) Diagram showing the  $Ct_{ss}/Ct_c$  ratio's in patient groups on the basis of atrial activity.

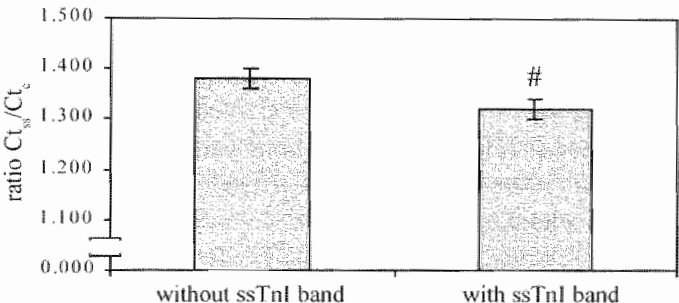
B) Diagram showing the  $Ct_{ss}/Ct_c$  ratio's in patient groups on the basis of both the atrial activity and the underlying valve disease.

C) Diagram showing the  $Ct_{ss}/Ct_c$  ratio in patients based on the presence of an additional (ssTnI) band in Western blotting. SR = sinus rhythm; PAF = paroxysmal AF; CAF = chronic AF; MVDSR is mitral valve disease combined with SR; lone PAF = lone paroxysmal AF; MVDAF = mitral valve disease combined with AF; lone CAF = lone chronic AF; \* p<0.050 vs. SR; † p<0.05 vs. SR; # p<0.05 vs. no additional band.

B



C



$Ct_c$  ratio indicating a shift towards ssTnI expression (Figure 3C). All data of the quantitative RT-PCR analysis are summarised in table 4.

Based on a standard curve, the  $Ct_c$  and  $Ct_{ss}$  values were also used to determine the absolute mRNA levels in each sample. During sinus rhythm, the amount of cTnI mRNA was approximately 600-fold higher as compared to ssTnI mRNA (Table 4). The presence of either MVD or AF increased this value significantly up to approximately 2,200-fold. When

**table 4**

Overall results from QRT-PCR analysis

SR = sinus rhythm; PAF is paroxysmal AF; CAF = chronic AF; MVDSR is mitral valve disease combined with SR; lone PAF = lone paroxysmal AF; MVDAF = mitral valve disease combined with AF; lone CAF = lone chronic AF; \* p<0.05 vs. SR (n=9); † p<0.05 vs. SR (n=5); # p<0.05 vs. no additional band

patient group	Ct <sub>ss</sub>	Ct <sub>c</sub>	Ratio Ct <sub>ss</sub> /Ct <sub>c</sub>	absolute cTnI/ssTnI mRNA
SR n=9	27.64+/-0.38	21.42+/-0.33	1.29+/-0.03	1,384+/-468
PAF n=6	28.27+/-0.61	20.62+/-0.49	1.37+/-0.03	2,124+/-578
CAF n=12	28.19+/-0.59	20.39+/-0.47*	1.38+/-0.02*	2,666+/-510*
NSR n=5	27.00+/-0.46	21.67+/-0.34	1.26+/-0.03	574+/-143
MVDSR n=4	28.44+/-0.35	21.11+/-0.63	1.36+/-0.03	2,396+/-816 <sup>†</sup>
MVDAF n=4	28.48+/-0.39 <sup>†</sup>	20.57+/-0.15 <sup>†</sup>	1.40+/-0.03 <sup>†</sup>	3,525+/-1,339 <sup>†</sup>
LPAF <sup>‡</sup> n=6	28.27+/-0.61	20.62+/-0.49	1.38+/-0.02 <sup>†</sup>	2,124+/-578 <sup>†</sup>
LCAF n=8	28.04+/-0.88	20.29+/-0.72	1.39+/-0.02 <sup>†</sup>	2,236+/-386 <sup>†</sup>
no add. band n=17	28.17+/-0.45	20.56+/-0.38	1.38+/-0.02	2,646+/-442
add. band n=10	27.77+/-0.39	21.16+/-0.33	1.32+/-0.02 <sup>#</sup>	1,220+/-166 <sup>#</sup>

patients suffered from both MVD and AF the value increased even up to 3,500-fold. As expected the amount of cTnI mRNA over ssTnI mRNA was significantly lower in patients which displayed an additional band in Western blotting as compared to those in which no additional band could be detected (1,200-fold vs. 2,600-fold, respectively).

#### 4 | Discussion

It has been shown that throughout cardiac development two different TnI isoforms are expressed in the heart. The expression of the skeletal isoform (ssTnI) decreases around birth while at the same time the cardiac isoform (cTnI) increases<sup>93,94</sup>. Consequently, the TnI isoform expression pattern reflects the differentiation state of the cardiomyocyte. Dedifferentiation of cardiomyocytes is a characteristic feature of AF and MVD<sup>32,79,88</sup>, and this dedifferentiation might lead to alterations in the expression of TnI isoforms. Furthermore, a relation was found between AF and the activity of Calpain I<sup>113</sup>, a protein which is involved in degradation of cTnI<sup>110,111</sup>. Both the degradation of cTnI and changes in the TnI isoform expression could contribute to the contractile dysfunction during AF. In this study we analysed the composition of TnI isoforms in the atria of patients with MVD and AF by Western blotting and quantitative RT-PCR.

In patients with SR, MVD, or PAF atrial expression of ssTnI

could be observed. This expression was not the result of cardiomyocyte dedifferentiation because patients with CAF did not show ssTnI expression. In addition, the expression of cTnI increased in patients with MVD, PAF, and CAF. These alterations in TnI isoform composition during MVD and AF are possibly involved in the contractile dysfunction of the atrium during AF.

#### 4.1 | Changes in TnI protein composition during AF

Western blot analysis with an antibody that recognises both cTnI and ssTnI revealed that apart from cTnI, an additional band with the same electrophoretic mobility as ssTnI could be detected in almost all patient groups, irrespective of the presence of MVD or PAF. Only in patients with longstanding (chronic) AF without any underlying disease no additional band could be detected. Western blotting on the same patients with a cTnI-specific antibody did not reveal any additional bands, even when a 10-fold increase in antibody concentration was used or after extensive elongation of the detection time following ECL. In other species the cTnI specific antibody also detects cTnI degradation which indicates that the absence of a degradation band in our patients is not due to a change in the epitope (Chapter 4). These results suggest that expression of ssTnI does occur in atrial tissue of patients irrespective of the presence of MVD or AF. Up to now, there have been no reports on the presence of ssTnI protein in adult cardiac tissue, except for Gorza *et al.* who did detect ssTnI mRNA in cells of the conductive tissue throughout adulthood<sup>96</sup>.

Although expression of ssTnI supports the hypothesis of cardiomyocyte dedifferentiation, patients with chronic AF did not express ssTnI. In contrast, chronic AF resulted in increased expression of cTnI. The discrepancy between these observations could be explained by a difference between the arrhythmic activity of paroxysmal AF and chronic AF. In a goat model on AF there appeared to be an increase in the mRNA level of ssTnI at the onset of AF, although not significant and ssTnI protein could not be detected by Western blot. The increased ssTnI mRNA level was no longer present after prolonged (chronic) AF (Chapter 4). Thus, in patients with CAF no ssTnI protein could be detected due to normalisation of expression in response to the persistent arrhythmic activity whereas in patients suffering from PAF, the repetitive cycles of AF followed by SR might

result in repeated activation of ssTnI expression subsequently leading to detectable levels of ssTnI protein. The fact that ssTnI expression was also observed in patients with sinus rhythm indicates that in these patients the underlying cardiac disease (coronary ischaemia) results in repetitive atrial stress (ischaemia, stretch), which in turn leads to increased ssTnI expression. The reason for re-expression of ssTnI is not known. ssTnI increases calcium sensitivity and renders the myofilaments resistant to acidosis<sup>101,102,118</sup>. Thus, re-expression of ssTnI could be a protective mechanism against increased cardiomyocyte stress/acidosis at the onset of AF.

There have been several reports on cTnI degradation as a result of increased preload, ischaemia/reperfusion, and in patients undergoing coronary artery bypass grafting<sup>107-109,111,119</sup>. In our patients, no degradation of cTnI could be detected. The discrepancy between our findings and those of other authors appears to be related to the duration and the severity of cardiac stress. Thomas *et al.* reported that in a swine model of stunned myocardium, representing mild cardiac stress, no increase in degradation of cTnI could be found<sup>120</sup>. In most studies that show degradation of cTnI, there was an acute and severe cardiac stress (increased pressure, ischaemia) and degradation was observed in the time-frame immediately following this cardiac stress<sup>107,108,111</sup>. We have also found some evidence of cTnI degradation at the onset of AF in the goat model. In goats subjected to sustained AF, limited cTnI degradation could be observed within the first 4 weeks following initiation of AF (1 out of 6 after one or two weeks of AF and 2 out of 6 after 4 weeks of AF). After longer periods of AF, degradation of cTnI was no longer detectable (Chapter 4). The degradation corroborated with the calcium overload in these goats which occurred in the first weeks of AF<sup>59</sup>. Calpain I, a calcium induced proteolytic protein that has been shown to be activated during AF<sup>112,113</sup> might be responsible for the observed degradation<sup>107,110,111</sup>. The patients described in this study all suffered for prolonged periods of time from MVD and repetitive paroxysms or chronic AF. Thus, the early phase of cardiac stress, calcium overload and subsequent cTnI degradation was not represented in this study. Furthermore, cTnI could be protected from degradation by a protective response of the cardiomyocytes by e.g. heat shock proteins<sup>121</sup> or by increased cTnI phosphorylation<sup>109</sup>. Phosphorylation also affects the calcium

sensitivity of cTnI<sup>122-124</sup> which might contribute to the contractile dysfunction of the atrium during chronic AF. Preliminary results on the phosphorylation state of cTnI in patients with AF indicate an increased amount of phosphorylated cTnI protein during AF (unpublished data).

#### 4.2 | Changes in TnI mRNA expression during AF

Further analysis of the changes in TnI isoform expression was performed by quantitative RT-PCR<sup>116,117</sup>. Rather than using a house-keeping gene like GAPDH to correct for differences in mRNA content and integrity we determined the ssTnI:cTnI ratio. Changes in this ratio are indicative of a shift in expression towards either ssTnI or cTnI. In the atria of patients with sinus rhythm, low levels of ssTnI expression could be detected. cTnI was the main isoform which was expressed at a 600-fold higher level as compared to ssTnI. Previous studies, using either in situ hybridisation or Northern blotting techniques, did not find any evidence for the presence of ssTnI mRNA in normal adult cardiac tissue or re-expression of ssTnI during cardiac disease<sup>93,95,96</sup>. However, quantitative RT-PCR is more sensitive than these techniques, which might explain the detection of the relatively low levels of ssTnI mRNA in the current study. In the presence of either MVD, PAF or CAF, the level of cTnI mRNA was approximately 2,200-fold higher as compared to ssTnI mRNA. The presence of both MVD and CAF increased the value even up to 3,500-fold. When patients with an additional band on the Western blot were compared with patients in which no additional band could be found, there was a significant decrease in the  $C_t_{ss}/C_t_c$  ratio which favours the idea of ssTnI re-expression. In patients with no additional band on the Western blot, the mRNA level of cTnI was 2,600 fold higher as compared to ssTnI, but this dropped to 1,200-fold when an additional band was detected. This value is in the same range as the value in patients with sinus rhythm (1,384-fold). Whether the increased expression of cTnI is a result of cardiac hypertrophy which also occurs during AF<sup>88,89</sup> or whether the mRNA turnover increases is unknown. The increased expression of cTnI might also be a response of the cardiomyocytes to compensate for the decreased calcium sensitivity as a result of increased cTnI phosphorylation<sup>122-124</sup>.

#### 4.3 | Limitations to the study

Although our data show re-expression of ssTnI in the atria of patients with MVD or lone PAF, it still needs to be established whether the ssTnI protein is functionally incorporated in the contractile apparatus of the cardiomyocytes. The simultaneous expression of both cTnI and ssTnI during embryogenesis<sup>93,94</sup> and the observation that adenovirus mediated replacement of cTnI with ssTnI results in functional sarcomere architecture<sup>118</sup> show that both isoforms can co-operate within a single cardiomyocyte. Whether this is also true for the low levels of ssTnI expression found in this study still needs to be established. All patients with sinus rhythm were either undergoing coronary artery bypass surgery or suffered from mitral valve disease. For both groups of patients it has been shown that the cardiac disease is accompanied by structural remodelling of the cardiomyocytes which, similar as for AF, is reminiscent of cardiomyocyte dedifferentiation<sup>40,88</sup>. Thus, rather than being a control group, the patients with SR might represent a group with similar cellular changes as the AF groups but to a lower extent and with a different underlying cause. Furthermore, the use of drugs might influence gene expression of TnI isoforms. To minimise this effect, drugs were discontinued before surgery, when possible. The use of an animal model on AF might provide a better way to determine the actual effect of AF on the expression of ssTnI and cTnI.

#### Acknowledgements

The authors would like to thank H. Kuijpers en M-H Lenders for their excellent technical assistance throughout this study.

# Chapter 4

## TROPONIN I ISOFORM EXPRESSION DURING CHRONIC ATRIAL FIBRILLATION IN THE GOAT

V. Thijssen, J. Ausma, L. Gorza, M. Allessie, M. Borgers, G. van Eys

In preparation

| 49

**Background:** Atrial fibrillation (AF) results in structural changes in the atrial myocytes. These changes are reminiscent of cardiomyocyte dedifferentiation and might be induced by activation of proteolytic enzymes. Both dedifferentiation and proteolysis are likely to influence the composition of Troponin I (TnI) isoforms during AF, either by re-expression of the foetal TnI isoform (slow-skeletal TnI; ssTnI) or by degradation of cardiac TnI (cTnI). We examined changes in the composition of TnI isoforms in a goat model of AF. **Methods:** Degradation of cTnI protein and re-expression of ssTnI protein were analysed by Western blotting in the atria of foetal goats, goats with normal sinus rhythm (SR), and goats after 1, 2, 4, 8, and 16 weeks of AF. Changes in the mRNA amount of both isoforms were quantified by means of the quantitative RT-PCR technique. **Results:** Similar to other species, cardiac development in the goat was accompanied by a switch from ssTnI to cTnI expression both at the level of protein and mRNA. Western blotting revealed degradation of cTnI in only a few samples during the first 4 weeks of AF (1 out of 6 after one and two weeks of AF and 2 out of 6 after 4 weeks of AF). During SR and after longer periods of AF no degradation of cTnI could be detected. ssTnI protein expression was undetectable up to 16 weeks of AF. There were also no significant differences in mRNA content of cTnI and ssTnI during AF as compared to SR. **Conclusions:** Limited cTnI degradation occurs during the first 4 weeks of AF. After longer periods of AF, cTnI degradation is inhibited. Surprisingly, cardiomyocyte dedifferentiation during AF was not accompanied by re-expression of the foetal ssTnI isoform.

## 1 | Introduction

Troponin I (TnI) is a subunit of the troponin complex which facilitates actin-myosin interaction during contraction of striated muscle. TnI is differentially expressed in distinct muscle types and during muscle development<sup>125</sup>. TnI isoforms have been described for fast-twitch skeletal muscle (fsTnI), slow-twitch skeletal muscle (ssTnI), and cardiac muscle (cTnI)<sup>91,92</sup>. The expression of these isoforms, encoded by three separate genes, is not completely restricted to a specific muscle type. Several species, including humans, show a switch in TnI isoform expression from ssTnI to cTnI during heart development<sup>93-95,97-100</sup>.

50 |  
TnI isoform composition is not only regulated during heart development, but appears to be affected by cardiac disease as well. Rather than regulation of mRNA expression<sup>93</sup>, the cTnI activity during cardiac disease appears to be regulated by protein phosphorylation<sup>103-106</sup> and/or protein degradation<sup>107-109</sup>. The importance of regulating cTnI activity is most likely related to altering the Ca<sup>2+</sup> sensitivity of the diseased myocardium<sup>101-103</sup>. Apart from cTnI modifications, several authors have looked at the expression of ssTnI during cardiac disease. No evidence of ssTnI re-expression was found during end-stage heart failure or decompensated cardiac hypertrophy<sup>93,104,105</sup>, suggesting that re-expression of ssTnI plays no role in cardiac disease. Our group could also not detect ssTnI expression in the atria of patients with chronic atrial fibrillation (CAF). However, in patients with paroxysmal atrial fibrillation (PAF) as well as in patients with mitral valve disease we did find indications of ssTnI re-expression (Chapter 3). The contribution of atrial fibrillation (AF) to the observed re-expression of ssTnI was not fully understood.

AF is characterised by morphological changes that are indicative of cardiomyocyte dedifferentiation<sup>32</sup>. Similar changes are also found in patients with hibernating myocardium and they consist of extensive myolysis, increased glycogen storage, mitochondrial shape changes and redistribution of heterochromatin<sup>32,126</sup>. These morphological changes are accompanied by expression patterns and subcellular organisation of structural and functional proteins, characteristic of foetal cardiomyocytes<sup>33</sup>. In addition, AF results in activation of calpains<sup>112,113</sup> which could result in increased TnI degradation

as previously shown during increased preload or hypoxia<sup>110,111</sup>. The exact effect of AF on TnI isoform expression in the atria is still poorly understood. During AF, TnI isoform expression might be influenced by calcium overload induced degradation or by dedifferentiation related changes in gene expression. To evaluate the role of AF in TnI isoform expression, we examined the composition of TnI isoforms in atrial cardiomyocytes during chronic atrial fibrillation in the goat.

## 2 | Materials and Methods

### 2.1 | Animal tissue

The goat model of AF, first described by Wijffels *et al.*<sup>127</sup>, was used to obtain tissues from right and left atrial appendages from animals in either sinus rhythm (SR) or after 1, 2, 4, 8, or 16 weeks of sustained AF as previously described by Ausma *et al.*<sup>59</sup>, (n=6 in each group). Briefly, under anaesthesia an Irelpacemaker (Medtronic®) was implanted in the neck of the goat and a bipolar screw-in electrode was inserted through the jugular vein in the right atrium. AF was maintained by burst pacing as described previously<sup>59</sup>. Thirty-six goats (61±13 kg) were used and animal handling was carried out according to the Dutch Law on Animal Experimentation (WOD) and The European Directive for Protection of Vertebrate Animals Used for Experimental and Other Scientific Purposes. At the end of the experimental period, the goats were anaesthetised and thoracotomy was performed. Foetuses (Foetal, n=5) at different days of gestation (from 4 weeks prior to end-term up to a few days before birth) were obtained from the abattoir. Of all animals, the right and left atrial appendages were excised and immediately frozen in liquid nitrogen precooled isopentane. From 1 adult animal, additional tissues were taken (skeletal muscle, diaphragm) and immediately frozen in liquid nitrogen precooled isopentane.

### 2.2 | Western blotting and antibodies

The monoclonal antibodies Ti-1, which reacts specifically with rat and bovine cTnI isoform and Ti-54 which reacts with both cTnI and ssTnI were used to detect changes in TnI isoform constitution<sup>98</sup>. Cryostat sections from tissue samples were

homogenised in electrophoresis sample buffer and boiled for 5 minutes. Equal protein amounts of each sample, together with molecular weight standards (Biorad), were run at 100 mA on a 13% gradient polyacrylamide gel, transferred onto a nitrocellulose filter, saturated for 1 hour with ovalbumin in TBST (10 mM Tris-HCl pH 8.0, 150 mM NaCl, 0.05% Tween20) and incubated with the primary antibody (Ti-54, 1:3000; Ti-1, 1:1000) for 1 hour at RT in TBST. After washing 3x10 min in TBST, filters were incubated for 1 hour with peroxidase conjugated secondary antibody (1:5000). Following 3x10 min washing in TBST, the peroxidase activity was determined by the ECL procedure.

### 2.3 | Isolation of goat TnI cDNA

To obtain the goat-specific sequence for cTnI, a goat atrial cDNA library (kindly provided by Dr. H.M.W. van der Velden<sup>128</sup>, Utrecht Medical Centre) was screened according to standard procedures. In short, cloned cDNAs were transferred onto Hybond N<sup>+</sup> filters (Amersham) and hybridised with a fragment of human cTnI cDNA. Positive clones were isolated and sequenced on the ABI PRISM® 310 genetic analyser (PE Applied Biosystems) using the ABI PRISM® Bigdye™ terminator cycle sequencing kit (PE Applied Biosystems). The goat-specific sequence of ssTnI was obtained by rapid amplification of cDNA ends with the 5'RACE-kit (Life Technologies), procedure as described by the manufacturer from 1 µg of RNA isolated from goat diaphragm tissue. Gene specific primer sequences (GSP-1: CCCGCAGATCCATGGACACCTTGTG; GSP-2: CGCTTGAACTTCCCACGGAGGTC) were selected according to optimal sequence homologies between ssTnI of human, rat and mouse. PCR products were cloned into pUC19 and subsequently sequenced on the ABI PRISM® 310 genetic analyser using ABI PRISM® Bigdye™ terminator cycle sequencing kit.

### 2.4 | Quantitative real-time RT-PCR

Total RNA from 30 mg atrial appendage tissue was isolated using the RNeasy mini kit (Qiagen) according to the manufacturer's instructions. To remove genomic DNA contamination, on-column DNase treatment with the RNase-

**Table 1 |**  
Specific primers and probes  
used for quantitative real-  
time RT-PCR

Target	Primers probe	Sequence/modification
goat cTnI	Forward	5' GCCCACCTCAAGCAGGTG 3'
	Reverse	5' TTGCGCCAGTCTCCTACCTC 3' <u>TAMRA</u>
	Probe	5' AGAAGGAGGACACGGAGAAGGAAAACCG 3' <u>DABCYL</u>
goat ssTnI	Forward	5' CATGCCGAAGTCGAGAGAAA 3'
	Reverse	5' CATCAGGCTTTCAGCAGGAG 3' <u>FAM</u>
	Probe	5' CCCAAGATCACTGCCTCCCGCA 3' <u>DABCYL</u>

free DNase set (Qiagen) was performed. Following incubation of the RNA at 65°C for 5 min, reverse transcription was performed for 1.5 hours at 37°C with 600 U of M-MLV reverse transcriptase (GibcoBRL) in 50 µL of 50 mM Tris-HCL, pH 8.3, 75 mM KCl, 3 mM MgCl<sub>2</sub>, 10 mM DTT, and 1mM dNTPs in the presence of 40 U RNase inhibitor RNasin® (Promega) and 0.5 µg oligo(dT) primer (GibcoBRL). Reverse transcriptase activity was inactivated by incubation at 95°C for 5 min and cDNAs were stored at -20°C. Quantitative real-time PCR (described elsewhere<sup>116,117</sup>), was performed using the Real-time PCR Taqman Kit (Eurogentec) with the ABI PRISM 7700® Sequence Detection System apparatus and software (PE Applied Biosystems). Primer Express software (PE Applied Biosystems) was used to design the specific primers and probes, based on the isolated cDNAs of cTnI or ssTnI, and all primers/probes were synthesised by Eurogentec. Primers and probes used for PCR are listed in table 1. Quantitative PCR was performed in a 50 µl volume containing 3 µl cDNA, 1x PCR buffer, 200 µM dATP, dGTP, dCTP, dTTP, and dUTP, 0.025 U/µl Hot Goldstar DNA polymerase, 100 nM probe, and 150 nM of each primer. Cycling conditions were as follows: a Hot Goldstar activation step of 10 min at 95°C, followed by 50 cycles of 15 sec at 95°C and 1 min at 60°C. After each cycle, the fluorescence of the reporter dye was measured and the parameter Ct (threshold cycle) was defined as the cycle number at which the fluorescent signal passed a fixed value (threshold). Thus, the Ct value reflects the point during the reaction at which a sufficient number of

amplicons have accumulated to be at a statistically significant point above the baseline. Data were analysed with the Sequence Detection System software (PE Applied Biosystems). The absolute mRNA amounts were calculated using a standard curve generated by quantitative real-time PCR on a dilution series of both cTnI and ssTnI.

## 2.5 | Statistical analysis

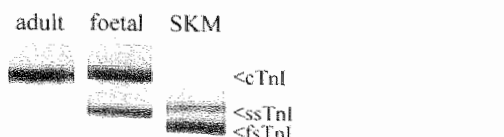
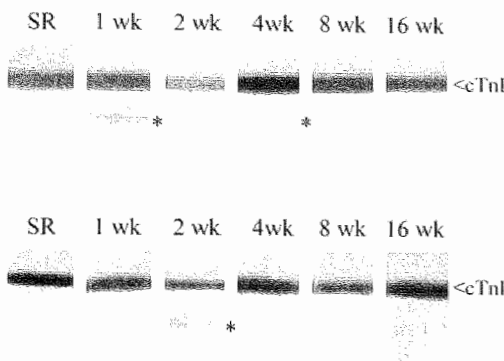
Data are given as mean values  $\pm$  SEM of 3 independent experiments. Significant differences between the groups were analysed by means of the Wilcoxon-Mann-Whitney rank sum test. All p-values are two-sided and p-values  $< 0.05$  were considered statistically significant. Statistical computations were performed in SPSS 10.0.5.

# 3 | Results

## 3.1 | TnI protein expression during chronic atrial fibrillation

To establish whether AF could affect TnI isoform expression we performed Western blotting on atrial tissue from goats in sinus rhythm and after 1, 2, 4, 8, and 16 weeks of AF. As in other species, there are three TnI isoforms expressed in goat muscle tissue<sup>94,98</sup>. In adult heart, only the cardiac TnI isoform could be detected by Western blotting. In foetal heart, both the cardiac and the slow-twitch skeletal isoform were present, and skeletal muscle contained the slow-twitch as well as the fast-twitch skeletal isoforms (Figure 1A). Western blotting with Ti-54 which recognises both cTnI and ssTnI revealed an additional band in only a few atrial samples (Table 2). To distinguish between ssTnI re-expression and cTnI degradation, Western blotting was also performed with an antibody specific for cTnI. Again, an additional band could be observed in the same atrial samples which displayed an additional band with Ti-54 (Figure 1B), indicating degradation of cTnI rather than re-expression of ssTnI.

All the results of the Western blot analysis are summarised in Table 2. Atrial fibrillation resulted in sporadic degradation of cTnI to a level that could be detected by Western blotting. This occasional degradation occurred both in the right and left atria but could only be observed within the first 4 weeks of AF. After

**A****B****Figure 1 |**

Western blot analysis of TnI isoform expression

Typical examples of Western blot analysis.

A) Western blot with Ti-54 on normal goat atrium, foetal goat atrium, and normal goat skeletal muscle (SKM).

B) Western blots with Ti-1 on atrial tissue from goats in sinus rhythm and after 1 week, 2 weeks, 4 weeks, 8 weeks, and 16 weeks of AF. The asterisk indicates the location of a band which was detected with both Ti-54 and Ti-1.

longer duration of AF no more cTnI degradation was detectable. Re-expression of ssTnI did not occur, at least not at a level detectable by Western blotting.

| 55

### 3.2 | Isolation of goat Troponin I cDNAs and primer design

In order to design goat-specific primers for quantitative RT-PCR analysis, cDNAs of the different TnI isoforms were isolated. A partial cDNA encoding 330 nt of the 3-prime end of cTnI (GenBank accession number: AY033589) was picked up from a goat heart cDNA library. Overall homology with human cTnI was approximately 90% at nucleotide level and 97% at the protein level (Figure 2A). ssTnI cDNA was isolated using 5' RACE on mRNA from goat diaphragm tissue. The partial cDNA of ssTnI (GenBank accession number: AY033587) contained 330 nt of the 5' end, and homologies at the nucleotide and the protein level were 88% and 93% respectively (Figure 2B).

Figure 2C shows the primers/probe combinations of cTnI and ssTnI used for real time quantitative RT-PCR which were based on the sequences derived from the partial cDNA's. In humans, the overall homology between the coding regions of cTnI and ssTnI is approximately 60%. Therefore, goat specific primers/probe combinations were confined to regions of poor homology

**Table 2 |**

TnI degradation during AF.

RA = right atrium; LA = left atrium; SR = sinus rhythm.

group	cTnI degradation		ssTnI expression	
	RA	LA	RA	LA
SR	0/6	0/6	0/6	0/6
AF1	1/6	1/6	0/6	0/6
AF2	1/6	1/6	0/6	0/6
AF4	2/6	0/6	0/6	0/6
AF8	0/6	0/6	0/6	0/6
AF16	0/6	0/6	0/6	0/6
FOETAL	0/5	0/5	5/5	5/5

between both sequences to avoid cross-reactivity. Furthermore, both the primers and the probes were designed to meet several requirements concerning G-C content, stretches of identical nucleotides, melting temperature, and the size of the amplicon, directed by the primer design software. The probes for cTnI and ssTnI were labelled with the reporter dyes TAMRA and 6-FAM respectively, in combination with DABCYL as the quencher (Table 1). This allows the use of the probes in a multiplex PCR analysis to analyse both isoforms simultaneously within the same sample. However, in this study both amplifications were performed separately because the detection software did not support the multiplex PCR approach.

### 3.3 | TnI mRNA expression during chronic atrial fibrillation

Real time quantitative RT-PCR was performed to analyse changes in the mRNA expression level of cTnI and ssTnI (Figure 3). A control PCR with cTnI primers on a dilution series of the partial cTnI cDNA from the goat generated an amplicon of the expected size (Figure 3A). Figure 3B shows the amplification plots obtained during real time RT-PCR on the same dilution series in the presence of both the cTnI primers and the cTnI probe. The cycle number at which the fluorescence crossed a fixed threshold value represented the Ct value which was used to generate a standard curve (inset). The standard curve had a linear detection range from 10 pg up to 100 ng. Similar results were obtained for ssTnI (data not shown). In figure 3C and 3D typical examples are shown of the amplification plots generated with cTnI and ssTnI primers on mRNA isolated from atrial tissue of goats in sinus rhythm, after 1, 2, 4, 8, and 16 weeks of atrial

**Figure 2 |**

Isolation of goat Troponin I cDNAs and primer design

A) Protein homology between human (hs, homo sapiens) cTnI and the 110 aa. fragment of goat (ch, *capra hircus*) cTnI.

B) Protein homology between human ssTnI and the 110 aa. fragment of goat ssTnI

C) Specificity of primers and probes used for quantitative RT-PCR. Primer sequences are shown in bold, probe sequences are underlined. The left panel shows the primers/probe for cTnI. The right panel shows the primers/probe for ssTnI. Mismatches with either the homologous ssTnI or cTnI sequence are indicated by X.

cTnI			
human	95	DLCRQLHARVDKVDEERYDIEAKVTKNITEIADLTQKIF	133
goat		HARVDKVDEERYDVEAKVTKNITEIADLNQKIF	
human	134	DLRGKFKRPTLRRVRISADAMMQALLGARAKESLDLRAH	172
goat		DLRGKFKRPTLRRVRISADAMMQALLGARAKETLDLRAH	
human	173	LKQVKKEDTEKENREVGDRKNI DALSGMEGRKKKFES	210
goat		LKQVKKEDTEKENREVGDRKNI DALSGMEGRKKKFEG	

ssTnI			
human	1	MPEVERKPKITASRKLLLKSLMLAKAKECWEQEHEEREA	39
goat		MPEVERKPKITASRKLLLKSLMLAKAKECWDQELEEREA	
human	40	EK VRYLAERIPTLQTRGLSLSALQDLCRELHAKVEVVDE	78
goat		EKKRYLAERVPSLQTRGLSLSALQDLCRDLHAKVEVVDE	
human	79	ERYDIEAKCLHNTREI KDLKLKVMDLRGKFKRPLRRV	116
goat		ERYDIEAKCLHNTREI KDLKLKVMDLRGKFKR	

C	cTnI	ssTnI
Forward	gcccacacctcaaggctg X XXX GCCAACCTCAAGTCTGTG	catggccggaaagtgcagagaaaa XX X XXX X CGAGCCGCACGCCAAGAAAAAA
	AGAAGGAGGACACGGAGAAGGGAAAACCGA X X XXXX XX AGAAGGAAGACACAGAGAAGGGAGCGGCCCT	CCCAAGATCACTGCCTCCCGA X X X X XX X TCTAAGATCCGCCTCGAGAA
Probe		
Reverse	gaggtaggagactggcgcaa X X X X GAGGTGGGTGACTGGAGAA	ctccctgtctgaagagactgtatg X X X XX X TTGCAGCTGAAGACTCTGCTG

| 57

fibrillation, and foetal goats. As expected, the expression of ssTnI was the highest in the foetal goat which results in a leftward shift of the foetal amplification curve. Figure 4 shows diagrams representing the mean Ct values of three independent QRT-PCR experiments on the different experimental groups. There was no significant change in the mRNA levels of cTnI between all groups (Figure 4A). The same was true for ssTnI mRNA levels. Only in the atria of foetal goats a significant drop in  $Ct_{ss}$  could be observed which indicates an increased level of ssTnI mRNA (Figure 4B). To exclude an effect of differences in the quantity or quality of the mRNA on the Ct values between the different

**Figure 3 |**

Real time quantitative RT-PCR analysis for cTnI and ssTnI in goats with AF

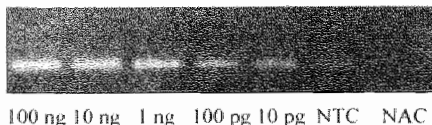
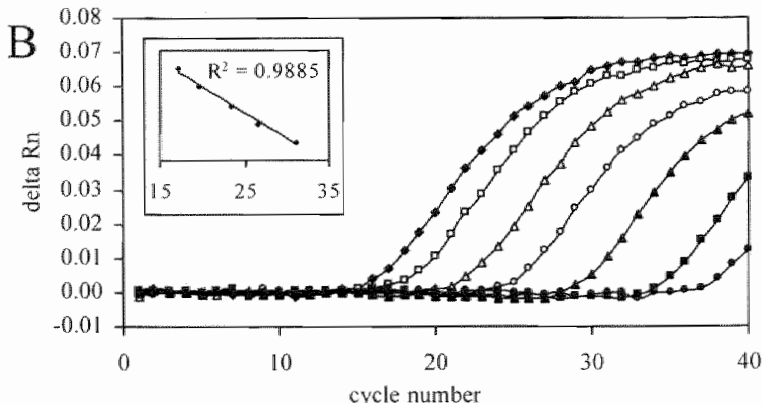
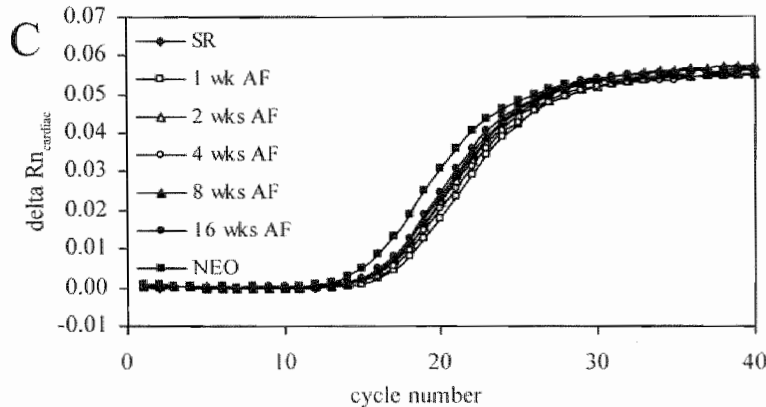
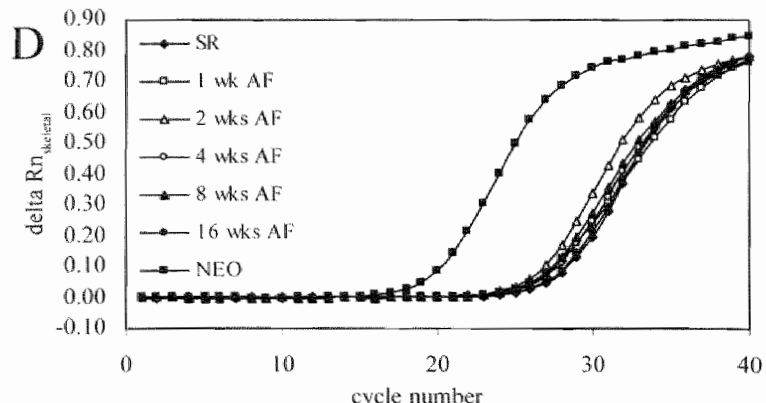
A) Amplicons generated during PCR with cTnI primers on a dilution series of goat cTnI cDNA. PCR products were analysed on a 2% agarose gel, stained with ethidium bromide. NTC = no template control; NAC = no amplification control.

B) Amplification curves generated during QRT-PCR on the same dilution series in the presence of both primers and the cTnI probe.

- ◆ = 100 ng; □ = 10 ng;
- △ = 1 ng; ○ = 100 pg;
- ▲ = 10 pg; ■ = NTC;
- = NAC.

Inset) Standard curve based on Ct values derived from QRT-PCR on cTnI dilution series.

C) cTnI amplification curves generated during QRT-PCR on atria from foetal goat, goat in SR and goats after 1, 2, 4, 8, and 16 weeks of AF. D) Amplification curves generated during QRT-PCR on same samples as in C) but now with primers/probe specific for ssTnI.

**A****B****C****D**

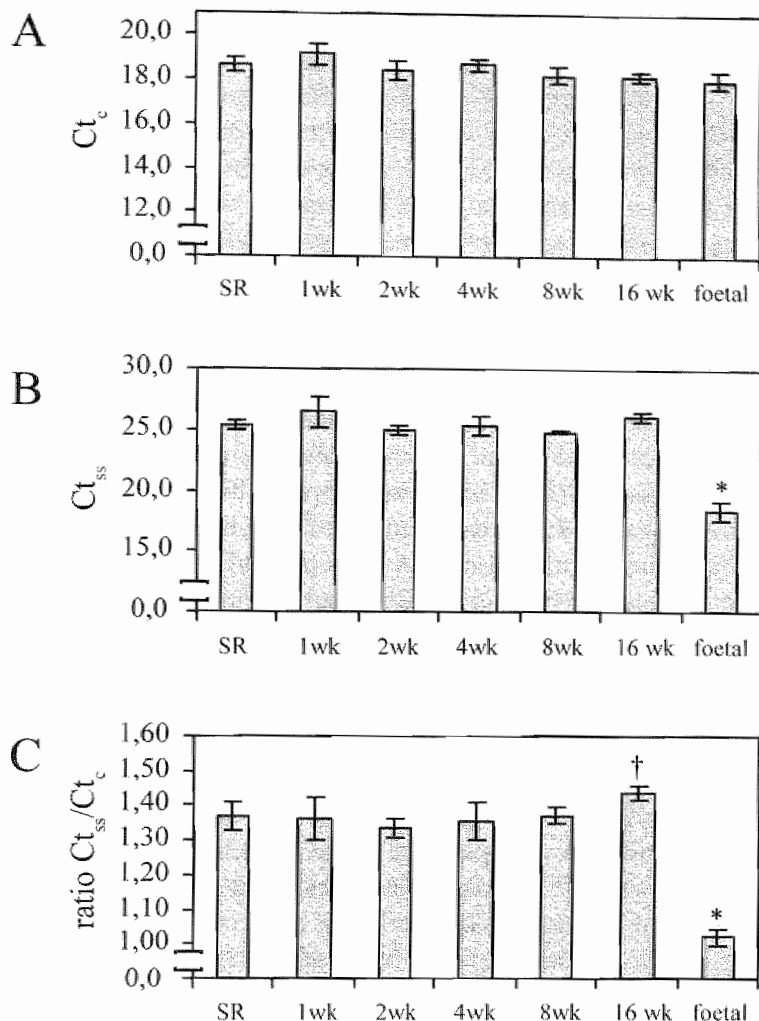


**Figure 4 |**  
Ct-values and Ct ratios of ssTnI and cTnI in goats with AF.

A) Diagram showing the mean Ct values derived from QRT-PCR for cTnI on the different experimental groups.

B) Diagram showing the mean Ct values derived from QRT-PCR for ssTnI on the different experimental groups. C) Diagram showing the mean  $Ct_{ss}/Ct_c$  ratio of the different experimental groups. \*  $p < 0.010$  vs. all other groups, †  $p < 0.050$  vs. 2 weeks AF.

groups, we determined the ratio between  $Ct_{ss}$  and  $Ct_c$  (Figure 4C). As expected, there was a significant decrease of the  $Ct_{ss}/Ct_c$  ratio in foetal goats as compared to all adult groups, due to the increased expression of ssTnI. There was no significant change in the  $Ct_{ss}/Ct_c$  ratio of any of the AF groups as compared to goats with SR. However, there appeared to exist a trend towards lower ratios at the onset of AF and increasing ratios after longer periods of AF. This trend was confirmed by a significant change in  $Ct_{ss}/Ct_c$  ratio after 16 weeks of AF as compared to 2 weeks of AF.

Based on the standard curves, we also calculated the ratio

**Table 3 |**

*Overall results of quantitative RT-PCR*

\*  $p < 0.010$  vs. all other groups, †  $p < 0.050$  vs. AF2

group	Ct <sub>ss</sub>	Ct <sub>c</sub>	ratio Ct <sub>ss</sub> /Ct <sub>c</sub>	absolute amount cTnI:ssTnI
SR	25.35+/- 0.32	18.65+/- 0.35	1.37+/- 0.04	11,277+/- 5,859
AF1	26.44+/- 1.25	19.15+/- 0.49	1.36+/- 0.06	8,302 +/- 2,899
AF2	24.95+/- 0.43	18.42+/- 0.41	1.33+/- 0.02	3,188+/- 601
AF4	25.42+/- 0.78	18.70+/- 0.22	1.36+/- 0.05	8,576+/- 3,516
AF8	24.85+/- 0.19	18.27+/- 0.41	1.37+/- 0.02	6,254+/- 1,968
AF16	26.15+/- 0.45	18.24+/- 0.18	1.44+/- 0.02†	12,125+/- 3,521
Foetal	18.35+/- 0.71*	18.03+/- 0.36	1.02+/- 0.02*	30+/- 10*

between the absolute amounts of cTnI and ssTnI which confirmed the observations that were made using the Ct values (Table 3). In the foetal heart the level of cTnI mRNA was approximately 30 fold higher as compared to ssTnI mRNA. In the adult heart this increased up to 11,000 fold. AF resulted in a drop of the cTnI:ssTnI mRNA ratio to nearly 3,000 fold after two weeks of AF but this gradually increased and after 16 weeks of AF the ratio had normalised. All the results of the quantitative real time RT-PCR analysis are summarised in Table 3.

#### 4 | Discussion

The results of the present study show that during heart development in the goat, the same switch in TnI isoform expression can be found as described for other species. Western blotting revealed that degradation of cTnI occurred in only a few samples during the first 4 weeks of AF (1 out of 6 after one and two weeks of AF and 2 out of 6 after 4 weeks of AF). Although quantitative RT-PCR did not show a significant change in the mRNA expression levels of cTnI and ssTnI there appeared to be a trend towards increasing expression of cTnI after 16 weeks of AF. Neither the limited degradation in the early phase of AF nor the increasing cTnI expression after longer duration of AF appeared to be accompanied by re-expression of ssTnI.

##### 4.1 | TnI isoform expression during cardiac development

Several authors have described the expression pattern of TnI during cardiac development in different species. TnI expression appears to follow a pattern that consists of three phases: expression of ssTnI during early development, co-expression of ssTnI and cTnI during late development, and exclusive

expression of cTnI in adulthood<sup>93,96,99,100</sup>. The same shift from ssTnI to cTnI can be found in the goat. Although we did not look at the early embryonic stages of goat heart development, Western blotting revealed the presence of both ssTnI and cTnI in foetal goat heart up to near end-term, whereas in adult heart only cTnI could be detected. These results support the general concept that TnI isoform expression during cardiac development is similarly regulated in a wide variety of species. The observations at the protein level were confirmed by QRT-PCR. Near end-term foetal heart displayed an almost 1:30 ratio with respect to ssTnI and cTnI mRNA levels. This ratio increased in the adult heart up to approximately 1:11,000, which shows that cTnI is the predominant isoform expressed in the adult heart. Nevertheless, QRT-PCR did reveal that a low level of ssTnI expression remains present in adult atrial myocardium. Previous studies did not find any ssTnI mRNA expression in adult myocardium<sup>93,95</sup>, except for Gorza *et al.* who showed by *in situ* hybridisation that cells of conductive tissues (e.g. AV node) did maintain some level of ssTnI mRNA throughout adulthood<sup>96</sup>. Whether the observed ssTnI mRNA expression actually results in the production of ssTnI protein and whether the protein is utilised in the contractile apparatus is unknown, but appears unlikely in view of the low mRNA expression level.

#### 4.2 | Degradation of cTnI protein during CAF

It has been suggested that AF results in calcium overload affecting both the contractile function and the electrical remodelling of the atrium<sup>56,58,127</sup>. Ausma *et al.*, who found evidence of increased calcium deposits at the sarcolemma and in the mitochondria in the first two weeks of AF, proposed that the increased calcium levels might activate proteolytic pathways thus initiating the structural remodelling of cardiomyocytes during AF<sup>59</sup>. Recent studies show that AF results in increased levels of Calpain I<sup>112,113</sup>, a calcium activated proteolytic protein involved in degradation of cTnI<sup>107,110,111</sup>. The Western blotting results in this study show that only a very limited amount of cTnI degradation can be detected in goat atria during AF, and only within the first 4 weeks of AF. This might be related to the increased calcium levels which are also limited to the first weeks of AF in the goat<sup>59</sup>. After prolonged periods of AF, no cTnI degradation could be detected by Western blotting, which could

indicate normalisation of calcium homeostasis, a decreased activity of Calpain I, or an increased protection against degradation. The absence of cTnI degradation after longer periods of AF is in agreement with our observation that in patients with paroxysmal and chronic AF no cTnI degradation can be detected (Chapter 3). The limited occurrence of cTnI degradation in the goat and the absence of degradation in patients with paroxysmal or chronic AF is suggestive of a protective response of the cardiomyocytes. This protective response might be the result of activation of heat shock proteins<sup>121</sup> or an increase in cTnI phosphorylation which protects cTnI from degradation<sup>109</sup>. We are currently analysing the phosphorylation state of cTnI in patients with CAF to determine whether or not increased cTnI phosphorylation protects cTnI from calpain mediated degradation.

#### 4.3 | Expression of cTnI and ssTnI mRNA during CAF

QRT-PCR is a sensitive and reliable technique to quantify mRNA levels within a population of cells<sup>117</sup>. In this study we quantified the levels of cTnI and ssTnI in the goat atrium during AF to analyse whether AF had any influence on the expression levels of both mRNAs. In late stages of foetal development, the amount of cTnI mRNA in goat atria was approximately 30-fold higher as compared to ssTnI. In adult atrium this number increased to 11,000-fold. AF appeared to have no significant effect on the mRNA concentration of either cTnI or ssTnI. However, when the  $C_{t_{ss}}/C_{t_c}$  ratio's were analysed there was a trend towards decreased cTnI expression in the first weeks of AF and an increase in cTnI expression after longer periods of AF. This trend was confirmed by a significant increase in the  $C_{t_{ss}}/C_{t_c}$  ratio after 16 weeks of AF as compared to 2 weeks AF. Indeed, after two weeks of AF, cTnI mRNA levels were only 3,200-fold higher as compared to ssTnI whereas after 8 and 16 weeks AF this number increased to 6,000-fold and 12,000-fold, respectively. Whether these changes are a response to altered mRNA turnover rate as a result of AF is not known. The increasing expression of cTnI after longer duration of AF could have several causes. First, a decreased stability of cTnI mRNA might be compensated for by increased expression levels of cTnI mRNA. Secondly, the increased expression might reflect cardiomyocyte hypertrophy which has been shown to occur during AF<sup>32,79,88</sup>.

Furthermore, cTnI expression upregulation could be a response to an altered calcium sensitivity of cTnI as a result of increased cTnI phosphorylation<sup>122-124</sup>. Finally, it has been shown that after an initial increase in calcium levels in the first 2 weeks of AF, the intracellular calcium levels decrease after 8 to 16 weeks of AF to levels below those during SR<sup>59</sup>. The increased expression of cTnI might represent the cardiomyocyte's response to counterbalance this effect and to maintain optimal contractile activity. This is supported by the observation of Schotten *et al.* that in patients with chronic AF the reduced contractile force could be completely restored by high calcium levels<sup>129</sup>.

It is unknown whether the shift towards ssTnI at 2 weeks of AF actually results in increased ssTnI protein because Western blotting did not detect any ssTnI expression. ssTnI expression increases calcium sensitivity and renders the myofilaments protected against acidosis<sup>101,102,118</sup>. As such, expression of ssTnI might be beneficial in the acute phase of AF when cellular stress is high. Nevertheless, the amount of cTnI over ssTnI is still in favour of cTnI (1:3,000). For comparison, in patients which displayed a ssTnI band with Western blotting, cTnI was only 800 fold higher as compared to ssTnI (Chapter 3).

| 63

#### 4.4 | Concluding remarks

We set out to analyse the expression of TnI isoforms in a goat model on AF. Induction of AF only occasionally resulted in degradation of cTnI in the first 4 weeks AF (1 out of 6 after 1 and 2 weeks of AF, and 2 out of 6 after 4 weeks of AF). Re-expressing ssTnI, which would coincide with the progressive changes reminiscent of cardiomyocyte dedifferentiation<sup>130</sup>, could not be detected. At the onset of AF, the limited cTnI degradation might be the result of calcium dependent activation of calpains. Following longer episodes of AF, cTnI seemed to be protected against degradation, possibly by heat shock proteins or increased protein phosphorylation.

#### Acknowledgements

The authors would like to thank H. Kuijpers en M-H Lenders for their excellent technical assistance throughout this study, and Dr. H.M.W. van der Velden (Utrecht Medical Centre) for providing them with the goat atrial cDNA library.



# Chapter 5

## ANALYSIS OF ALTERED GENE EXPRESSION DURING SUSTAINED ATRIAL FIBRILLATION IN THE GOAT

V. Thijssen, H. van der Velden, E. van Ankeren, J. Ausma,  
M. Allessie, M. Borgers, G. van Eys, H. Jongsma

Cardiovasc Res 2002; 54: 427-437

| 65

**Objective:** Atrial fibrillation (AF) is characterised by electrical, gap junctional and structural remodelling. However, the underlying molecular mechanisms of these phenomena are largely unknown. To get more insight into atrial remodelling at the molecular level we have analysed changes in gene expression during sustained AF in the goat. **Methods:** The differential display technique (DD) was used to identify genes differentially expressed during sustained AF ( $13.9 \pm 5.2$  weeks) as compared to sinus rhythm (SR). Dot-blot analysis was performed to confirm the altered gene expression and to establish the changes in expression after 1, 2, 4, 8 and 16 weeks of AF. Immunohistochemistry and Western blotting were used to validate the DD approach and to further characterise the changed expression of the  $\beta$ -myosin heavy chain gene at the protein level. **Results:** Of the approximately 125 fragments that showed changed expression levels during AF, 34 were cloned and sequenced. Twenty-one of these represented known genes involved in cardiomyocyte structure, metabolism, expression regulation, or differentiation status. The changed expression of 70% of the isolated clones could be confirmed by dot-blot analysis. In addition, time course analysis revealed different profiles of expression as well as transient re-expression of genes, e.g. the gene for hypoxia-inducible factor 1a during the first week of AF. During sustained AF the frequency of cardiomyocytes expressing  $\beta$  myosin heavy chain (BMHC) increased from  $21.8 \pm 2.1\%$  to  $47.9 \pm 2.5\%$  (SEM). The overall expression of MHC (a+ $\beta$ ) appeared to be down regulated during AF. **Conclusions:** AF is accompanied by changes in expression of proteins involved in cellular structure, metabolism, gene expression regulation and (de-)differentiation. Most alterations in expression confirm or support the hypothesis of cardiomyocyte de-differentiation. Furthermore, the results suggest a role for ischaemic stress in the early response of cardiomyocytes to AF, possibly via activation of hypoxia-inducible factor 1a.

## 1 | Introduction

Atrial fibrillation (AF) is characterised by extensive electrical and structural remodelling of the atrium, both at the level of the single myocyte and the atrial tissue as a whole. Electrophysiological remodelling is characterised by shortening of the atrial effective refractory period (AERP), which (in part) is the result of changes in expression of the L-type  $\text{Ca}^{2+}$  channel. Several authors have reported, both in animal models<sup>131,132</sup> and in patients<sup>133,134</sup>, a downregulated expression of the L-type  $\text{Ca}^{2+}$  channel during AF. In patients with paroxysmal or persistent AF reduced protein levels of L-type  $\text{Ca}^{2+}$  channel were shown to correlate with AERP shortening<sup>135</sup>. Besides the L-type  $\text{Ca}^{2+}$  channel, the expression of several  $\text{K}^+$  channel subunits appears to be downregulated<sup>65,131-133,136,137</sup>.

Since it was shown that time courses of AERP shortening and the increase in the duration of AF episodes did not match, it was concluded that other factors must be important for making the arrhythmia sustained<sup>127</sup>. A candidate is gap junctional remodelling, which was shown to occur both in a goat model of AF and in patients suffering from sustained AF<sup>128,138-141</sup>. Another factor involved in the stabilisation of AF appears to be structural remodelling<sup>142</sup>. Structural remodelling during AF includes a significant reduction in sarcomere number (myolysis), the accumulation of glycogen, changes in mitochondrial morphology, altered chromatin distribution and last but not least changes in cellular size (hypertrophy), phenomena known from hibernating myocardium in patients with chronic ischaemic heart disease<sup>32,40,79,89</sup>. In addition, the expression pattern of several (structural) proteins adapts a foetal phenotype indicative of cardiomyocyte de-differentiation; e.g. re-expression of alpha-smooth muscle actin and the disappearance of cardiotin<sup>33</sup>.

Apart from its effect on the stability of AF, structural remodelling of atrial myocytes is likely to be co-responsible for the temporarily impaired contractile function of the atria after cardioversion from AF<sup>129</sup>. It has been shown that following brief periods of AF, the electrical remodelling and contractile dysfunction are completely reversible within a few days<sup>143</sup>. However, after longer periods of AF, a discrepancy occurs between the normalisation of electrical properties (days to weeks)<sup>144-146</sup> and the recovery of contractile function (weeks to months)<sup>25-27,147</sup>. Structural remodelling might be important in this

context, although the downregulation and/or altered function of L-type  $\text{Ca}^{2+}$  channels seems to be largely responsible<sup>143</sup>.

Many aspects of AF-induced remodelling have been studied extensively in the goat model of AF. In fact, the principles of ‘AF begets AF’ and ‘AF-induced de-differentiation’ originate from studies in which this model was used<sup>148</sup>. However, the exact molecular mechanisms underlying various aspects of atrial remodelling still remain unknown. In order to identify factors involved in the electrical and structural remodelling, we studied alterations in gene expression in the fibrillating goat atrium using the method of differential display<sup>68</sup>.

## 2 | Materials and Methods

### 2.1 | Animal model of atrial fibrillation

For the first part of our studies 12 female goats were used (average weight 55 kg). Of these, 6 were kept in SR while in the others sustained AF was induced as described by Wijffels *et al.*<sup>127</sup>. In brief, silicon strips containing multiple electrodes were stitched to the epicardial surface of both atria as well as to Bachmann’s bundle. After recovery, the electrodes were connected to an external automatic fibrillator programmed to deliver a 1 second-burst of stimuli (50Hz, 4 times threshold) each time an iso-electrical segment longer than 300 ms was detected. Following this protocol AF becomes sustained (episodes >24 hours) in most animals after 1-2 weeks. After at least two months of sustained AF samples of the right (RAA) and left atrial appendages (LAA) were immediately frozen in liquid N<sub>2</sub> and stored at -80°C until use.

For the second part of our studies 36 female goats were used (average weight 61 kg) and instrumented as described by Ausma *et al.*<sup>59</sup>. Six were kept in SR and used as controls. In the other animals an electrode was inserted via the jugular vein in the right atrium and connected to a pacemaker. Sustained (chronic) AF was induced by switching on the pacemaker, producing 2 second bursts (50Hz, 4 times threshold) at 1-second intervals. Initially AF was self-terminating within seconds whereas during the following days AF episodes became longer and more stable. The inter-burst period could gradually be prolonged to 30 min while sustained AF was being maintained. Animals were sacrificed after 1, 2, 4, 8 or 16 weeks of AF (n=6) and RAA and

LAA samples were prepared and stored as described above. All animal handling was according to the Dutch Law on Animal Experimentation (WOD) and The European Directive for Protection of Vertebrate Animals used for Experimental and Other Scientific Purposes.

## 2.2 | Differential display

From pulverised atrial samples, total RNA was isolated using RNeasy (Qiagen). Chromosomal DNA contaminations were removed during incubation with RNase-free DNase (10 U/ $\mu$ l; Boehringer Mannheim) in the presence of an RNase inhibitor (1 U/ $\mu$ l RNA-guard; Pharmacia). Concentrations were adjusted to 0.2  $\mu$ g/ $\mu$ l and aliquots were frozen and stored at -80°C. For reverse transcription 1  $\mu$ l (0.2  $\mu$ g) DNA-free total RNA and 1  $\mu$ l 25  $\mu$ M anchored primer (T12VA (V is 3-fold degenerate for A, C and G), T12VC, T12VG or T12VT; final concentration 2.5  $\mu$ M) in 8  $\mu$ l DEPC treated dH<sub>2</sub>O was heated in a thermal cycler for 5 min at 65°C and quickly cooled down to 37°C. Then 10  $\mu$ l of a mixture of M-MLV Reverse Transcriptase (200 U; GibcoBRL) in 100 mM Tris-HCl, pH 8.3, 150 mM KCl, 6 mM MgCl<sub>2</sub>, 20 mM DTT, 40  $\mu$ M dNTPs and 2U/ $\mu$ l RNA-guard was added and incubations were performed for an additional 1h at 37°C, followed by 5 min at 95°C to heat inactivate the enzyme. Aliquots of 2  $\mu$ l were transferred to thin walled 200  $\mu$ l PCR tubes and used for differential display (DD) analysis. To each aliquot an equal volume of 25  $\mu$ M of the appropriate anchored primer was added followed by a mixture of 1 unit Taq DNA polymerase (recombinant; Gibco-BRL) and 0.5  $\mu$ M of a specific arbitrary 10-mer primer (twenty-six different ones; Operon) in 20 mM Tris-HCl, pH 8.4, 50 mM KCl, 3 mM MgCl<sub>2</sub>, 2  $\mu$ M of each dNTP, 0.02  $\mu$ Ci/ $\mu$ l { $\alpha$ -<sup>32</sup>P}-dCTP (all final concentrations). Incubations were performed in a Perkin Elmer GeneAmp PCR System 2400 thermal cycler (Perkin Elmer Applied Biosystems) according to the following program; 1 min at 94°C was followed by 40 cycles {30 sec 94°C, 90 sec 40°C, 30 sec 72°C} and an extension of 5 min at 72°C. Stop buffer (10 mM ethylenediaminetetraacetic acid, pH 7.5, 97.5% deionised formamide and 0.3% Bromophenol Blue) was added, samples were heated to 80°C for 2 min and 3  $\mu$ l aliquots were electrophoresed on 6% denaturing sequencing gels. Each gel was dried without fixation and exposed to Fuji RX safety film.

Gel strips containing DD PCR fragments were excised, dried and soaked in 100 µl dH<sub>2</sub>O for 10 min at room temperature, followed by incubation for 15 min in a boiling water bath. Eluted DNA in the presence of a glycogen carrier was ethanol precipitated and re-amplified by Taq DNA polymerase (2 units) in 40 µl of 20 mM Tris-HCl, pH 8.4, 50 mM KCl, 3 mM MgCl<sub>2</sub>, containing 2.5 µM each of the appropriate anchored primer and specific 10-mer primer and 20 µM of each dNTP. PCR conditions were as described above. Finally, DNAs were cloned into a T/A cloning vector (pGEM-T Easy, Promega) or pBluescript (Stratagene) and at least three clones of each ligation were sequenced using an ABI PRISM® 310 Genetic Analyzer (Perkin Elmer Applied Biosystems).

### 2.3 | Slot(dot)-blot analysis

For the screening of the DD DNA products a slot-blot procedure was applied as described by Mou *et al.*<sup>149</sup>. Of each plasmid DNA 250 ng was denatured for 10 minutes at 100°C in 0.4 M NaOH, 10 mM EDTA and transferred onto a pre-cut nylon membrane (Zeta-Probe, Biorad). The DNA in each well was washed with 0.4 M NaOH, 10 mM EDTA and immobilised by UV cross-linking. Each membrane was pre-hybridised for 1 hour at 60°C in 0.5M Na<sub>2</sub>HPO<sub>4</sub>, pH7.2, 1mM EDTA, 7% SDS. For probes, 10 µg of pooled (from 5 goats) total RNA and 2.5 µg oligodT primers were incubated at 65°C for 10 minutes. Reverse transcription was performed for 1.5 hour at 37°C with 600 U M-MLV reverse transcriptase (GibcoBRL) in 50 µl 50mM Tris-HCl, pH 8.3, 75 mM KCl, 3 mM MgCl<sub>2</sub>, 10mM DTT, 1 mM of dATP, dGTP and dTTP, in the presence of 40 U RNase inhibitor RNasin (Promega) and 50 µCi {α-<sup>32</sup>P}dCTP. Following purification over Sephadex G50, probes were denatured for 5 minutes at 95°C and added to the pre-hybridisation mix. Following overnight incubation at 60°C, membranes were washed in phosphate buffer/SDS with increasing stringency and exposed to a phosphorimaging screen (Biorad). For image analysis either Image Quant® (Molecular Dynamics) or Quantity One® version 4.2.1. (Biorad) software was used. For analysis of the time series, 500 ng amplified DNA fragments were transferred onto Hybond N<sup>+</sup> membranes (Amersham) following the same procedure.

The expression level of each clone was normalised to that of at

least two out of four different controls; a clone from a goat atrium cDNA library encoding part of the GAPDH housekeeping gene and three cloned DD-DNAs selected on the basis of equal gel display in AF and SR.

#### 2.4 | Immunohistochemistry

Unfixed cryostat sections (8 µm) were stained essentially as described before<sup>150</sup>. They were incubated at room temperature in phosphate-buffered saline (PBS) containing 0.2% (v/v) Triton X-100 for 1 hour, followed by 30 min in 2% (w/v) Bovine Serum Albumin (BSA) in PBS. Sections were washed with PBS and incubated overnight with primary mouse anti- $\alpha$ -MHC (Alexis Biochemicals, clone F88-12.F8) or mouse anti- $\beta$ -MHC (169-ID5; gift from Dr. A.F.M. Moorman, AMC) antibodies (1:5 and 1:10 dilution in PBS containing 10% Normal Goat Serum, respectively). Samples were incubated for 2.5 hours with secondary antibodies against mouse IgG, conjugated with Fluorescein Isothiocyanate (FITC; Jackson Laboratories) or Texas Red (TR; Jackson Laboratories). Sections were mounted with Vectashield (Vector Laboratories) and examined using a Nikon Optiphot-2 light microscope equipped for epifluorescence. Within each section, percentages of myocytes that did (++) or did not (-) stain for  $\beta$ -MHC were assessed.

#### 2.5 | Western blotting

Tissue samples were homogenised in RIPA solubilisation buffer (50 mM Tris-HCl pH 7.4, 150 mM NaCl, 1% Nonidet-P40, 1% sodium deoxycholate, 0.1% sodium dodecylsulfate) with protease inhibitors (2 mM phenylmethylsulfonyl fluoride, 1 mM iodoacetamide, 1 mM phenanthroline, 1 mM benzamidine, 0.5 mM pefabloc, 5 mM sodium bisulfate, 20 µg/ml pepstatin A). They were treated as described<sup>151</sup>. Heparin anti-coagulated blood control samples were immediately mixed with concentrated Laemmli's sample buffer. Of each sample 40 µg of total cellular protein was electrophoresed on 8% SDS-polyacrylamide gels and transferred onto nitrocellulose membranes. Efficiency of transfer was checked by Ponceau Red staining. Membranes were blocked for 1h at room temperature with 5% Protifar in 0.1% Tween 20 in PBS (T-PBS). They were probed for the presence of  $\alpha$  and  $\beta$ -MHC in an overnight incubation at 4°C using the

antibodies (1:40 and 1:10, respectively) described in the previous section. After the primary antibody incubation, membranes were incubated for 1 h at 4°C with a horseradish peroxidase labelled secondary antibody (Bio-Rad; 1:7000). Peroxidase activity was detected using ECL detection reagents (Amersham). Film exposure times were 20 seconds for detection of  $\alpha$ -MHC and 30 minutes for detection of  $\beta$ -MHC expression. Scans (Microtek ScanMaker 630) were analysed using Image Quant software (Molecular Dynamics).

## 2.6 | Statistical analysis

To identify statistically significant changes in expression between AF and SR, a Mann-Whitney rank sum test was used to compare the average normalised values (see methods 2.3) of 5 independent slot(dot)-blot analyses. Beta-MHC expression in AF was compared to SR using a paired Student's t-test or whenever the data did not have a normal distribution a Mann-Whitney rank sum test. Statistical significance was defined as  $P < 0.05$ .

## 3 | Results

### 3.1 | Analysis of differential gene expression between SR and chronic AF

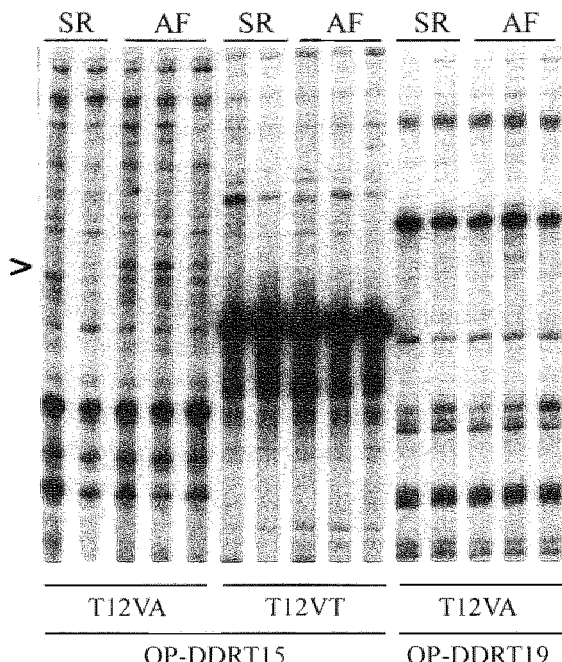
To identify genes involved in AF-induced remodelling of the atrium, we used the DD technique<sup>68</sup> to compare atrial mRNA expression patterns from 6 goats in sustained AF (induced as described by Wijffels *et al.*<sup>127</sup>) with those from 6 goats in SR. For PCR amplification primer combinations of one out of 4 degenerate anchored oligo(dT) primers with one out of 26 short arbitrary 10-mers (OP-DDRT1 through OP-DDRT26)<sup>152</sup> were used. A typical example of expression patterns generated by DD is shown in figure 1.

About 125 bands of amplified gene products, reproducibly displayed differently in AF as compared to SR, were excised from the gels. DNAs from 34 DD fragments, ranging from 90-375 bp (average of 227 bp), were cloned and sequenced. They represented 16 (47%) downregulated and 15 (44%) upregulated genes, while 3 (clone 2.2, 3.3, and 4.1) of them did not show any change in expression and were used as controls. Apart from

## Figure 1 |

Differential display expression patterns.

Typical examples of DD expression patterns obtained by using two different anchored primers in combination with two 10-mer primers. Gel patterns from 2 goats in SR and 3 goats in sustained AF were compared. The arrowhead indicates a DD band, representing a gene whose expression is up regulated in AF.



72 |

these controls, 21 (62%) clones could be identified based on sequence homology to database entries of known eukaryotic genes. Most clones could be placed into one of four functional categories; “structure” (7/21), “metabolism” (4/21), “expression” (7/21) and “embryogenesis/(de-)differentiation” (3/21). Genes in the first category mainly encoded proteins involved in cardiomyocyte contractility, like  $\alpha$ -cardiac actin ( $\alpha$ -CA),  $\beta$ -myosin heavy chain ( $\beta$ -MHC), titin, and cardiac troponin I (cTnI). In addition, a sarcolemma associated protein (SLAP-2) and a nuclear matrix protein (matrin 3) were identified. Genes involved in metabolic pathways included the VLDL receptor (VLDLR) gene, the myoglobin gene and the ubiquitin hydrolyzing enzyme I (UBH1) gene, encoding a deubiquitinating enzyme which prevents ubiquitinated substrates from degradation, like “fat facets” in *Drosophila*<sup>153</sup>. In the category “expression”, several genes were identified encoding ribosomal proteins, together with a transcriptional repressor (of c-myc) and a translational activator of EIF2 $\alpha$  (EIF2 $\alpha$  kinase). The remaining known genes (3/21) encoded proteins (H beta 58, LAK-4p, KIAA1610/ ER1) that have been associated with the

differentiation status of an eukaryotic cell<sup>154,155</sup>. The 10 DD fragments placed in the category “unknown” matched with EST sequences, which means that they represent either unknown genes or known genes whose 3' non-translated sequences are not in the GenBank database.

### 3.2 | Confirmation of altered gene expression

Since one of the criticisms of the DD technique is the relatively high number of false positives, reported to range from 5% to 50%<sup>156</sup>, it is essential to confirm differential gene expression by a hybridisation-based assay such as Northern blotting. In order to screen large numbers of DD-products simultaneously without the need for large amounts of RNA, we used a reverse Northern-like procedure, essentially as described by Mou *et al.*<sup>149</sup>. A total of five independent experiments were performed to determine the ratios of normalised signals between AF and SR. It was assessed whether each ratio was statistically higher or lower than 1, indicating upregulation or downregulation of gene expression (table 1).

The 4 controls showed a maximal deviation of 10% in AF as compared to SR, which suggests that their expression level is stable. The DD data for 20 (65%) of the remaining 31 clones could be confirmed by dot-blot analyses and ratios for 15 of these were statistically significant ( $P < 0.05$ ). The dot-blot data from 10 clones did not corroborate those from the DD analyses and showed either no change (1) or an opposite change (9) in expression. Although statistically significant, overall changes in the levels of expression for most genes were not very large; upregulation ranged from +22% to +107% and downregulation from -7% to -38%.

### 3.3 | Time course of altered gene expression

Changes in AF-induced gene expression levels were studied in a time course series by comparing dot-blot data after 1, 2, 4, 8 and 16 weeks of AF with those in SR. We also investigated a number of genes that were likely to undergo changes in expression during AF, i.e. the genes for  $\alpha$ -smooth muscle actin ( $\alpha$ -SMA), slow skeletal troponin I (ssTnI), and hypoxia-inducible factor 1 $\alpha$  (HIF1 $\alpha$ ). The results are listed in table 2. After 1 week of AF, 5 out of 13 genes investigated showed a

**Table 1.**

Differential Display results.

▲ = up-regulated;  
 ▼ = down-regulated;  
 ♦ = unchanged;  
 \* P < 0.05

21 known						
DD clone	length (bp)	dd blot	ratio AF/SR	mRNA sequence, homology (%)	GenBank acc. no.	
3	180	▼ ▼ *	0.70	mouse cardiac $\alpha$ actin ( $\alpha$ CA), (94%)	NM_009608	
3A	273	▲ ▲	2.07	rat matrin 3 (90%)	M63485	
4A	200	▼ ▼ *	0.88	rabbit sarcolemma associated protein-2 (SLAP-2), (93%)	U21156	
4H	375	▲ ▼ *	0.67	pig cardiac $\beta$ myosin heavy chain ( $\beta$ MHC), (90%)	X91846	
11	200	▼ ▼ *	0.91	bovine beta-actin pseudogene (90%)	U02295	
13	90	▲ ▼ *	0.80	human titin (90%)	NM_003319	
25	125	▼ ▼ *	0.70	rat cardiac troponin I (cTnI), (95%)	NM_017144	
III	282	▼ ▲	1.33	bovine CI-B14 subunit ubiquin. oxred. complex, (91%)	X63211	
4	130	▼ ▼ *	0.62	bovine VI.DL receptor (VLDL.r), (100%)	AF016537	
6H	325	▼ ♦	0.98	bovine myoglobin mRNA, (97%)	D00409	
7II	150	▼ ▼ *	0.93	human ubiquitin hydrolyzing enzym I (UBH1), (94%)	AF022789	
1A	326	▼ ▼ *	0.87	human c-myc transcriptional repressor protein (92%)	D89667	
3H	195	▼ ▼ *	0.92	human ribosomal protein L31 (90%)	X15940	
5II	161	▲ ▼ *	0.75	human ribosomal protein L17 (92%)	X52839	
16	250	▼ ▼ *	0.73	human 17S rRNA (90%)	M13932	
16A	224	▼ ▼ *	0.78	human Csa-19 or ribosomal protein L10a (86%)	U12404	
17	270	▲ ▼ *	0.70	mouse RNA dep. EIF2 $\alpha$ kinase (96%)	M93663	
22	300	▲ ▼ *	0.72	human 28S rRNA (100%)	M11167	
5A	285	▲ ▲	1.44	human H beta 58 homolog	AF054179	
7A	347	▲ ▲ *	2.05	human LAK-4p (84%)	AB002405	
11A	220	▲ ▲	2.00	human KIAA1610, (95%)/ frog ER1, (85%)	XM_040622/ AF015454	
						STRUCTURE
						METABOLISM
						EXPRESSION
						EMBRYO-GENESIS

10 unknown						
2	180	▲ ▼	0.89	unknown	-	
7	320	▼ ♦	1.00	unknown	-	
8	300	▼ ▼ *	0.79	unknown	-	
8A	215	▲ ▲	1.22	unknown	-	
10A	256	▼ ▲	1.78	unknown	-	
12A	175	▲ ▼ *	0.68	unknown	-	
13A	125	▲ ▲ *	1.81	unknown	-	
14	150	▼ ▼ *	0.89	unknown	-	
15A	234	▲ ▲ *	2.05	unknown	-	
18	180	▲ ▼ *	0.69	unknown	-	
4 controls						
G	275	♦ ♦	0.91	bov. glycerald.-phosph. dehydrogenase (GAPDH), (99%)	U85042	
2.2	224	♦ ♦	1.02	goat mitochondrial genome (99%)	X72965	
3.3	198	♦ ♦	0.97	human regulator of G- protein signalling 4 (90%)	NM005613	
4.1	211	♦ ♦	1.10	mouse mapk/erk kin. kinase2 (95%)	AI472964	

UNKNOWN

similar change in expression as observed during sustained AF (average 12.7 weeks). At 4 weeks, this number had increased to 8 out of 13 and at 16 weeks, the expression level of most of the clones (12 out of 13) was similar or comparable to that measured before. Several genes were downregulated throughout the time course (titin, UBH1,  $\alpha$ -SMA, EIF $\alpha$ 2 kinase), whereas others changed progressively ( $\beta$ -MHC, cTnI, ssTnI, VLDLr) or displayed transient alterations (HIF1 $\alpha$ ,  $\alpha$ -CA). In addition, genes that had not changed their overall expression in sustained AF as compared to SR did show changes during the time course. For example, the gene represented by DD-DNA 7 appeared to follow an expression pattern (0-8 weeks) similar to HIF1 $\alpha$ , while the gene represented by DD-DNA 2 showed a transient decreased expression early (1 week) in AF.

### 3.4 | Changes in myosin heavy chain isoform expression

Since the results from the DD and dot-blot analyses with respect to the  $\beta$ -MHC mRNA expression were rather contradictory, we investigated the protein expression of  $\alpha$ -MHC and  $\beta$ -MHC by

**Table 2 |**

Time course analysis of changes in expression during atrial fibrillation.

▲ = up-regulated;  
▼ = down-regulated;

◆ = unchanged;

NA = not applicable;

α-CA = alpha cardiac actin;  
β-MHC = beta myosin heavy chain;

cTnI = cardiac Troponin I;  
ssTnI = slow skeletal Troponin I

α-SMA = alpha-smooth muscle actin;

VLDLr = very low density lipoprotein receptor;

UBH = ubiquitin

hydrolyzing enzyme I;

HIF1α = hypoxia inducible factor 1 alpha;

\* p < 0.05

DD clone	homologue	known					profile
		1 wk	2 wks	4 wks	8 wks	16 wks	
3	α-CA	▲ * +39%	▼ -20%	▼ -25%	▲ +18%	▼ -29%	
3A	matrin 3	▲ +1%	▲ +2%	▼ -17%	▲ +7%	▲ +8%	
4H	β-MHC	▼ -14%	▲ +4%	▼ -15%	▼ -6%	▼ -31%	
13	titin	▼ * -25%	▼ * -18%	▼ * -27%	▼ * -32%	▼ * -20%	
25	cTnI	▼ * -22%	▲ +1%	▼ * -27%	▼ * -12%	▼ * -30%	
NA	ssTnI	▲ -4%	▼ * -19%	▼ * -36%	▼ * -12%	▼ * -30%	
NA	α-SMA	▼ -9%	▼ -9%	▼ * -23%	▼ * -14%	▼ * -15%	
4	VLDLr	▲ -2%	▲ -4%	▼ -22%	▼ -3%	▼ -38%	
6H	myoglobin	▼ -24%	▼ -29%	▲ +28%	▼ -5%	▼ -23%	
7H	UBH	▼ -28%	▼ -19%	▼ -22%	▼ -16%	▼ -28%	
17	EIF2 kinase	▼ * -34%	▼ * -34%	▼ * -37%	▼ * -34%	▼ * -30%	
NA	HIF1α	▲ * +58%	▼ -4%	▼ -18%	▼ +6%	▼ * -36%	
unknown							
2	unknown	▼ * -24%	▲ +6%	▼ -11%	▲ +6%	▼ -11%	
7	unknown	▲ * +22%	▲ +4%	▼ * -23%	▼ * -22%	▼ +1%	
8	unknown	▲ +4%	0%	▲ +3%	▼ -8%	▼ -21%	
18	unknown	▼ * -19%	▼ -11%	▼ -24%	▼ +2%	▼ -31%	

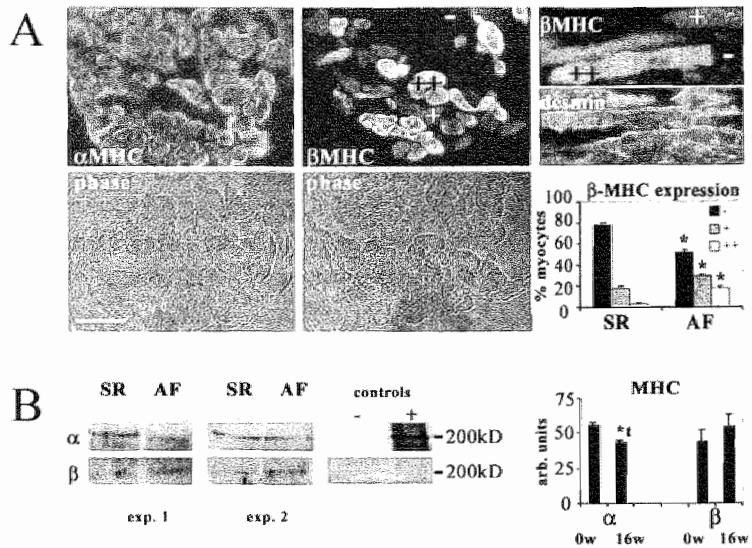
immunohistochemistry and Western blotting.

Fig.2A shows immunolabelling patterns of representative sections of the atrial appendage from a goat in SR incubated with antibodies against  $\alpha$ -MHC or  $\beta$ -MHC. Most cardiomyocytes ( $>90\%$ ) stained positive for  $\alpha$ -MHC while only a sub-population ( $21.8 \pm 2.1\%$  (SEM)) expressed the  $\beta$ -isoform of MHC (+ and ++). Within this sub-population a small fraction of cardiomyocytes ( $3.2 \pm 0.7\%$ ) expressed  $\beta$ -MHC at high levels (++). During sustained AF the percentage of cardiomyocytes expressing  $\alpha$ -MHC seemed unaffected, while the percentage of those expressing  $\beta$ -MHC (+ and++) had clearly increased ( $47.9 \pm 2.5\%$  (SEM)). The percentage of cardiomyocytes expressing  $\beta$ -MHC at high levels (++) had increased even more ( $18.0 \pm 2.5\%$  (SEM)). The observed AF-induced increase in the relative numbers of  $\beta$ -MHC expressing cells is in support of the DD-data. The relative levels of expressed  $\alpha$ - and  $\beta$ -MHC protein were assessed by Western blot analysis (fig. 2B). Contrary to what has been shown for chicken atrium<sup>157</sup>, both antibodies reacted with several bands in the goat atrium extracts. We focused on bands with the same electrophoretic mobility as the 200 kD marker, representing rabbit skeletal muscle myosin. Competitor studies could not be performed since specific peptides were not available. Consequently, we used adult mouse heart and goat blood extracts for controls. Cross-reactivity of the  $\alpha$ -(human)MHC antibody to mouse cardiac myosin in a Western blot was stated by the supplier. Indeed a prominent 200 kD band showed up, as can be seen in the positive (+) control lane. There was no reaction with the goat blood sample (negative (-) control). The  $\beta$ -MHC antibody was (almost) negative with the mouse cardiac extract, which is in accordance with the negligible expression of  $\beta$ -MHC in adult mouse heart<sup>158</sup>. There was no specific reaction with goat blood. However, a non-specific band with a higher molecular weight became visible, possibly as a result of the almost 100 times longer exposure time needed for ECL detection of  $\beta$ -MHC (30 min) as compared to  $\alpha$ -MHC (20 sec). Fig.2B shows the goat atrial myosin expression in two representative experiments. The quantitative analysis of the data from 4 experiments revealed a significantly lower expression of  $\alpha$ -MHC in AF as compared to SR and a tendency of upregulated  $\beta$ -MHC expression (not statistically significant).

## Figure 2 |

Protein expression of  $\alpha$ - and  $\beta$ -MHC in goat atrial myocytes.

A). Immunolabelling of successive transversely cut thin sections of atrial appendage from a goat in AF with antibodies against  $\alpha$ - or  $\beta$ -MHC. Matching phase contrast images are given underneath each panel. Longitudinally sectioned myocytes were double stained with antibodies against  $\beta$ -MHC and desmin. Bar=100 $\mu$ m. The histogram shows the data of an immunohistochemical evaluation of thin sections from 6 goats in SR and 6 goats in sustained AF. Frequencies are given of atrial myocytes that did not stain (-), stained positive (+) for  $\beta$ -MHC or expressed it at very high levels (++). B). Western blot analysis of the  $\alpha$ - and  $\beta$ -MHC protein levels in SR and sustained AF (16 weeks) from two representative experiments. Positions of the 200 kD rabbit skeletal muscle myosin marker are indicated. For controls, adult mouse cardiac (+) and goat blood (-) extracts were used. Band intensities were measured and average data from 4 experiments are given in the bar plot.



## 4 | Discussion

AF is accompanied by electrical<sup>127,159</sup>, gap junctional<sup>128,138</sup> and structural remodelling<sup>32,89</sup> of the atria. In this study we have used the goat model of AF to obtain more insight into the underlying molecular processes. To identify genes involved in atrial remodelling, we have compared their expression profiles in SR with those during AF by means of the differential display (DD) technique. DD was used because at present no goat-specific micro-arrays are available. In addition, DD allows the direct identification of both upregulated and downregulated genes between multiple samples within one experiment<sup>68</sup>. We have isolated a number of genes that were either upregulated or downregulated during sustained (chronic) AF. For approximately 60% of these genes differential expression could be confirmed by dot-blot analysis. Less than 10% of the DD-signals turned out to be false positive, which is within the margins reported for the technique. In those situations, in which the dot-blot data did not corroborate the DD results, heterogeneity between tissue samples is the likely cause. Since relatively large tissue samples from 5 goats had to be pooled for the preparation of probes, relative numbers of remodelled cardiomyocytes in these mixed samples might be significantly different from those in the much smaller individual goat samples used for DD analysis. This might account for relatively mild overall changes in gene expression.

However, locally these (focal) changes might be very pronounced and promote arrhythmogenic activity that could affect the atrial tissue as a whole.

Characteristic of AF-induced structural remodelling of cardiomyocytes is that several structural proteins adopt a foetal-like expression<sup>33</sup>. The expression of several genes that were detected in our DD analyses and placed in the category “structure” appears to be in line with this phenomenon. The observed downregulation of the mRNA expression of titin is in agreement with observations at the protein level<sup>33</sup>. Downregulation of cTnI and  $\alpha$ -CA mRNA also correlates with the observed reduction in sarcomeres. It has been suggested that the 3' non-translated regions of both genes are involved in inhibition of proliferation and promotion of differentiation<sup>160</sup>, which suggests that downregulation of their expression might favour cellular de-differentiation. Yet, re-expression of the embryonically expressed ssTnI and  $\alpha$ -SMA<sup>94,100,161,162</sup> could not be detected. The absence of an increase in  $\alpha$ -SMA mRNA is in contrast with the observed increase in  $\alpha$ -SMA protein in the cardiomyocytes during AF<sup>33</sup>. However, since cTnI and  $\alpha$ -CA are abundantly expressed and highly homologous to their embryonically expressed counterparts, the inconsistency is likely due to cross-reactivity of their mRNAs with the ssTnI and  $\alpha$ -SMA DNA on the filter, which would obscure any AF-induced effect in mRNA expression of the latter two. In addition, it has been reported that the expression of  $\alpha$ -SMA is predominantly regulated at a post-transcriptional level<sup>163</sup>.

Cross-reactivity of  $\alpha$ -MHC mRNA with  $\beta$ -MHC DNA (homology in humans 95%<sup>164</sup>) on the filters is possibly also responsible for the observed inconsistency between DD and dot-blot data. The relative proportions of the 2 isoforms of myosin heavy chain in mammalian heart are affected by a wide variety of pathological and physiological stimuli<sup>165</sup>. Cardiomyocytes that predominantly express the faster (higher ATPase activity)  $\alpha$ -MHC can generate more force than those expressing the slower  $\beta$ -isoform<sup>166</sup>. Human ventricular myocardium contains 93%  $\beta$ -MHC and 7%  $\alpha$ -MHC, whereas  $\alpha$ -MHC mRNA makes up 30% of total MHC mRNA<sup>167</sup>. During heart failure  $\alpha$ -MHC decreases to a level 15-fold less for mRNA, while protein could hardly be detected anymore. Adult bovine atrium consists of 80-90%  $\alpha$ -MHC and 10-20%  $\beta$ -MHC<sup>168</sup>. Also in adult human left atria  $\alpha$ -MHC comprises about 90% of total MHC, whereas

this relative amount dropped to around 50% in individuals with dilated or ischaemic cardiomyopathy<sup>169</sup>. Concomitant changes at the mRNA level are not known. An increase in the relative amount of  $\beta$ -MHC of the left atrium during the development of heart failure has been suggested to be beneficial by increasing the economy of contraction<sup>170</sup>. Consequently, an AF-induced increase in  $\beta$ -MHC expression in combination with a reduction in  $\alpha$ -MHC expression would be in support of an observed reduction in atrial contractility. Since a downregulation of MHC expression could already be detected early (1 week) in the time course, it might be partly responsible for the developing atrial dysfunction.

Apart from structural remodelling, AF is accompanied by electrical and gap junctional remodelling and many authors including ourselves have described changes in the expression or distribution of channel proteins that might underlie these processes<sup>131,132,135,142</sup>. In the present study no changes in the levels of mRNAs that encode ion or gap junction channel proteins were identified. This might be due to the fact that these mRNAs are relatively low abundant or that their 3' non-translated sequences are not in the database.

We did find changes in expression of several genes involved in cellular metabolic pathways. Altered expression of proteins like myoglobin and the VLDLR are indicative of changes in energy utilisation. Downregulation of the VLDLR has been shown to occur in hypertrophied rat hearts<sup>171</sup>. A shift in the metabolic balance as a result of AF had already been suggested by Ausma *et al.*<sup>130</sup>. They concluded that a temporary metabolic imbalance was not the result of ischaemic injury<sup>130</sup>. However, the transient increase in the expression of HIF1 $\alpha$  as was observed in the present study, indicates that a certain amount of ischaemic stress during the onset of AF cannot be ruled out. It has been reported that HIF1 $\alpha$  upregulates the glucose transporter 1 and several glycolytic enzymes<sup>172,173</sup>. This, in combination with the observed downregulation of the VLDLR, is indicative of a switch from fatty acid metabolism to glucose metabolism, subsequently leading to increased glycogen storage, either due to excessive influx of glucose or to a decreasing energy demand as a result of impaired contractile activity.

Apart from known genes, we isolated a number of DD fragments without homology to any of the genes that are currently present in the GenBank database. Some of these might represent genes

whose products play an important role in early response mechanisms, for they show an expression pattern similar to that of HIF1 $\alpha$  (clones 2 and 7, downregulated and upregulated in the first week of AF, respectively). We are currently trying to isolate and characterise full-length cDNAs of these unknown mRNA species.

In conclusion, we have used DD in our search for changes in gene expression due to AF in the goat. That this approach is feasible was proven by the identification of genes whose protein products are known to be involved in AF-induced structural remodelling. In addition, we found genes that might play an important role in this process, genes potentially involved in "AF induced de-differentiation", as well as genes whose expression is in favour of a short period of ischaemic stress during the onset of AF.

### Acknowledgements

The authors like to thank Dr. A.F.M. Moorman (Academic Medical Centre, Amsterdam) for providing them with the monoclonal antibody (169-ID5) against  $\beta$ -MHC, and M. van Zijverden and A.J.C.G.M. Hellemons for their technical assistance. Part of this study was supported by grants from the Dutch Heart Foundation (NHS M93.002 to H.M.W.v.d.V.; NHS 96.155 to J.A.) and the Dutch organisation for Scientific Research (NWO 900-516-318; M.A.A.).



# Chapter 6

## | Discussion |

adapted from  
STRUCTURAL REMODELLING DURING  
CHRONIC ATRIAL FIBRILLATION  
'ACT OF PROGRAMMED CELL SURVIVAL'

V. Thijssen, J. Ausma, M. Borgers

Cardiovasc Res 2001; 52: 14-20

| 83

- 1 | Background
- 2 | Structural remodelling during AF
- 3 | Molecular remodelling during AF
  - 3.1 | Channel proteins
  - 3.2 | Gap junctional proteins
  - 3.3 | Metabolic proteins
  - 3.4 | Contractile and structural proteins
- 4 | Mechanisms of remodelling
  - 4.1 | Calcium overload
  - 4.2 | Cardiac adaptation
- 5 | Future perspectives
  - 5.1 | Molecular remodelling during AF
  - 5.2 | Molecular remodelling during cardiac disease
  - 5.3 | Reversibility of molecular remodelling
- 6 | Conclusions

## 1 | Background

Atrial fibrillation (AF) is the most common arrhythmia observed in the western civilisation, with an overall prevalence of almost 1 percent. Based on 4 major population studies, Feinberg *et al.* calculated that the prevalence of AF ascends with increasing age, ranging from less than 1 percent in young adults to 2.3 percent in people over 40 years and over 5 percent in those older than 65 years<sup>2</sup>. In addition, the prevalence of AF is strongly influenced by the presence of underlying diseases like hypertension, valve disease, myocardial infarction, and ischaemic heart disease<sup>4,174</sup>. The growing prevalence together with the increased risk of stroke<sup>5</sup> and mortality<sup>7</sup> will increase the burden on the medical health care at the beginning of this new century. The development of safe and more effective medical treatments requires a better understanding of the pathophysiological aspects underlying AF.

## 2 | Structural remodelling during AF

84 |

In animal models it has been shown that AF changes the electrophysiological properties of the atrium which facilitates the maintenance of AF<sup>127</sup>. During the first days of pacing-induced AF, the atrial effective refractory period is markedly shortened (electrical remodelling)<sup>23,127,147,175,176</sup> and within the same period, the atrial contractility measured during slow rate pacing, is completely abolished<sup>143</sup>. After short periods of AF, both phenomena are completely reversible and normal values are reached within 2-3 days<sup>127,143</sup>. After longer periods of AF (weeks to months), the atrial effective refractory period still normalises within a few days<sup>127,144,177</sup> and atrial conduction recovers within a few weeks<sup>145,146,178</sup>. However, recovery from contractile dysfunction may take several weeks to months<sup>25-27,147</sup>. Thus, besides an early time window of atrial remodelling, which involves rapid and reversible electrical and contractile remodelling, a second time window exists during AF. This second time window is characterised by a considerably slower functional recovery following cardioversion. This discrepancy suggests the involvement of a second factor that plays a role in stabilisation of AF<sup>179</sup>. Recent studies support the existence of a slower second factor that is involved in the increasing stability of AF<sup>180,181</sup>.

In chapter 2 the structural changes in patients with cardiac valve disease and AF are described. Light microscopy revealed that besides some degree of cardiomyocyte degeneration, the cellular changes in these patients mainly consisted of cardiomyocyte hypertrophy, depletion of sarcomeres and accumulation of glycogen. Remarkably, the localisation of glycogen differed between two groups of patients and was either found throughout the cytoplasm or confined to large vacuoles<sup>88</sup>. The difference in localisation as well as the presence of vacuoles appeared to be the result of the different underlying diseases<sup>88</sup>. Atrial vacuolisation has also been observed in patients undergoing coronary artery bypass grafting. Ninety percent of the patients which displayed large perinuclear vacuoles in most of the atrial cells, developed postoperative AF whereas AF occurred in only five percent of the patients with no or mild vacuolisation<sup>87</sup>. Many studies in which atrial structural remodelling is related to AF report similar observations. Both in patients and in animal models with AF, common characteristics are atrial dilatation, cardiomyocyte volume increase, myolysis, accumulation of glycogen and increased extracellular space<sup>29,31,32,77,88,129</sup>.

In addition to the light microscopic observations, Chapter 2 describes the structural changes revealed by electron microscopy. Several alterations of a non-degenerative nature were observed in atrial samples of patients suffering from cardiac valve disease, with or without AF. Characteristic observations were: i) The presence of a large number of small, abnormally shaped mitochondria, embedded in a matrix of glycogen granules. ii) The depletion of smooth sarcoplasmic reticulum. iii) The frequent occurrence of strands of rough endoplasmic reticulum. iv) Nuclei with dispersed heterochromatin. With respect to degenerative changes, cytosolic blebs filled with membrane-bound vesicles and amorphous bodies of unknown but most probably autophagic origin were observed, and in some samples, features were visible that might indicate the presence of apoptosis. The latter cells were, in contrast to the above mentioned myolytic cells, not hypertrophied and showed no loss of sarcomeres. In fact, a distinction could be made between adaptive and maladaptive (degeneration) changes<sup>88</sup>.

These observations with light and electron microscopy indicate that in patients, part of the cardiomyocytes dedifferentiate to a survival state in order to endure the altered environmental conditions during AF. In experimental models of AF,

cardiomyocytes mainly adapt to a survival phenotype<sup>35,36,130</sup> whereas in patients with AF both cellular degeneration and cellular adaptation occur<sup>29-31,34,147,175</sup>. This difference might be due to species variance but is probably related to differences in duration of AF and underlying cardiac pathology.

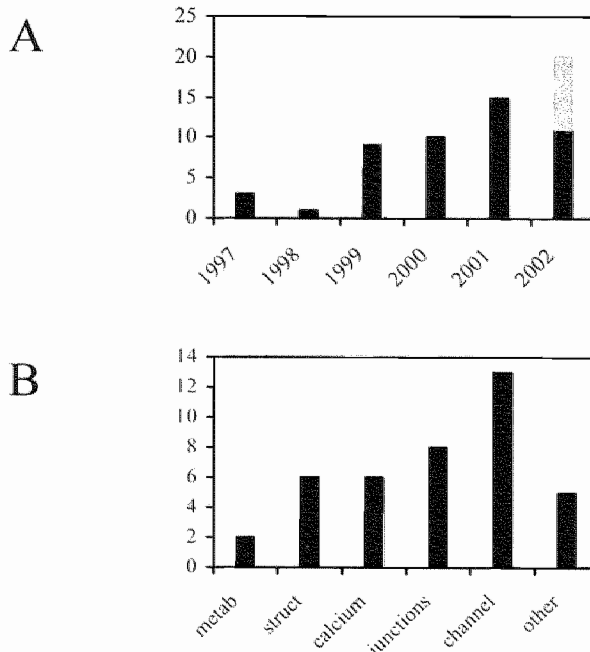
### 3 | Molecular remodelling during AF

The histological studies show that cardiomyocytes undergo marked adaptive remodelling during AF. The altered morphology as well as the diminished functionality are a reflection of transitions that take place at the molecular level. The cardiomyocytes have to cope with abnormal conditions and consequently they change the expression and organisation pattern of proteins involved in atrial activation, conduction, and contraction. Over the last 5 years, the interest in the role of molecular remodelling in electrical and structural remodelling during AF increased, which resulted in a growing number of publications (Figure 1A). However, most studies have focussed on finding a molecular correlate for the observed electrical, structural, and contractile alterations during AF, i.e. expression of channel, gap junctional, and structural proteins (Figure 1B).

**Figure 1 |**

Publications on molecular remodelling during AF over the last 5 years.

- A) The number of publications on molecular remodelling during AF in the last 5 years (1997-2001). In the first eight months of 2002, 11 papers on molecular remodelling were published and a estimate of the final score for 2002 is represented by the grey bar.
- B) The distribution of the publications over five main topics: metabolism, structure, calcium homeostasis, gap junctions, and channel proteins.



In the following paragraphs the contribution of this thesis to the current knowledge on molecular remodelling during AF will be discussed.

### 3.1 | Channel proteins

The most apparent outcome of molecular adaptations is probably the electrical remodelling because it occurs immediately at the onset of AF. Ions like calcium, sodium, and potassium are important players in the excitation/contraction cycle, and the expression patterns of their channels and other proteins involved in ion homeostasis have been extensively studied. Several authors have found altered mRNA and/or protein levels of ion channels during AF<sup>65,133-137</sup>. Downregulation has been described for the L-type calcium channel<sup>115,133,134,182</sup>, the sarcoplasmic reticulum calcium ATPase<sup>115,133,134</sup>, and several potassium channel subunits<sup>65,115,133,135-137,183</sup>. The decreased level of L-type calcium channel expression was correlated with the shortening of the atrial effective refractory period<sup>135</sup>. Previously, it had been shown in patients and animals with AF that the reduced density of potassium currents, were influenced by alterations at the expression level of potassium channel subunits<sup>24,65,66,131,183</sup>.

These data show that the cardiomyocytes regulate channel expression, alter channel properties, and co-ordinate channel interactions, which all contribute to the electrical remodelling during AF. Surprisingly, a survey of the overall changes in gene expression during AF in goats (Chapter 5) did not identify any genes representing channel proteins. This is in contrast with the observation that AF in the goat decreased the expression of calcium and potassium channel subunits<sup>132</sup>. This discrepancy can be explained by the fact that only 34 out of the 125 DNA fragments that were identified as being differentially expressed were characterised. Probably, several genes encoding channel proteins are present among the remaining 91 DNA fragments. In addition, the technique used to detect the changes in gene expression (differential display) is prone to pick up the 3' untranslated regions of mRNAs. Apart from the high variability amongst these regions between different species, the non-coding sequences are not always submitted to the databanks. This could hamper the proper identification of the clones and some of the unknown sequences that were picked up might actually represent channel proteins.

### 3.2 | Gap junctional proteins

Similar to the channel proteins, the analysis of altered gene expression did not pick up any changes in expression of gap junctional proteins (connexins) during AF. Changes in connexin distribution and expression have been described in literature. Persistent AF was shown to affect connexin40 distribution in the goat model on AF<sup>128</sup>. A time course experiment in this model revealed that from two weeks onward, the heterogeneity in connexin40 distribution increased leading to a reduction in the levels of connexin40. The localisation of connexin43 remained unaltered but the changes in connexin40 distribution correlated with AF stability<sup>142</sup>. In contrast, rapid atrial pacing-induced AF in dogs resulted in increased expression of connexin43<sup>184</sup>. Unfortunately, in the latter study the connexin40 levels were not addressed. Patients with persistent AF also displayed a heterogeneous distribution of connexin40 and, to a lesser extent, of connexin43<sup>139</sup>. A recent clinical study indicated that the heterogeneous distribution of connexin40, as observed in goats during AF, is a common feature in humans, irrespective of the presence of AF. Furthermore it was shown that patients susceptible to postoperative AF had elevated levels of connexin40<sup>141</sup>. However, AF patients with complex atrial activation (chronic AF) had lower levels of connexin40 compared to patients with induced AF (no history of AF)<sup>140</sup>. All in all, there appear to exist some discrepancies concerning the gap junctional remodelling during AF. This might be due to species differences, variations in experimental set up in the case of animal models or differences in underlying heart disease whenever patients were involved.

### 3.3 | Metabolic proteins

The effect of AF on the expression of proteins that are involved in the cardiomyocyte metabolism has not been well studied. In pigs with AF, the creatine phosphate content in atrial tissue declined slightly, ATP and lactate remained unchanged<sup>44</sup>. In sheep, two hours of AF resulted in activation of the proton-translocating ATPase, while the activity of cytochrome c oxidase remained unchanged<sup>185</sup>. The proton-translocating ATPase activity was not altered in goats with AF<sup>130</sup>. The discrepancy between sheep and goats in activation of proton-translocating

ATPase is most likely related to the duration of AF (hours and weeks, respectively). In the goat model of AF, no changes in the concentration of adenine nucleotides and their degradation products could be detected. The activity of mitochondrial cytochrome c oxidase and mitochondrial NADH-oxidase was also unaltered<sup>130</sup>. Only a decrease in the tissue content of phosphocreatine occurred during the first 8 weeks of AF, which is indicative of an increased energy demand<sup>130</sup>.

Circumstantial evidence does indicate that the metabolism of cardiomyocytes is altered in response to AF (Chapter 5)<sup>186</sup>. First, during cardiac development the glucose metabolism is a major energy source for the cardiomyocyte. Adult cardiomyocytes rely on the fatty acid metabolism for energy production<sup>187-191</sup>. The observation that one of the features of structural remodelling, i.e. increased glycogen storage, is also found in foetal cardiomyocytes suggests that cardiomyocytes switch to the glucose metabolism during AF. Fujii *et al.* recently described an increased uptake of fluoro-2-deoxy-D-glucose in the right atrial wall of patients suffering from cardiac disease, and mainly AF, which is suggestive of an increased glucose metabolism<sup>186</sup>. Second, the altered expression of the very low density lipoprotein receptor (VLDLr) also suggests a switch from fatty acid to glucose metabolism (Chapter 5). Expression of the VLDLr has been found in the heart, where it is presumed to supply the cardiomyocytes with triglycerides for the fatty acid metabolism<sup>192-194</sup>. During AF, the expression of the VLDLr was downregulated by approximately 40%. Finally, in the first week of AF, the hypoxia inducible factor 1α (HIF1α) is upregulated by approximately 60% (Chapter 5) which indicates a reduced oxygen tension<sup>195</sup>. The transcription factor HIF1α has been shown to upregulate expression of the glucose transporter 1 and enzymes involved in the glycolytic pathway, e.g. aldolase A, phosphoglycerate kinase 1, and pyruvate kinase M<sup>172,173</sup>.

Altogether, a possible oxygen deficit at the onset of AF might induce a switch from the fatty acid metabolism to the glucose metabolism. When the oxygen supply is limited, the glucose metabolism is a more economic way to generate energy because it requires less oxygen. In addition, the increase in glucose uptake and glycolytic activity could explain the observed accumulation of glycogen in the cardiomyocytes as a result of AF. This corroborates with the important role of glycolysis in the maintenance of intracellular calcium homeostasis during severe overload<sup>196</sup>.

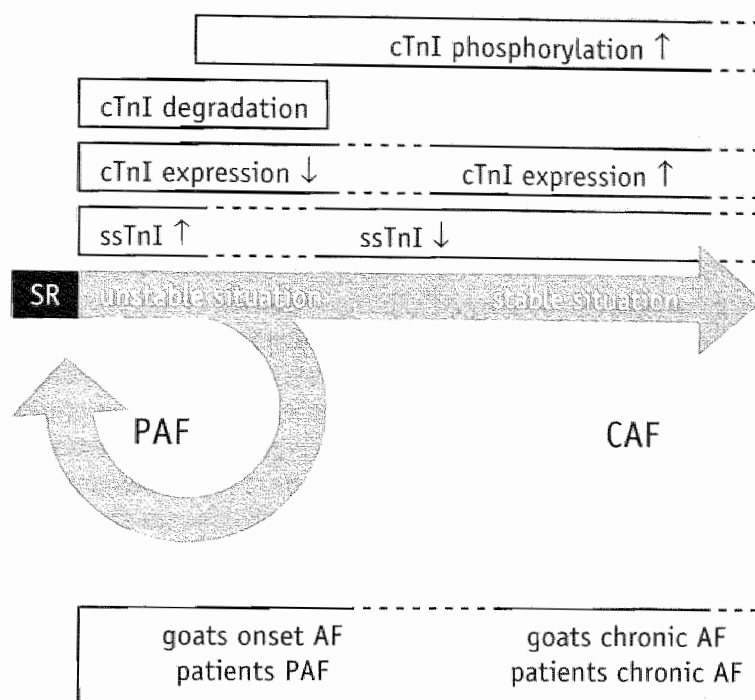
### 3.4 | Contractile and structural proteins

The expression of contractile and structural proteins has been extensively studied in the goat model on AF. Immunohistochemical staining was used to assess the effect of AF on protein levels and organisation, and to establish the degree of cardiomyocyte remodelling. During AF, myolytic cardiomyocytes reduced the concentration of several of their structural proteins like myosin, tropomyosin, actin and alpha-actinin<sup>33</sup>. Only at the periphery of the cells, where the remaining sarcomeres resided, normal cross-striation patterns of these proteins could be observed<sup>33</sup>. In the myolytic areas the distribution of desmin appeared disorganised and other proteins adapted a foetal expression pattern, i.e. titin and cardiotin<sup>33</sup>. In line with the previously described observations, the remodelling of structural proteins became apparent after 1-2 weeks of AF and progressively increased<sup>37,90</sup>. The changes occurred without signs of apoptosis<sup>35</sup> and re-expression of alpha-smooth muscle actin supported the hypothesis of cardiomyocyte adaptation through dedifferentiation<sup>33,37,88</sup>.

90 |

The alterations in TnI isoform expression during AF in humans and goats are described in chapter 3 and 4, respectively. The expression of Troponin I (TnI) isoforms in cardiomyocytes is related to the degree of differentiation during embryonic development<sup>93-95,97-100</sup>. In the heart the slow-skeletal TnI (ssTnI) isoform is normally only expressed during foetal or neonatal stages and re-expression of ssTnI in adult hearts could be an indication of cardiomyocyte dedifferentiation. In addition, the expression of the different isoforms in cardiomyocytes influences the calcium sensitivity and renders the myofilaments protected against acidosis<sup>101,102,118</sup> which could underlie the altered contractile properties of the atrium during AF. In patients with cardiac disease with or without AF, the expression of slow-twitch skeletal TnI (ssTnI) protein could be detected (Chapter 3). Only the atrial cardiomyocytes of patients with chronic AF did not show expression of ssTnI. Instead, the expression of the adult cardiac isoform (cTnI) was increased, which is in disagreement with cardiomyocyte dedifferentiation. In goats with AF there was a trend towards increased ssTnI mRNA expression after 2 weeks of AF although no ssTnI protein could be detected (Chapter 4). Degradation of cTnI which was only sporadically observed in the first 4 weeks of AF was absent

**Figure 2 |**  
Hypothetical expression regulation of TnI during AF.



The early stage of AF is characterised by an unstable situation, caused by calcium overload and acidosis which might result in degradation of cTnI, re-expression of ssTnI and downregulation of cTnI expression. To protect cTnI from degradation the protein is phosphorylated and its expression is upregulated. Following the early unstable period, the situation stabilises, and ssTnI expression is downregulated. In the *in vivo* situation, the unstable condition is represented by patients with PAF and goats at the onset of AF (cTnI degradation, ssTnI expression) whereas patients and goats with CAF represent the stable situation (no ssTnI expression, increased cTnI expression).

after longer periods of AF. Similar to the observations in patients, the expression of cTnI appeared to increase after prolonged duration of AF.

The functional implications of the changes in TnI isoform expression are not fully understood. Figure 2 shows a hypothetical mechanism of TnI expression regulation that could explain the observations in humans as well as in goats.

Early during AF, some degradation of cTnI might occur, possibly as a result of activation of the proteolytic enzyme Calpain<sup>113</sup> which has been shown to degrade cTnI<sup>107,110,111</sup>. Re-expression of ssTnI which protects the cardiomyocyte from acidic stress<sup>118</sup> and improves the calcium sensitivity<sup>101,102</sup> is a response to the unstable early phase characterised by acidic stress, and ischaemia. Following longer episodes of AF, the calcium homeostasis normalises, ssTnI expression decreases and protection against cTnI degradation is achieved by protein phosphorylation<sup>109</sup>. However, phosphorylation decreases the calcium sensitivity of cTnI<sup>122-124</sup> which could be compensated for by upregulation of cTnI expression. In patients with paroxysmal AF, the repetitive nature of AF episodes might

compromise the stabilisation which results in continuous activation of ssTnI expression. During chronic AF, normalisation may occur and the expression of ssTnI returns to normal levels. In addition, the expression of cTnI is upregulated, either as a response to compensate for the decreased calcium sensitivity of phosphorylated cTnI or because of an increased protein/mRNA turnover. Thus, rather than cardiomyocyte dedifferentiation, the expression of TnI isoforms appears to be involved in protection of the contractile apparatus against the cellular stress induced by AF. The mechanisms of this protective response, i.e. cTnI degradation, cTnI phosphorylation, and ssTnI expression are likely to contribute to the contractile dysfunction. An additional contributor to contractile dysfunction might be the altered expression of myosin heavy chain (MHC) isoforms (Chapter 5). Cardiomyocytes that express  $\alpha$ -MHC can generate more force than those expressing  $\beta$ -MHC due to the lower ATPase activity of the latter isoform<sup>166</sup>. Immunohistochemistry on atrial cardiomyocytes indicated that during SR more than 90% of the cells expressed  $\alpha$ -MHC. Beta-MHC was present in almost 22% of the cells, and 3% of this population expressed  $\beta$ -MHC at high levels. During sustained AF the percentage of cardiomyocytes expressing  $\beta$ -MHC increased up to almost 50%. The percentage of cardiomyocytes expressing  $\beta$ -MHC at high levels increased up to 18%. Although the percentage of cells expressing  $\alpha$ -MHC seemed unaffected, Western blotting revealed a significant decrease in the expression level of this isoform. This observed increase in  $\beta$ -MHC expression during AF in combination with a reduction in  $\alpha$ -MHC expression might explain the observed reduction in atrial contractility. Because the downregulation of MHC expression could already be detected after 1 week of AF, it might be partly responsible for the developing atrial dysfunction. The exact involvement of changes in expression of TnI, MHC, or other structural proteins in the altered contractile function of the atrium during AF still needs to be established.

## 4 | Mechanisms of remodelling

### 4.1 | Calcium overload

One of the main actors in the complex regulation of electrical and morphological remodelling appears to be calcium, a

common messenger in signalling pathways<sup>197</sup>. It has been shown that the calcium antagonist verapamil is able to reduce the electrical remodelling<sup>57,198,199</sup> and attenuate the contractile dysfunction<sup>27,44,56</sup> during short term AF. After longer duration of AF, the protective effect of verapamil disappears<sup>200</sup> indicating a transient calcium overload at the onset of AF. There are several mechanisms by which AF might induce a calcium overload:

*i | atrial activity rate*

At the onset of AF the atrial activation rate is high which causes an excessive influx of calcium<sup>44,201</sup>. In dogs, atrial tachycardia increased cellular calcium loading, which induced abnormalities in intracellular calcium handling<sup>60,201</sup>. In the goat model of AF, the levels of sarcolemma-bound and mitochondria bound calcium increased within the first two weeks of AF. From four weeks onward, the calcium level normalised, and control values are reached at 16 weeks of AF<sup>59</sup>.

*ii | atrial stretch:*

During AF, the atrial contractile function is depressed<sup>27,56,60,201</sup> which will lead to volume overload and subsequently increased passive stretch. Increased atrial pressure has been shown to induce calcium overload<sup>199</sup> and shortening of the atrial effective refractory period<sup>52,199,202</sup>. In addition, atrial stretch influences protein expression<sup>45-48</sup> and has a positive effect on cell size<sup>49-51</sup>. Thus apart from calcium overload, atrial stretch could be involved in the observed structural remodelling and cardiomyocyte hypertrophy during AF.

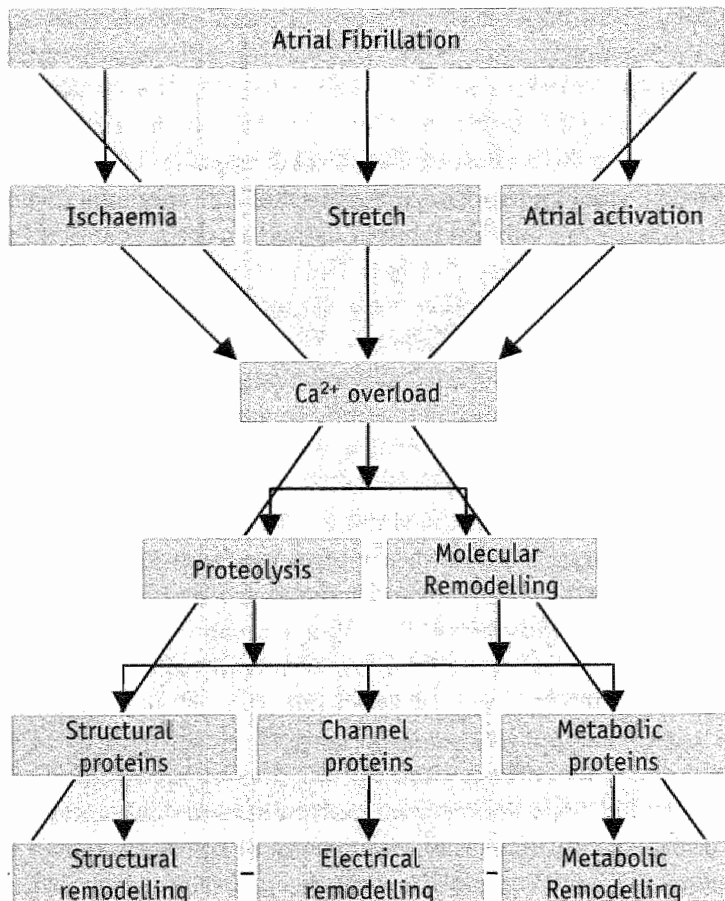
*iii | atrial ischaemia:*

It is well established that ischaemia results in cellular acidosis and calcium overload. However, the role of ischaemia during AF is controversial. The viable appearance of mitochondria during AF suggests that severe ischaemic stress does not occur AF<sup>29-32,88</sup>. The absence of changes in the metabolites of cardiomyocytes, such as ATP, also indicates that severe ischaemia is absent during AF<sup>44,130</sup>. Nevertheless, it was found that during acute AF the atrial flow was high and the flow reserve was limited<sup>38,203</sup>. As a consequence, additional metabolic demands

**Figure 3 |**

Cardiac response to AF.

See text for explanation of the figure



94 |

could lead to a metabolic mismatch<sup>18</sup>. This could explain the transient decrease in phosphocreatine content in atrial cells at the onset of AF<sup>43,44</sup>. Furthermore, the observed upregulation of the hypoxia inducible factor 1 $\alpha$  in the first weeks of AF indicates that oxidative stress does occur at the onset of AF (Chapter 5). Thus, although severe ischaemia does not seem to play a role during AF, some degree of ischaemic stress could be involved in atrial remodelling. Figure 3 shows the most likely mechanism by which AF induces the changes that are characteristic of atrial remodelling.

At the onset of AF, calcium overload occurs in response to an increased activation rate, stretch, and/or ischaemia. Excess calcium results in the activation of proteolytic pathways. A recent study in patients with persistent and paroxysmal AF described increased levels of the calcium activated proteolytic protein

calpain I, located in the nucleus, the cytoplasm and at the intercalated discs<sup>112</sup>. The induction of calpain activity correlated with shortening of the atrial effective refractory period, increased structural alterations in the atrial myocytes, and decreased protein levels of channel proteins<sup>112</sup>. Degradation of calcium channel proteins<sup>204</sup> and contractile/structural proteins by calpain was also observed by others<sup>107,110,205,206</sup>.

Besides the activation of proteolytic proteins like calpains, calcium overload is involved in the altered expression of proteins during AF, i.e. molecular remodelling (Figure 3). Calcium overload has been shown to downregulate sodium channel expression<sup>67</sup> which could explain the reduced sodium current density in atrial myocytes from dogs with pacing induced AF<sup>66</sup>. A recent study found a relation between calcium overload and HIF1 $\alpha$  protein levels. In H9c2 cardiomyoblasts the hypoxia-induced increase in HIF1 $\alpha$  protein could be attenuated by verapamil<sup>207</sup>. Salnikow *et al.* did not find alterations in HIF1 $\alpha$  protein or expression levels but observed a calcium-induced activation of signalling pathways involving transcription factor AP-1. They concluded that the co-operation between the HIF1 $\alpha$  and AP-1 pathways allowed the fine regulation of gene expression during hypoxia<sup>208</sup>.

In all, these data show that calcium overload does occur during AF and that calcium overload is involved in activation of protein degradation and initiation of protein expression regulation. The subsequent alterations in structural, channel, and metabolic proteins results in structural, electrical and metabolic remodelling which are responsible for induction and maintenance of atrial dysfunction during AF.

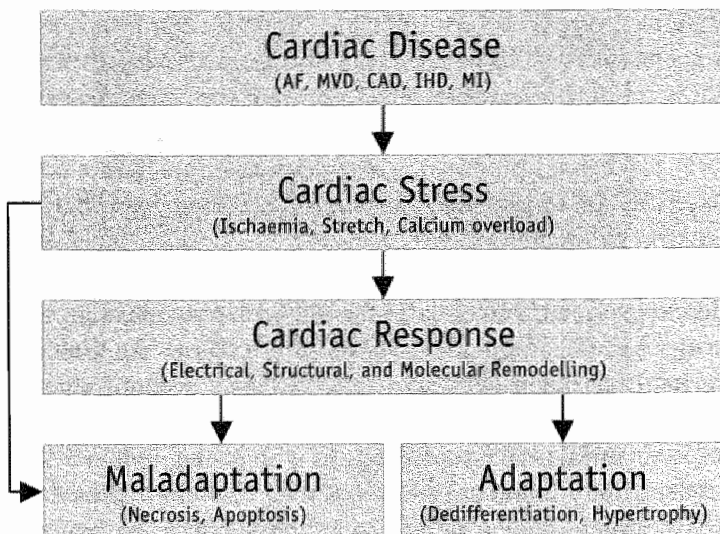
#### 4.2 | Cardiac adaptation

As described in the previous section, calcium overload is an important regulator of cardiomyocyte structural remodelling in response to cardiac stresses like ischaemia and stretch. However, the observed response appears not to be restricted to AF. Several studies have shown that structural remodelling occurs in several other cardiac diseases, e.g. cardiac valve disease, chronic hibernating myocardium, myocardial infarction<sup>32,33,40,41,88,209</sup>. This observation, together with the knowledge that many cardiac diseases induce ischaemia and/or stretch suggests the existence of an uniform response mechanism of cardiomyocytes in

**Figure 4 |**

General cardiac response to cardiac disease.

See text for explanation of the figure.



jeopardy. Figure 4 shows a model of how cardiac disease in general could induce an adaptive and/or maladaptive response of the cardiomyocytes. As depicted in the figure, a broad spectrum of cardiac diseases induces common cardiac stresses like ischaemia or stretch. Cardiac stress usually induces calcium overload which initiates proteolysis and molecular remodelling. Depending on the degree of cardiomyocyte stress, the cells either die by necrosis and apoptosis, or they adapt through dedifferentiation and hypertrophy. The observations in patients and goats with AF suggest that the adaptive response occurs apart from necrosis and apoptosis or programmed cell death<sup>35,88</sup>. The adaptive response might be considered as ‘programmed cell survival’, as it appears to render the cardiomyocytes the ability to survive stress conditions including ischaemia and stretch<sup>42</sup>. This would also explain the capacity of cells to regain function, although delayed, once environmental conditions have become normalised<sup>25-27,147,210</sup>.

## 5 | Future perspectives

### 5.1 | Molecular remodelling in AF

Since the first description of AF in 1628 by the English physician William Harvey (1578-1657)<sup>211</sup> our knowledge of this arrhythmic disease has increased substantially. The multiple wavelet hypothesis of Gordon K. Moe<sup>12,13</sup>, the paradigm of AF

begets AF<sup>127</sup>, and the theory of AF-induced cardiomyocyte dedifferentiation<sup>32,33</sup> are examples of the scientific contributions to our current understanding of the cause and maintenance of AF. Despite the increasing comprehension of atrial remodelling during AF, many questions concerning the molecular mechanisms that underlie atrial remodelling remain unanswered. Most research has focussed on molecular alteration in the more obvious proteins like ion channels and structural proteins. The use of techniques that allow a random screen of the overall changes in gene expression (differential display, expression arrays) might contribute to resolving the exact molecular pathways that are involved in molecular remodelling during AF. However, the aetiology of patients with AF is often diverse which conceals the true contribution of AF to altered gene expression. Although the use of animal models can overcome this problem, the mix of different cell types within the atrial tissue, the heterogeneity in the response of the atrial cells to AF, and the interspecies differences complicate the gene expression analysis. Only *in vitro* systems provide the most optimal conditions to perform gene expression analysis because they consist of an indefinite source of well defined cells. Unfortunately, up to now no good *in vitro* models for AF induced remodelling exist. When most of the problems using expression screening techniques have been overcome, such techniques might be used successfully in basic science to unravel the molecular aspects of AF. Furthermore, they might be used in the clinical setting as a diagnostic tool to determine the degree or stage of cardiac remodelling during AF. Eventually, expression screening techniques might provide clinicians with information on which specific and individual patient treatment can be based.

## 5.2 | Molecular remodelling in cardiac disease

Different cardiac diseases may result in a general response at the level of cardiomyocyte morphology and protein expression patterns. Atrial fibrillation, chronic hibernating myocardium, and cardiac valve disease all result in changes that are reminiscent of cardiomyocyte dedifferentiation<sup>33,40,41,88</sup>. A switch towards foetal gene expression programs and metabolism has also been described in cardiac hypertrophy<sup>212,213</sup>. This indicates that the primary response of the heart to cardiac stress consists of a return to a less differentiated phenotype. One of the questions

that has to be answered in the near future is whether the dedifferentiation is a response in order to survive the altered conditions or is it an attempt to enter the cell cycle again, as a countermeasure against cell loss? A comparison of the similarities and the differences between the molecular responses during different cardiac diseases could reveal the nature of cardiomyocyte dedifferentiation, not only in AF, but in cardiac diseases in general.

### 5.3 | Reversibility of molecular remodelling

Little is known about the reversibility of molecular remodelling after restoration of sinus rhythm. The observed changes in expression of ion channels, e.g. L-type calcium channel, and alterations in the atrial effective refractory period indicate that changes in cardiac gene expression are responsible for electrical remodelling during AF<sup>65,133-135,214</sup>. After restoration of sinus rhythm the atrial effective refractory period normalises within a few days<sup>127,144,177</sup>. Atrial conduction normalises somewhat slower but still recovers within a few weeks<sup>145,146</sup>. These data indicate that upon normalisation of the atrial rhythm, the changes in atrial activation and conduction are completely reversible and that the underlying changes in gene expression of channels and connexins most likely also return to normal values. Indeed, in the goat model, the expression of connexin40 normalised within 8 weeks of SR following 16 weeks of AF<sup>215,216</sup>.

As stated before, the rapid normalisation of the electrical properties after normalisation of SR is not in line with the slow recovery of contractile function<sup>25,27,147</sup>. A slow recovery of function is also noted in patients with hibernating myocardium<sup>215,216</sup>, a cardiac disease which is characterised by cardiomyocyte dedifferentiation<sup>40,41</sup>. In goats, 8 or 16 weeks of SR following 16 weeks of AF resulted in a slow recovery of the structural changes<sup>217</sup>, which could explain the delay in functional improvement. Whether the structural remodelling is completely reversible and whether or not the slow recovery of structural remodelling is accompanied by an equal slow normalisation in the expression levels of structural proteins is not known. In goats, the expression of titin had not reached normal levels 16 weeks post cardioversion whereas the expression of cardiotin looked normal<sup>217</sup>. A factor that could hamper the complete normalisation of structural remodelling is fibrosis. Several authors have

described the presence of substantial fibrosis besides the structural changes in patients with AF<sup>217</sup>. The removal of this fibrotic tissue, if possible at all, might take a long time. Thus, the concept that ‘SR begets SR’<sup>159</sup>, analogous to ‘AF begets AF’<sup>127</sup>, might not hold true when molecular and structural remodelling is too extended. The reversibility of molecular remodelling and subsequent electrical and structural remodelling will be one of the important issues in the future research of AF.

## 6 | Conclusions

AF induces electrical and structural remodelling which results in contractile dysfunction of the atrium. It has been shown that electrical and structural remodelling during AF are the result of far-reaching molecular remodelling that affects the function of cardiomyocytes in various ways, e.g. excitation, contraction, metabolism. The triggers for molecular remodelling might involve calcium overload, stretch, and ischaemia. The observed cardiomyocyte remodelling is not restricted to AF but appears to be a common response mechanism to cardiac stress. Unravelling the exact mechanisms and triggers that are involved in molecular remodelling and the reversibility of remodelling should be main targets in future research, not only to provide a better understanding of AF but also to generate new tools for better treatment.



# Appendix

## | *Summary* |

Atrial fibrillation (AF) is a cardiac arrhythmia that is characterised by irregular and disorganised atrial activity with respect to rate and rhythm. It has an overall prevalence of almost one percent and it is the most common arrhythmia encountered in the clinical setting. It has been shown that AF is accompanied by electrical remodelling and contractile dysfunction. Both phenomena are reversible but after prolonged periods of AF, a discrepancy occurs between a rapid normalisation of electrical function and the delay in recovery of contractility. One possible explanation for this incongruity is the occurrence of structural remodelling of the cardiomyocytes during AF.

Structural remodelling could be observed in atrial cardiomyocytes of patients suffering from cardiac valve disease with or without AF (**Chapter 2**). The size of cardiomyocytes increased in patients with AF as compared to patients with no AF. Additional structural changes were present in patients with or without AF and mainly consisted of extensive myolysis, glycogen accumulation, sarcoplasmic reticulum disorganisation, mitochondrial changes, and redistribution of the nuclear heterochromatin. These changes are indicative of an adaptive response through cardiomyocyte dedifferentiation and the

observations were in agreement with previous studies in humans and animal models.

Because AF is accompanied by cardiomyocyte dedifferentiation and contractile dysfunction the effect of AF on the expression of Troponin I isoforms was analysed (**Chapter 3 and 4**). Troponin I (TnI) is a sub-unit of the troponin complex which regulates actin-myosin interaction during contraction. Different isoforms of TnI are expressed in different muscle types and several species, including humans, show a switch in expression from the foetal slow-twitch skeletal isoform (ssTnI) to the adult cardiac isoform (cTnI) during heart development. Furthermore, degradation of AF might occur during AF as a result of increased proteolytic activity. First, the changes in TnI expression were analysed in patients with cardiac valve disease and/or AF (**Chapter 3**). Several patients showed expression of ssTnI, irrespective of the presence of cardiac valve disease or AF. Although the re-expression of ssTnI is indicative of cardiomyocyte dedifferentiation, patients with chronic AF did not re-express ssTnI. Rather than re-expression of ssTnI, chronic AF resulted in increased expression of cTnI. In none of the patients degradation of cTnI could be detected. Because of the differences between the individual patients with respect to duration of AF and underlying cardiac disease, changes in the expression of TnI isoforms were further characterised in the goat model of lone AF (**Chapter 4**). In contrast to the observations in patients, AF in the goat did not result in detectable protein levels of ssTnI. Degradation of TnI could only be observed in a few samples but was confined to the first 4 weeks of AF. After prolonged duration of AF the degradation of cTnI was no longer detectable and cTnI expression appeared to be increased, although not significantly. The results in the goat together with the observations in patients suggest that the alterations in TnI expression are not the result of ongoing cardiomyocyte dedifferentiation. Nevertheless, the changes in TnI expression might be one of the contributors to the contractile dysfunction.

To obtain a more complete picture of the effect of AF on atrial gene expression the goat model was used to isolate and characterise genes of which the expression changed during AF (**Chapter 5**). The differential display technique was used to isolate genes that might be involved in atrial remodelling. The majority of these genes were involved in cardiomyocyte

structure, metabolism, expression regulation, or (de)differentiation. Several of the genes that were isolated confirmed or supported the current knowledge on structural remodelling and AF-induced cardiomyocyte dedifferentiation. Time course analysis of the expression revealed an increased expression of the transcription factor HIF1 $\alpha$  in the first week of AF, which is indicative of atrial ischaemia at the onset of AF and that provides evidence for a switch in metabolism and subsequent glycogen accumulation.

In short, the studies presented in this thesis show that AF is accompanied by altered gene expression in the atria. Part of the changes in expression are involved in the structural remodelling of the atrial cells. In addition, a stress response appears to occur at the onset of AF which could not only initiate the structural remodelling but may also account for a metabolic remodelling of the cardiomyocyte. Future studies on the exact role of molecular remodelling in atrial adaptation and the involvement of ischaemia, stretch, and calcium overload in this process might provide new tools for a better treatment of AF.



# Appendix

## | Samenvatting |

Boezemfibrilleren is een hartritmestoornis die zich kenmerkt door onregelmatigheden en disorganisatie in zowel het tempo als het ritme van de boezemcontracties. Ongeveer 1 procent van de bevolking lijdt aan boezemfibrilleren en daarmee is het de meest voorkomende ritmestoornis. Onderzoek heeft aangetoond dat boezemfibrilleren gepaard gaat met veranderingen in de electrische eigenschappen van de boezem. Daarnaast vindt er een verslechtering plaats in het samentrekken van de boezem. Hoewel beide fenomenen normaliter volledig omkeerbaar zijn, is gebleken dat naarmate de duur van boezemfibrilleren toeneemt het herstel van de contractie langer duurt dan het herstel van de electrische patronen. Een mogelijke verklaring voor dit ongelijk herstel kan liggen in het feit dat de hartspiercellen structurele veranderingen ondergaan ten gevolge van het boezemfibrilleren.

Structurele veranderingen waren aanwezig in de hartspiercellen uit de boezems van patienten met een hartklep aandoening met of zonder boezemfibrilleren (**Hoofdstuk 2**). De hartspiercellen van patienten met boezemfibrilleren waren groter dan de cellen van patienten zonder boezemfibrilleren. Tevens waren in alle patienten, ongeacht de aanwezigheid van boezemfibrilleren,

structurele veranderingen zichtbaar die voornamelijk bestonden uit het verdwijnen van de contractiele elementen, het opstapelen van glycogeen, een verminderde organisatie van het sarcoplasmatisch reticulum, veranderingen in de grootte en de vorm van de mitochondriën en een regelmatige verdeling van het heterochromatine in de kern. Al deze veranderingen kwamen overeen met waarnemingen uit andere studies in zowel mensen als dieren en ze wijzen op een mechanisme waarbij de hartspiercel zich aanpast aan een nieuwe situatie door terug te gaan naar een vroeger ontwikkelingsstadium (dedifferentiatie). Aangezien boezemfibrilleren gepaard gaat met hartspiercel dedifferentiatie en verminderde contractiliteit is effect van boezemfibrilleren op de expressie van Troponine I onderzocht (**Hoofdstuk 3 en 4**). Troponine I is een eiwit dat onderdeel uitmaakt van het Troponine complex. Dit complex regelt de interactie tussen actine en myosine tijdens het samentrekken van hartspiercellen. Verschillende spiertypes hebben elk hun eigen specifieke isovorm van Troponine I, aangepast aan de contractiele eigenschappen van het spiertype. Tijdens de ontwikkeling van het hart vindt er wisseling plaats in de expressie van deze isovormen. In het foetale hart wordt voornamelijk een variant tot expressie gebracht die ook te vinden is in skeletspieren. In het volwassen hart komt alleen nog maar de hartspecifieke isovorm tot expressie. Kortom, als er tijdens het boezemfibrilleren veranderingen plaatsvinden in de expressie van de Troponine I isovormen zou dit een aanwijzing kunnen zijn voor de dedifferentiatie van hartspiercellen. Daarnaast zou er ook afbraak kunnen plaatsvinden van het Troponine I eiwit. Allereerst is er gekeken naar veranderingen in de Troponine I expressie in de boezems van patienten die lijden aan een hartklepandoening en/of boezemfibrilleren (**Hoofdstuk 3**). Hierbij is zowel de samenstelling van de Troponine eiwitten als de expressie van het mRNA bestudeerd. Bij een aantal patienten kon de aanwezigheid van de skeletspier isovorm van Troponine op eiwitniveau worden aangetoond, ongeacht of deze patienten een hartklepandoening dan wel boezemfibrilleren hadden. Hoewel de aanwezigheid van ssTnI een indicatie is voor hartspiercel dedifferentiatie kon het eiwit niet aangetoond worden in patienten met chronisch boezemfibrilleren. In plaats van een toename in ssTnI ging bij patienten met chronisch boezemfibrilleren de expressie van de hartsierspecifieke isovorm omhoog. In geen van de patienten was afbraak van het

hartspecifieke eiwit meetbaar.

Aangezien de patienten nogal verschillend waren ten aanzien van de duur van boezemfibrilleren en onderliggende hartziekten, is de expressie van de Troponine I eiwitten verder onderzocht in een diermodel (geit) van boezemfibrilleren (**Hoofdstuk 4**). In tegenstelling tot wat we bij de patienten hadden gevonden resulteerde boezemfibrilleren in de geit niet tot een waarneembare toename van het skeletsierspecifieke eiwit. Afbraak van het hartspecifieke Troponine I was maar in een zeer klein aantal gevallen zichtbaar en alleen maar in de eerste 4 weken van boezemfibrillatie. Na een langere periode van boezemfibrilleren was er geen afbraak meer zichtbaar en leek de mRNA expressie van de hartspecifieke isovorm weer toe te nemen. Samen met de observaties in de patienten lijken deze resultaten aan te geven dat de verschuivingen in de expressie van Troponine I isovormen tijdens boezemfibrilleren geen gevolg zijn van hartspiercel dedifferentiatie. De verandering in de expressie zouden wel een bijdrage kunnen leveren aan de verslechterde contractiliteit van de boezem.

Om een completer beeld te krijgen van het effect van boezemfibrilleren op de expressie van genen in het algemeen is vervolgens het geit model gebruikt om genen te isoleren waarvan de expressie veranderde ten gevolge van boezemfibrilleren (**Hoofdstuk 5**). Met behulp de ‘differential display’ techniek werd, naast een aantal nog onbekende genen, een aantal genen geïsoleerd dat mogelijk een rol speelt tijdens boezemfibrilleren. Het merendeel van de geïdentificeerde genen speelt een rol in de structuur van hartspiercellen, de energiehuishouding van cellen, de regulatie van gen-expressie, of in de (de)differentiatie van hartspiercellen. Een aantal van de geïsoleerde genen bevestigde of ondersteunde onze huidige kennis van zaken met betrekking tot de structuele veranderingen en dedifferentiatie van hartspiercellen. Het verloop van de expressiepatronen van genen gedurende het boezemfibrilleren werd ook onderzocht en het bleek dat in de eerste week van AF een eiwit tot overexpressie werd gebracht (HIF1 $\alpha$ ) dat aangeeft dat er bij de aanvang van boezemfibrilleren wel eens sprake kon zijn van een zuurstoftekort en dat de hartspiercellen hun energiehuishouding dusdanig veranderden dat er glycogeenstapeling kon plaatsvinden.

Kortom, de in dit proefschrift gepresenteerde studies geven aan dat boezemfibrilleren gepaard gaat met vergaande moleculaire

veranderingen. Een deel van deze veranderingen is betrokken bij de structurele veranderingen van hartspiercellen in de boezem. Verder is gebleken dat bij aanvang van boezemfibrilleren een tijdelijke stress wel eens verantwoordelijk zou kunnen zijn voor het inzetten van de structurele veranderingen en het aanpassen van de energiehuishouding door hartspiercellen. Toekomstig onderzoek naar de exacte rol van de moleculaire veranderingen en de invloed van het mogelijke zuurstoftekort, rek en calcium op het proces van de verminderde boezemfunctie zou nieuwe handvatten kunnen reiken voor een betere behandeling van boezemfibrilleren.

# Appendix

## | Curriculum Vitae |

Personal	109
Name	Victor L.J.L. Thijssen
Date of birth	March 8, 1972
Place of birth	Tegelen, The Netherlands
Education	
1978 - 1984	Primary school (Basisschool) St. Jozefschool, Beesel
1984 - 1990	Secondary (high) school (VWO) Bisschoppelijke College, Roermond
1990 - 1997	Msc programme Biotechnology Agricultural University, Wageningen
1997 - 2001	PhD Student Dept. Molecular cell biology & Genetics, University of Maastricht (UM)
2001 - 2002	Research fellow Dept. Cardiologie Academic Hospital Maastricht (azM) / UM
2002 - present	Research fellow Dept. Internal medicine / Pathology azM / UM



# Appendix

## | *List of publications* |

Papers |

| 111

V.L.J.L. Thijssen, J. Ausma, G-S. Liu, M.A. Allessie, G.J. van Eys, M. Borgers. Structural Changes Of Atrial Myocardium During Chronic Atrial Fibrillation. *Cardiovasc Pathol* 2000;9(1):17-28

L Wouters, G-S Liu, W Flameng, V Thijssen, F Thone, M Borgers. Structural remodelling of atrial myocardium in patients with cardiac valve disease and atrial fibrillation. *Exp Clin Cardiol* 2001;5(3): 158-163

V.L.J.L. Thijssen, J. Ausma, M Borgers. Structural remodelling during chronic atrial fibrillation: act of programmed cell survival. *Cardiovasc Res* 2001;52: 14-20

V.L.J.L. Thijssen, H.M.W. van der Velden, E.P. van Ankeren, J.Ausma, M.A. Allessie, M.Borgers, G.J.J.M. van Eys, H.J. Jongsma. Analysis of altered gene expression during sustained atrial fibrillation in the goat. *Cardiovasc Res*, 2002;54(2): 427-437

V.L.J.L. Thijssen, J. Ausma, L. Gorza, I.C. van Gelder, G.J.J.M. van Eys, M. Borgers. Expression of Troponin I isoforms in patients with atrial fibrillation. In preparation.

V.L.J.L. Thijssen, J. Ausma, L. Gorza, M.A. Allessie, M. Borgers, G.J.J.M. van Eys. Troponin I isoform expression during chronic atrial fibrillation in the goat. In preparation

S.S.M. Rensen, V.L.J.L. Thijssen, C.J. de Vries, P.A. Doevedans, S.D. Detera-Wadleigh, G.J.J.M. van Eys. Expression of the smoothelin gene is mediated by alternative promoters. Accepted for publication in *Cardiovasc Res.*

## Chapters |

G.J.J.M. van Eys, C.J.M. de Vries, S.S.M. Rensen, V.L.J.L. Thijssen, E.L.C. Verhaar, G.P.G.M. Coolen, W.M.H. Debie, M.C. de Ruiter, S.D. Wadleigh-Detera. Smoothelins: one gene, two proteins, three muscle cell types ... so far. In: *Cardiovascular specific gene expression*, P.A. Doevedans, R.S. Reneman, and M. van Bilsen, Editors. 1999, Kluwer Academic Publishers: Dordrecht, The Netherlands. p. 49-66.

## Abstracts |

V.L.J.L. Thijssen, G.J.J.M. van Eys, J. Ausma, M. Borgers, M. Allessie. Identification Of Genes Involved In Dedifferentiation Of Cardiomyocytes. *J Mol Cell Cardiol*, 1999;31:A93

V.L.J.L. Thijssen, G.J.J.M. van Eys, J. Ausma, M. Borgers. Dedifferentiation Of Cardiomyocytes During Atrial Fibrillation: Analysis Of Gene Expression By Differential Display. *J Muscle Res Cell Motil*. 1999;20(8): 845

V.L.J.L. Thijssen, J. Ausma, L. Gorza, M. Borgers, G.J.J.M. van Eys. Expression Of Troponin I Isoforms During Chronic Hibernation And Chronic Atrial Fibrillation. *Exp Clin Cardiol* 2000;5(1): 49





# Appendix

## | Dankwoord |

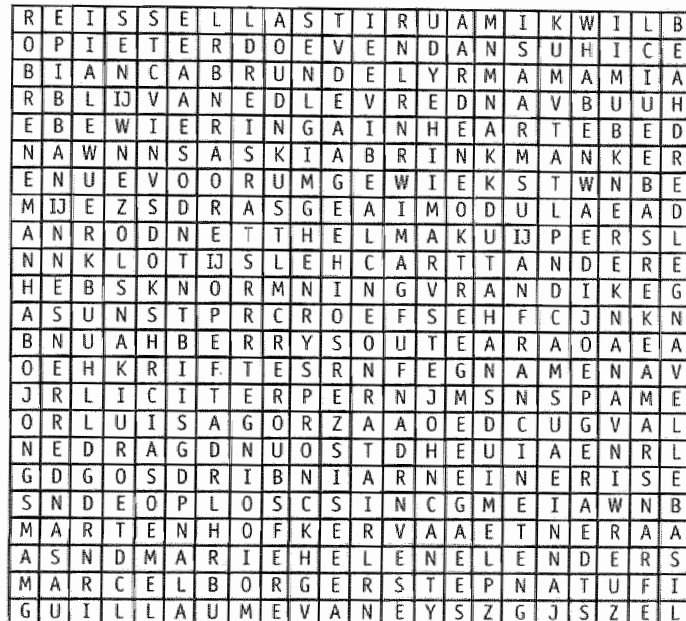
*Er zou weinig van mij overblijven als ik alles terug moest geven wat ik aan anderen te danken heb.*

Johann Wolfgang von Goethe

### BedankPuzzel |

Helaas is een dankwoord nooit volledig. Voor eenieder die teleurgesteld, verdrietig danwel verontwaardigd is omdat zijn/haar naam niet in het dankwoord voorkomt vormt deze puzzel de oplossing. Het doel van de puzzel is tweeledig. Allereerst stelt hij je in staat je frustraties bot te vieren op alle mensen die wel genoemd zijn in het dankwoord. Daarnaast streeft de oplossing van de puzzel het gedeukte ego.

Zoek de namen van de lijst in het diagram en streep ze door met een pen danwel een dikke zwarte stift. De namen staan horizontaal, verticaal en diagonaal verborgen in de letterbrij. Een aantal namen staat zelfs achtersteven (hoe moeilijk kun je het maken...). De letters die overblijven vormen een troostende en heilzame oplossing.  
Veel succes...



| 115

#### Promotion Team

Marcel Borgers  
Guillaume van Eys

Jannie Ausma

#### Review Board

Rob Reneman  
Harry Crijns  
Marten Hofker  
Frans Ramaekers  
Be Wieringa  
**Paranimfen**  
Hans Duimel  
Sander Rensen

#### Last line of Defense

John Canty  
Joep Geraedts  
Maurits Allessie  
Pieter Doevedans

Habo Jongsma

#### Technical support

Geert Koene  
Saskia Brinkman  
Mayriam Stijns  
Marie-Helene Lenders  
Erwin van Ankeren  
Francine Teng  
**Collaborators**  
Luisa Gorza  
Bianca Brundel

Isabelle van Gelder  
Huub van der Velden

#### Students

Berry Soute  
Henry Spronck  
**Sequencing Team**  
Rainbirds  
Soundgarden

#### Left-overs

MCB  
Huub Kreuwel  
Kanslozen  
**Last but not Least**  
LudoMia  
GeWiekst  
MamaMia  
Rachel



# Appendix

## | References |

1. Myerburg RJ, Kessler KM, Castellanos A, O'Rourke RA, Roberts R, Sonnenblick EH. Recognition, clinical assessment, and management of arrhythmias and conduction disturbances. In: Alexander RW, Schlant RC, Fuster V, eds. *Hurst's The Heart*. 9 ed. New York: McGraw-Hill; 1998:873-941.
2. Feinberg WM, Blackshear JL, Laupacis A, Kronmal R, Hart RG. Prevalence, age distribution, and gender of patients with atrial fibrillation. Analysis and implications. *Arch Intern Med*. 1995;155:469-73.
3. Benjamin EJ, Levy D, Vaziri SM, D'Agostino RB, Belanger AJ, Wolf PA. Independent risk factors for atrial fibrillation in a population-based cohort. The Framingham Heart Study. *Jama*. 1994;271:840-4.
4. Krahn AD, Manfreda J, Tate RB, Mathewson FA, Cuddy TE. The natural history of atrial fibrillation: incidence, risk factors, and prognosis in the Manitoba Follow-Up Study. *Am J Med*. 1995;98:476-84.
5. Wolf PA, Abbott RD, Kannel WB. Atrial fibrillation as an independent risk factor for stroke: the Framingham study. *Stroke*. 1991;22:983-988.
6. Truelsen T, Lindenstrom E, Boysen G. Comparison of probability of stroke between the Copenhagen City Heart Study and the Framingham Study. *Stroke*. 1994;25:802-7.
7. Benjamin EJ, Wolf PA, D'Agostino RB, Silbershatz H, Kannel WB, Levy D. Impact of atrial fibrillation on the risk of death: the Framingham Heart Study. *Circulation*. 1998;98:946-52.
8. Lewis T, Drury AN, Iliescu CC. A demonstration of circus movement in clinical atrial fibrillation. *Br Heart J*. 1971;34:63-70.
9. Michelassi F. The recognition of the circus motion of the heart by electrocardiographic criteria. *Continuing Education in Cardiology*. 1994;15:203-6.
10. Michelassi F. On dynamic equilibrium in the heart. *Continuing Education in Cardiology*. 1994;15:207-13.
11. Michelassi F. On the reciprocal generation of normal and fibrillatory contractions in the heart. *Continuing Education in Cardiology*. 1994;15:221-2.
12. Michelassi F, Abildstrøm JAA. Atrial fibrillation as a self-reinforcing fibrillation independent of its initial trigger. *Acta Physiol Scand*. 1993;145:47-50.
13. Michelassi F. On the multiple mechanisms of fibrillation. *Acta Physiol Pharmacol Belg*. 1963;27:301.
14. Adelsohn MA, Lümmelius W, Rydt B, Roskjaer F, Elmer Hansen SG. Experimental evaluation of the amplitude and frequency of atrial fibrillation in sheep. *Acta Physiol Scand*. 1961;53:273-81.
15. Adelsohn MA, Wijffels M, Verheyen CG. Experimental induced fibrillation in sheep. *Acta Physiol Scand*. 1994;141:589-602.
16. O'Malley WM. The pharmacological consequences of fibrillation - a literature review and summary. *Acta Physiol Scand*. 1994;141:531.
17. Goldberger AL, Pinsky ZZ. Very low medication for fibrillation in older persons with atrial fibrillation. *Ann Geriatr Cardiol*. 1998;1:347-55.

- 118 |
18. Powell AC, Garan H, McGovern BA, Fallon JT, Krishnan SC, Ruskin JN. Low energy conversion of atrial fibrillation in the sheep. *J Am Coll Cardiol.* 1992;20:707-11.
  19. Whittington JR, Cross MR, Raftery EB. An effective conscious animal model of atrial fibrillation. *Cardiovasc Res.* 1979;13:105-12.
  20. Elvan A, Pride HP, Eble JN, Zipes DP. Radiofrequency catheter ablation of the atria reduces inducibility and duration of atrial fibrillation in dogs. *Circulation.* 1995;91:2235-44.
  21. Iskos D, Lurie KG, Adler SW, Shultz JJ, Coffeen PR, Mulligan KA, Benditt DG. Effect of parenteral d-sotalol on transvenous atrial defibrillation threshold in a canine model of atrial fibrillation. *Am Heart J.* 1996;132:116-9.
  22. Gray RA, Pertsov AM, Jalife J. Incomplete reentry and epicardial breakthrough patterns during atrial fibrillation in the sheep heart. *Circulation.* 1996;94:2649-61.
  23. Gaspo R, Bosch RF, Talajic M, Nattel S. Functional mechanisms underlying tachycardia-induced sustained atrial fibrillation in a chronic dog model. *Circulation.* 1997;96:4027-35.
  24. Yue L, Feng J, Gaspo R, Li GR, Wang Z, Nattel S. Ionic remodeling underlying action potential changes in a canine model of atrial fibrillation. *Circ Res.* 1997;81:512-25.
  25. Manning WJ, Silverman DI, Katz SE, Riley MF, Come PC, Doherty RM, Munson JT, Douglas PS. Impaired left atrial mechanical function after cardioversion: relation to the duration of atrial fibrillation. *J Am Coll Cardiol.* 1994;23:1535-40.
  26. Shapiro EP, Effron MB, Lima S, Ouyang P, Siu CO, Bush D. Transient atrial dysfunction after conversion of chronic atrial fibrillation to sinus rhythm. *Am J Cardiol.* 1988;62:1202-7.
  27. Daoud EG, Marcovitz P, Knight BP, Goyal R, Man KC, Strickberger SA, Armstrong WF, Morady F. Short-term effect of atrial fibrillation on atrial contractile function in humans. *Circulation.* 1999;99:3024-7.
  28. Van Gelder IC, Crijns HJ, Blanksma PK, Landsman ML, Posma JL, Van Den Berg MP, Meijler FL, Lie KI. Time course of hemodynamic changes and improvement of exercise tolerance after cardioversion of chronic atrial fibrillation unassociated with cardiac valve disease. *Am J Cardiol.* 1993;72:560-6.
  29. Mary-Rabine L, Albert A, Pham TD, Hordof A, Fenoglio JJ, Jr., Malm JR, Rosen MR. The relationship of human atrial cellular electrophysiology to clinical function and ultrastructure. *Circ Res.* 1983;52:188-99.
  30. Frustaci A, Chimenti C, Bellocchi F, Morgante E, Russo MA, Maseri A. Histological substrate of atrial biopsies in patients with lone atrial fibrillation. *Circulation.* 1997;96:1180-4.
  31. Thiedemann KU, Ferrans VJ. Left atrial ultrastructure in mitral valvular disease. *Am J Pathol.* 1977;89:575-604.
  32. Ausma J, Wijffels M, Thone F, Wouters L, Allessie M, Borgers M. Structural changes of atrial myocardium due to sustained atrial fibrillation in the goat. *Circulation.* 1997;96:3157-63.
  33. Ausma J, Wijffels M, van Eys G, Koide M, Ramaekers F, Allessie M, Borgers M. Dedifferentiation of atrial cardiomyocytes as a result of chronic atrial fibrillation. *Am J Pathol.* 1997;151:985-97.
  34. Boyden PA, Tilley LP, Pham TD, Liu SK, Fenoglio JJ, Jr., Wit AL. Effects of left atrial enlargement on atrial transmembrane potentials and structure in dogs with mitral valve fibrosis. *Am J Cardiol.* 1982;49:1896-908.
  35. Dispersyn GD, Ausma J, Thoné F, Flameng W, Vanoverschelde JL, Allessie MA, Ramaekers FC, Borgers M. Cardiomyocyte remodelling during myocardial hibernation and atrial fibrillation: prelude to apoptosis. *Cardiovasc Res.* 1999;43:947-57.

36. Ausma J, Lenders M-H, Mast F, Allessie MA, Ramaekers F, Wouters L, Thoné F, Borgers M. Time course of structural changes due to atrial fibrillation in the goat. *Circulation*. 1998;98:1683 (abstract).
37. Ausma J, Ramaekers FCS, Allessie MA, Mast F, Borgers M. Time course of cardiomyocyte dedifferentiation due to atrial fibrillation in a goat model. *J Mol Cel Card.* 1999;31:A62.
38. White CW, Kerber RE, Weiss HR, Marcus ML. The effects of atrial fibrillation on atrial pressure-volume and flow relationships. *Circ Res*. 1982;51:205-15.
39. Jayachandran V, Winkle W, Sih HJ, Zipes DP, Olgin JE. Chronic atrial fibrillation from rapid atrial pacing is associated with reduced atrial blood flow: a positron emission tomography study. *Circulation*. 1998;98:I209.
40. Borgers M, Thoné F, Wouters L, Ausma J, Shivalkar B, Flameng W. Structural correlates of regional myocardial dysfunction in patients with critical coronary artery stenosis: chronic hibernation? *Cardiovasc Pathol*. 1993;2:237-245.
41. Ausma J, Schaart G, Thoné F, Schivalkar B, Flameng W, Depré C, Vanoverschelde J-L, Ramaekers F, Borgers M. Chronic ischemic viable myocardium in man: aspects of dedifferentiation. *Cardiovasc Pathol*. 1995;4:29-37.
42. Ausma J, Thoné F, Dispersyn GD, Flameng W, Vanoverschelde JL, Ramaekers FC, Borgers M. Dedifferentiated cardiomyocytes from chronic hibernating myocardium are ischemia-tolerant. *Mol Cell Biochem*. 1998;186:159-68.
43. Ausma J, Coumans W, Duimel H, van der Vusse GJ, Allessie MA, Borgers M. Atrial high energy phosphate content and mitochondrial enzyme activity during chronic atrial fibrillation. *Cardiovasc Res*. 2000;47:788-96.
44. Leistad E, Aksnes G, Verburg E, Christensen G. Atrial contractile dysfunction after short-term atrial fibrillation is reduced by verapamil but increased by BAY K8644. *Circulation*. 1996;93:1747-54.
45. Buttrick PM, Malhotra A, Brodman R, McDermott L, Lam L. Myosin isoenzyme distribution in overloaded human atrial tissue. *Circulation*. 1986;74:477-83.
46. Naruse M, Hiroe M, Naruse K, Nagata M, Ohno H, Hashimoto A, Koyanagi H, Sekiguchi M, Demura H, Hirosawa K, et al. Increased levels of beta-human atrial natriuretic peptide-like immunoreactivity in chronically overloaded atrial tissue. *Am J Hypertens*. 1990;3:105-10.
47. Sadoshima J, Takahashi T, Jahn L, Izumo S. Roles of mechano-sensitive ion channels, cytoskeleton, and contractile activity in stretch-induced immediate-early gene expression and hypertrophy of cardiac myocytes. *Proc Natl Acad Sci USA*. 1992;89:9905-9.
48. Christensen G, Leistad E. Atrial systolic pressure, as well as stretch, is a principal stimulus for release of ANF. *Am J Physiol*. 1997;272:H820-6.
49. Yamazaki T, Komuro I, Kudoh S, Zou Y, Shiojima I, Mizuno T, Takano H, Hiroi Y, Ueki K, Tobe K, et al. Angiotensin II partly mediates mechanical stress-induced cardiac hypertrophy. *Circ Res*. 1995;77:258-65.
50. Yamazaki T, Komuro I, Yazaki Y. Molecular mechanism of cardiac cellular hypertrophy by mechanical stress. *J Mol Cell Cardiol*. 1995;27:133-40.
51. Yamazaki T, Komuro I, Kudoh S, Zou Y, Shiojima I, Hiroi Y, Mizuno T, Maemura K, Kurihara H, Aikawa R, Takano H, Yazaki Y. Endothelin-1 is involved in mechanical stress-induced cardiomyocyte hypertrophy. *J Biol Chem*. 1996;271:3221-8.
52. Sideris DA, Toumanidis ST, Tselepatiotis E, Kostopoulos K, Stringli T, Kitsiou T, Moulopoulos SD. Atrial pressure and experimental atrial fibrillation. *Pacing Clin Electrophysiol*. 1995;18:1679-85.
53. Zipes DP. The seventh annual Gordon K. Moe Lecture. Atrial fibrillation: from cell to bedside. *J Cardiovasc Electrophysiol*. 1997;8:927-38.

54. Nijjar MS, Dhalla NS. Biochemical basis of calcium handling in developing myocardium. In: Ost'adal B, Nagano M, Takeda N, Dhalla NS, eds. *The developing heart*. 1 ed. Philadelphia: Lippincott-Raven publishers; 1997:189-217.
55. Vornanen M. Postnatal changes in cardiac calcium regulation. In: Ost'adal B, Nagano M, Takeda N, Dhalla NS, eds. *The developing heart*. Philadelphia: Lippincott-Raven publishers; 1997:219-229.
56. Leistad E, Borgers M, Christensen G. Atrial contractile dysfunction after short-term atrial fibrillation can be explained by changes in intracellular calcium, but not by atrial ischemia. *Circulation*. 1996;94:I386-387.
57. Goette A, Honeycutt C, Langberg JJ. Electrical remodeling in atrial fibrillation. Time course and mechanisms. *Circulation*. 1996;94:2968-74.
58. Tielemans RG, De Langen C, Van Gelder IC, de Kam PJ, Grandjean J, Bel KJ, Wijffels MC, Allessie MA, Crijns HJ. Verapamil reduces tachycardia-induced electrical remodeling of the atria. *Circulation*. 1997;95:1945-53.
59. Ausma J, Dispersyn GD, Duimel H, Thoné F, Ver Donck L, Allessie MA, Borgers M. Changes in ultrastructural calcium distribution in goat atria during atrial fibrillation. *J Mol Cell Cardiol*. 2000;32:355-64.
60. Sun H, Gaspo R, Leblanc N, Nattel S. Cellular mechanisms of atrial contractile dysfunction caused by sustained atrial tachycardia. *Circulation*. 1998;98:719-27.
61. Sun H, Leblanc N, Nattel S. Mechanisms of inactivation of L-type calcium channels in human atrial myocytes. *Am J Physiol*. 1997;272:H1625-35.
62. Gomez JP, Potreau D, Branka JE, Raymond G. Developmental changes in Ca<sup>2+</sup> currents from newborn rat cardiomyocytes in primary culture. *Pflugers Arch*. 1994;428:241-9.
63. Wetzel GT, Chen F, Klitzner TS. Ca<sup>2+</sup> channel kinetics in acutely isolated fetal, neonatal, and adult rabbit cardiac myocytes. *Circ Res*. 1993;72:1065-74.
64. Sharp WW, Terracio L, Borg TK, Samarel AM. Contractile activity modulates actin synthesis and turnover in cultured neonatal rat heart cells. *Circ Res*. 1993;73:172-83.
65. Van Wagoner DR, Pond AL, McCarthy PM, Trimmer JS, Nerbonne JM. Outward K<sup>+</sup> current densities and Kv1.5 expression are reduced in chronic human atrial fibrillation. *Circ Res*. 1997;80:772-81.
66. Gaspo R, Bosch RF, Bou-Abboud E, Nattel S. Tachycardia-induced changes in Na<sup>+</sup> current in a chronic dog model of atrial fibrillation. *Circ Res*. 1997;81:1045-52.
67. Duff HJ, Offord J, West J, Catterall WA. Class I and IV antiarrhythmic drugs and cytosolic calcium regulate mRNA encoding the sodium channel alpha subunit in rat cardiac muscle. *Mol Pharmacol*. 1992;42:570-4.
68. Liang P, Pardee AB. Differential display of eukaryotic messenger RNA by means of the polymerase chain reaction. *Science*. 1992;257:967-71.
69. Tyagi SC, Kumar S, Voelker DJ, Reddy HK, Janicki JS, Curtis JJ. Differential gene expression of extracellular matrix components in dilated cardiomyopathy. *J Cell Biochem*. 1996;63:185-98.
70. Sirokman G, Humphries DE, Bing OH. Endogenous retroviral transcripts in myocytes from spontaneously hypertensive rats. *Hypertension*. 1997;30:88-93.
71. Singh K, Sirokman G, Communal C, Robinson KG, Conrad CH, Brooks WW, Bing OH, Colucci WS. Myocardial osteopontin expression coincides with the development of heart failure. *Hypertension*. 1999;33:663-70.
72. Venkataraman R, Presser J, Vaillancourt RE, West AK. Identification of a new noradrenaline induced gene in the rat heart by differential mRNA display. *Cardiovasc Res*. 1995;29:490-4.
73. Cormier-Regard S, Egeland DB, Tannoch VJ, Claycomb WC. Differential display: identifying genes involved in cardiomyocyte proliferation. *Mol Cell Biochem*. 1997;172:111-20.

74. Utans U, Liang P, Wyner LR, Karnovsky MJ, Russell ME. Chronic cardiac rejection: identification of five upregulated genes in transplanted hearts by differential mRNA display. *Proc Natl Acad Sci U S A.* 1994;91:6463-7.
75. Manning WJ, Leeman DE, Gotch PJ, Come PC. Pulsed Doppler evaluation of atrial mechanical function after electrical cardioversion of atrial fibrillation. *J Am Coll Cardiol.* 1989;13:617-23.
76. Cote G, Mohiuddin SM, Roy PE. Occurrence of Z-band widening in human atrial cells. *Exp Mol Pathol.* 1970;13:307-18.
77. Aimé-Sempé C, Folliguet T, Rucker-Martin C, Krajewska M, Krajewska S, Heimbigner M, Aubier M, Mercadier JJ, Reed JC, Hatem SN. Myocardial cell death in fibrillating and dilated human right atria. *J Am Coll Cardiol.* 1999;34:1577-86.
78. Flameng W, Wouters L, Sergeant P, Lewi P, Borgers M, Thoné F, Suy R. Multivariate analysis of angiographic, histologic, and electrocardiographic data in patients with coronary heart disease. *Circulation.* 1984;70:7-17.
79. Thijssen VLJL, Ausma J, Liu GS, Allessie MA, van Eys GJ, Borgers M. Structural Changes of Atrial Myocardium During Chronic Atrial Fibrillation. *Cardiovasc Pathol.* 2000;9:17-28.
80. Haunstetter A, Izumo S. Apoptosis: basic mechanisms and implications for cardiovascular disease. *Circ Res.* 1998;82:1111-29.
81. Anversa P, Leri A, Beltrami CA, Guerra S, Kajstura J. Myocyte death and growth in the failing heart. *Lab Invest.* 1998;78:767-86.
82. Elsasser A, Schlepper M, Klovekorn WP, Cai WJ, Zimmermann R, Muller KD, Strasser R, Kostin S, Gagel C, Munkel B, Schaper W, Schaper J. Hibernating myocardium: an incomplete adaptation to ischemia. *Circulation.* 1997;96:2920-31.
83. Freude B, Masters TN, Kostin S, Robicsek F, Schaper J. Cardiomyocyte apoptosis in acute and chronic conditions. *Basic Res Cardiol.* 1998;93:85-9.
84. Schaper J, Lorenz-Meyer S, Suzuki K. The role of apoptosis in dilated cardiomyopathy. *Herz.* 1999;24:219-24.
85. Olivetti G, Abbi R, Quaini F, Kajstura J, Cheng W, Nitahara JA, Quaini E, Di Loreto C, Beltrami CA, Krajewski S, Reed JC, Anversa P. Apoptosis in the failing human heart. *N Engl J Med.* 1997;336:1131-41.
86. Pirolo JS, Hutchins GM, Moore GW. Myocyte vacuolization in infarct border zones is reversible. *Am J Pathol.* 1985;121:444-50.
87. Ad N, Snir E, Vidne BA, Golomb E. Potential preoperative markers for the risk of developing atrial fibrillation after cardiac surgery. *Semin Thorac Cardiovasc Surg.* 1999;11:308-13.
88. Wouters L, Liu G-S, Flameng W, Thijssen V, Thoné F, Borgers M. Structural remodelling of atrial myocardium in patients with cardiac valve disease and atrial fibrillation. *Exp Clin Cardiol.* 2001;5:158-163.
89. Thijssen V, Ausma J, Borgers M. Structural remodelling during chronic atrial fibrillation: act of programmed cell survival. *Cardiovasc Res.* 2001;52:14-20.
90. Ausma J, Borgers M, Allessie MA. Structural changes due to atrial fibrillation: resemblance with hibernation and dedifferentiation. In: Santini M, ed. *Progress in Clinical Pacing 2000.* Rome: Tipolithografia Fernando Begliomini; 2000:198-205.
91. Wilkinson JM, Grand RJ. Comparison of amino acid sequence of troponin I from different striated muscles. *Nature.* 1978;271:31-5.
92. Cummins P, Perry SV. Troponin I from human skeletal and cardiac muscles. *Biochem J.* 1978;171:251-9.
93. Sasse S, Brand NJ, Kyriianou P, Dhoot GK, Wade R, Arai M, Periasamy M, Yacoub MH, Barton PJ. Troponin I gene expression during human cardiac development and in end-stage heart failure. *Circ Res.* 1993;72:932-8.

94. Bhavsar PK, Dhoot GK, Cumming DV, Butler-Browne GS, Yacoub MH, Barton PJ. Developmental expression of troponin I isoforms in fetal human heart. *FEBS Lett.* 1991;292:5-8.
95. Hunkeler NM, Kullman J, Murphy AM. Troponin I isoform expression in human heart. *Circ Res.* 1991;69:1409-14.
96. Gorza L, Ausoni S, Merciai N, Hastings KE, Schiaffino S. Regional differences in troponin I isoform switching during rat heart development. *Dev Biol.* 1993;156:253-64.
97. L'Ecuyer TJ, Schulte D, Lin JJ. Thin filament changes during *in vivo* rat heart development. *Pediatr Res.* 1991;30:232-8.
98. Saggin L, Gorza L, Ausoni S, Schiaffino S. Troponin I switching in the developing heart. *J Biol Chem.* 1989;264:16299-302.
99. Sabry MA, Dhoot GK. Identification and pattern of expression of a developmental isoform of troponin I in chicken and rat cardiac muscle. *J Muscle Res Cell Motil.* 1989;10:85-91.
100. Ausoni S, De Nardi C, Moretti P, Gorza L, Schiaffino S. Developmental expression of rat cardiac troponin I mRNA. *Development.* 1991;112:1041-51.
101. Martin AF, Ball K, Gao LZ, Kumar P, Solaro RJ. Identification and functional significance of troponin I isoforms in neonatal rat heart myofibrils. *Circ Res.* 1991;69:1244-52.
102. Reiser PJ, Westfall MV, Schiaffino S, Solaro RJ. Tension production and thin-filament protein isoforms in developing rat myocardium. *Am J Physiol.* 1994;267:H1589-96.
103. Zakhary DR, Moravec CS, Stewart RW, Bond M. Protein kinase A (PKA)-dependent troponin-I phosphorylation and PKA regulatory subunits are decreased in human dilated cardiomyopathy. *Circulation.* 1999;99:505-10.
104. Bodor GS, Oakeley AE, Allen PD, Crimmins DL, Ladenson JH, Anderson PA. Troponin I phosphorylation in the normal and failing adult human heart. *Circulation.* 1997;96:1495-500.
105. McConnell BK, Moravec CS, Bond M. Troponin I phosphorylation and myofilament calcium sensitivity during decompensated cardiac hypertrophy. *Am J Physiol.* 1998;274:H385-96.
106. Luss H, Meissner A, Rolf N, Van Aken H, Boknik P, Kirchhefer U, Knapp J, Laer S, Linck B, Luss I, Muller FU, Neumann J, Schmitz W. Biochemical mechanism(s) of stunning in conscious dogs. *Am J Physiol Heart Circ Physiol.* 2000;279:H176-84.
107. Gao WD, Atar D, Liu Y, Perez NG, Murphy AM, Marban E. Role of troponin I proteolysis in the pathogenesis of stunned myocardium. *Circ Res.* 1997;80:393-9.
108. Van Eyk JE, Powers F, Law W, Larue C, Hodges RS, Solaro RJ. Breakdown and release of myofilament proteins during ischemia and ischemia/reperfusion in rat hearts: identification of degradation products and effects on the pCa-force relation. *Circ Res.* 1998;82:261-71.
109. McDonough JL, Arrell DK, Van Eyk JE. Troponin I degradation and covalent complex formation accompanies myocardial ischemia/reperfusion injury. *Circ Res.* 1999;84:9-20.
110. Kositprapa C, Zhang B, Berger S, Cantly JJ, Lee T. Calpain-mediated proteolytic cleavage of troponin I induced by hypoxia or metabolic inhibition in cultured neonatal cardiomyocytes. *Mol Cell Biochem.* 2000;214:47-55.
111. Feng J, Schaus BJ, Fallavollita JA, Lee TC, Cantly JM, Jr. Preload Induces Troponin I Degradation Independently of Myocardial Ischemia. *Circulation.* 2001;103:2035-2037.
112. Brundel BJM, Ausma J, van Gelder IC, Crijns HJGM, van Gilst WH, Tielemans RG, Van Der Want JJL, Henning RH. Calpain activity is related to ion-channel, structural and electrical remodeling in human paroxysmal and persistent atrial fibrillation. (*Thesis*). 2000.

113. Brundel BJM, Ausma J, van Gelder IC, van der Want JJ, van Gilst WH, Crijns HJGM, Henning RH. Activation of proteolysis by calpains in human paroxysmal and persistent atrial fibrillation. *Cardiovasc Res.* 2002;54:380-9.
114. Tuinenburg AE, Brundel BJ, Van Gelder IC, Henning RH, Van Den Berg MP, Driessen C, Grandjean JG, Van Gilst WH, Crijns HJ. Gene expression of the natriuretic peptide system in atrial tissue of patients with paroxysmal and persistent atrial fibrillation. *J Cardiovasc Electrophysiol.* 1999;10:827-35.
115. Brundel BJ, van Gelder IC, Henning RH, Tuinenburg AE, Deelman LE, Tielemans RG, Grandjean JG, van Gilst WH, Crijns HJ. Gene expression of proteins influencing the calcium homeostasis in patients with persistent and paroxysmal atrial fibrillation. *Cardiovasc Res.* 1999;42:443-54.
116. Gibson UE, Heid CA, Williams PM. A novel method for real time quantitative RT-PCR. *Genome Res.* 1996;6:995-1001.
117. Heid CA, Stevens J, Livak KJ, Williams PM. Real time quantitative PCR. *Genome Res.* 1996;6:986-94.
118. Westfall MV, Albayya FP, Metzger JM. Functional analysis of troponin I regulatory domains in the intact myofilament of adult single cardiac myocytes. *J Biol Chem.* 1999;274:22508-16.
119. McDonough JL, Labugger R, Pickett W, Tse MY, MacKenzie S, Pang SC, Atar D, Ropchan G, Van Eyk JE. Cardiac troponin I is modified in the myocardium of bypass patients. *Circulation.* 2001;103:58-64.
120. Thomas SA, Fallavollita JA, Lee TC, Feng J, Carty JM, Jr. Absence of troponin I degradation or altered sarcoplasmic reticulum uptake protein expression after reversible ischemia in swine. *Circ Res.* 1999;85:446-56.
121. Vitadello M, Ausma J, Borgers M, Gambino A, Casarotto DC, Gorza L. Increased myocardial GRP94 amounts during sustained atrial fibrillation: a protective response? *Circulation.* 2001;103:2201-6.
122. Wattanapermpool J, Guo X, Solaro RJ. The unique amino-terminal peptide of cardiac troponin I regulates myofibrillar activity only when it is phosphorylated. *J Mol Cell Cardiol.* 1995;27:1383-91.
123. Ray KP, England PJ. Phosphorylation of the inhibitory subunit of troponin and its effect on the calcium dependence of cardiac myofibril adenosine triphosphatase. *FEBS Lett.* 1976;70:11-6.
124. Noland TA, Jr., Guo X, Raynor RL, Jideama NM, Averyhart-Fullard V, Solaro RJ, Kuo JF. Cardiac troponin I mutants. Phosphorylation by protein kinases C and A and regulation of  $Ca^{2+}$ -stimulated MgATPase of reconstituted actomyosin S-1. *J Biol Chem.* 1995;270:25445-54.
125. Adamcova M, Pelouch V. Isoforms of troponin in normal and diseased myocardium. *Physiol Res.* 1999;48:235-47.
126. Borgers M, De Nollin S, Thone F, Wouters L, Van Vaeck L, Flameng W. Distribution of calcium in a subset of chronic hibernating myocardium in man. *Histochem J.* 1993;25:312-8.
127. Wijffels MC, Kirchhoff CJ, Dorland R, Allessie MA. Atrial fibrillation begets atrial fibrillation. A study in awake chronically instrumented goats. *Circulation.* 1995;92:1954-68.
128. van der Velden HM, van Kempen MJ, Wijffels MC, van Zijlverden M, Groenewegen WA, Allessie MA, Jongasma HJ. Altered pattern of connexin40 distribution in persistent atrial fibrillation in the goat. *J Cardiovasc Electrophysiol.* 1998;9:596-607.
129. Schotten U, Ausma J, Stellbrink C, Sabatichus I, Vogel M, Frechen D, Schoendube F, Hanrath P, Allessie MA. Cellular Mechanisms of Depressed Atrial Contractility in Patients With Chronic Atrial Fibrillation. *Circulation.* 2001;103:691-698.
130. Ausma J, Coumans WA, Duimel H, Van der Vusse GJ, Allessie MA, Borgers M. Atrial high energy phosphate content and mitochondrial enzyme activity during chronic atrial fibrillation. *Cardiovasc Res.* 2000;47:788-96.

131. Yue L, Melnyk P, Gaspo R, Wang Z, Nattel S. Molecular mechanisms underlying ionic remodeling in a dog model of atrial fibrillation. *Circ Res.* 1999;84:776-84.
132. van der Velden HMW, van der Zee L, Wijffels MC, van Leuven C, Dorland R, Vos MA, Jongsma HJ, Allessie MA. Atrial fibrillation in the goat induces changes in monophasic action potential and mRNA expression of ion channels involved in repolarization. *J Cardiovasc Electrophysiol.* 2000;11:1262-9.
133. Van Gelder IC, Brundel BJ, Henning RH, Tuinenburg AE, Tielemans RG, Deelman L, Grandjean JG, De Kam PJ, Van Gilst WH, Crijns HJ. Alterations in gene expression of proteins involved in the calcium handling in patients with atrial fibrillation. *J Cardiovasc Electrophysiol.* 1999;10:552-60.
134. Lai LP, Su MJ, Lin JL, Lin FY, Tsai CH, Chen YS, Huang SK, Tseng YZ, Lien WP. Down-regulation of L-type calcium channel and sarcoplasmic reticular Ca(2+)-ATPase mRNA in human atrial fibrillation without significant change in the mRNA of ryanodine receptor, calsequestrin and phospholamban: an insight into the mechanism of atrial electrical remodeling. *J Am Coll Cardiol.* 1999;33:1231-7.
135. Brundel BJ, Van Gelder IC, Henning RH, Tielemans RG, Tuinenburg AE, Wietsema M, Grandjean JG, Van Gilst WW, Crijns HJ. Ion Channel Remodeling Is Related to Intraoperative Atrial Effective Refractory Periods in Patients With Paroxysmal and Persistent Atrial Fibrillation. *Circulation.* 2001;103:684-690.
136. Lai LP, Su MJ, Lin JL, Lin FY, Tsai CH, Chen YS, Tseng YZ, Lien WP, Huang SK. Changes in the mRNA levels of delayed rectifier potassium channels in human atrial fibrillation. *Cardiology.* 1999;92:248-55.
137. Brundel BJMM, Van Gelder IC, Henning RH, Tuinenburg AE, Wietsema M, Grandjean JG, Wilde AAM, Van Gilst WH, Crijns HJGM. Alterations in potassium channel gene expression in atria of patients with persistent and paroxysmal atrial fibrillation: differential regulation of protein and mRNA levels for K<sup>+</sup> channels. *J Am Coll Cardiol.* 2001;37:926-932.
138. van der Velden HM, Jongsma HJ. Connexin types and distribution in normal and electrically remodeled atria. In: Santini M, ed. *Progress in Clinical Pacing 2000.* Rome: Tipolitografia Fernando Begliomini; 2000:190-197.
139. van der Velden HM, van Kempen MJ, Groenewegen WA, Jongsma HJ. Comparative analysis of the distribution of the gap junction proteins connexins 40 and 43 in chronic atrial fibrillation (AF) in patients and a goat model. *Circulation.* 1997;96:I-237 (abstract).
140. Kangaratnam P, Severs NJ, Peters NS. The relationship between conduction, activation pattern and quantity of immunoreactive connexin in chronic human atrial fibrillation. *Eur Heart J.* 2000;21:240 (abstract).
141. Dupont E, Ko Y, Rothery S, Coppen SR, Baghai M, Haw M, Severs NJ. The Gap-junctional protein connexin40 is elevated in patients susceptible to postoperative atrial fibrillation. *Circulation.* 2001;103:842-9.
142. van der Velden HM, Ausma J, Rook MB, Hellemons AJ, van Veen TA, Allessie MA, Jongsma HJ. Gap junctional remodeling in relation to stabilization of atrial fibrillation in the goat. *Cardiovasc Res.* 2000;46:476-86.
143. Schotten U, Allessie M. Electrical and contractile remodeling during atrial fibrillation go hand-in-hand. *PACE.* 2001;24:572 (abstract).
144. Yu WC, Lee SH, Tai CT, Tsai CF, Hsieh MH, Chen CC, Ding YA, Chang MS, Chen SA. Reversal of atrial electrical remodeling following cardioversion of long-standing atrial fibrillation in man. *Cardiovasc Res.* 1999;42:470-6.
145. Manios EG, Kanouppakis EM, Chlouverakis GI, Kaleboubas MD, Mavrakis HE, Vardas PE. Changes in atrial electrical properties following cardioversion of chronic atrial fibrillation: relation with recurrence. *Cardiovasc Res.* 2000;47:244-53.

146. Elvan A, Wylie K, Zipes DP. Pacing-induced chronic atrial fibrillation impairs sinus node function in dogs. *Electrophysiological remodeling*. *Circulation*. 1996;94:2953-60.
147. Everett TH, Li H, Mangrum JM, McMurry ID, Mitchell MA, Redick JA, Haines DE. Electrical, morphological, and ultrastructural remodeling and reverse remodeling in a canine model of chronic atrial fibrillation. *Circulation*. 2000;102:1454-60.
148. Allessie MA. Atrial electrophysiologic remodeling: another vicious circle? *J Cardiovasc Electrophysiol*. 1998;9:1378-93.
149. Mou L, Miller H, Li J, Wang E, Chalifour L. Improvements to the differential display method for gene analysis. *Biochem Biophys Res Commun*. 1994;199:564-9.
150. Gros D, Jarry-Guichard T, Ten Velde I, de Maziere A, van Kempen MJ, Davoust J, Briand JP, Moorman AF, Jongsma HJ. Restricted distribution of connexin40, a gap junctional protein, in mammalian heart. *Circ Res*. 1994;74:839-51.
151. Delorme B, Dahl E, Jarry-Guichard T, Marics I, Briand JP, Willecke K, Gros D, Theveniau-Ruissy M. Developmental regulation of connexin 40 gene expression in mouse heart correlates with the differentiation of the conduction system. *Dev Dyn*. 1995;204:358-71.
152. Bauer D, Muller H, Reich J, Riedel H, Ahrenkiel V, Warthoe P, Strauss M. Identification of differentially expressed mRNA species by an improved display technique (DDRT-PCR). *Nucleic Acids Res*. 1993;21:4272-80.
153. Chen X, Overstreet E, Wood SA, Fischer JA. On the conservation of function of the Drosophila fat facets deubiquitinating enzyme and Fam, its mouse homolog. *Dev Genes Evol*. 2000;210:603-10.
154. Paterno GD, Li Y, Luchman HA, Ryan PJ, Gillespie LL. cDNA cloning of a novel, developmentally regulated immediate early gene activated by fibroblast growth factor and encoding a nuclear protein. *J Biol Chem*. 1997;272:25591-5.
155. Radice G, Lee JJ, Costantini F. H beta 58, an insertional mutation affecting early postimplantation development of the mouse embryo. *Development*. 1991;111:801-11.
156. Martin KJ, Pardee AB. Principles of differential display. *Methods Enzymol*. 1999;303:234-58.
157. de Groot IJ, Hardy GP, Sanders E, Los JA, Moorman AF. The conducting tissue in the adult chicken atria. A histological and immunohistochemical analysis. *Anat Embryol*. 1985;172:239-45.
158. Lyons GE, Ontell M, Cox R, Sasoon D, Buckingham M. The expression of myosin genes in developing skeletal muscle in the mouse embryo. *J Cell Biol*. 1990;111:1465-76.
159. Nattel S, Li D, Yue L. Basic mechanisms of atrial fibrillation—very new insights into very old ideas. *Annu Rev Physiol*. 2000;62:51-77.
160. Rastinejad F, Blau HM. Genetic complementation reveals a novel regulatory role for 3' untranslated regions in growth and differentiation. *Cell*. 1993;72:903-17.
161. Ya J, Markman MW, Wagenaar GT, Blommaart PJ, Moorman AF, Lamers WH. Expression of the smooth-muscle proteins alpha-smooth-muscle actin and calponin, and of the intermediate filament protein desmin are parameters of cardiomyocyte maturation in the prenatal rat heart. *Anat Rec*. 1997;249:495-505.
162. Woodcock-Mitchell J, Mitchell JJ, Low RB, Kieny M, Sengel P, Rubbia L, Skalli O, Jackson B, Gabbiani G. Alpha-smooth muscle actin is transiently expressed in embryonic rat cardiac and skeletal muscles. *Differentiation*. 1988;39:161-6.
163. Harder BA, Hefti MA, Eppenberger HM, Schaub MC. Differential protein localization in sarcomeric and nonsarcomeric contractile structures of cultured cardiomyocytes. *J Struct Biol*. 1998;122:162-75.

164. Kurabayashi M, Tsuchimochi H, Komuro I, Takaku F, Yazaki Y. Molecular cloning and characterization of human cardiac alpha- and beta- form myosin heavy chain complementary DNA clones. Regulation of expression during development and pressure overload in human atrium. *J Clin Invest.* 1988;82:524-31.
165. Wessels A. Spatial distribution of "Tissue-specific" antigens in the developing human heart. In: Amsterdam: University of Amsterdam; 1991.
166. Pope B, Hoh JF, Weeds A. The ATPase activities of rat cardiac myosin isoenzymes. *FEBS Lett.* 1980;118:205-8.
167. Miyata S, Minobe W, Bristow MR, Leinwand LA. Myosin heavy chain isoform expression in the failing and nonfailing human heart. *Circ Res.* 2000;86:386-90.
168. Komuro I, Nomoto K, Sugiyama T, Kurabayashi M, Takaku F, Yazaki Y. Isolation and characterization of myosin heavy chain isozymes of the bovine conduction system. *Circ Res.* 1987;61:859-65.
169. Reiser PJ, Portman MA, Ning XH, Schomisch Moravec C. Human cardiac myosin heavy chain isoforms in fetal and failing adult atria and ventricles. *Am J Physiol Heart Circ Physiol.* 2001;280:H1814-20.
170. Holubarsch C, Goulette RP, Litten RZ, Martin BJ, Mulieri LA, Alpert NR. The economy of isometric force development, myosin isoenzyme pattern and myofibrillar ATPase activity in normal and hypothyroid rat myocardium. *Circ Res.* 1985;56:78-86.
171. Masuzaki H, Jingami H, Matsuoka N, Nakagawa O, Ogawa Y, Mizuno M, Yoshimasa Y, Yamamoto T, Nakao K. Regulation of very-low-density lipoprotein receptor in hypertrophic rat heart. *Circ Res.* 1996;78:8-14.
172. Semenza GL, Roth PH, Fang HM, Wang GL. Transcriptional regulation of genes encoding glycolytic enzymes by hypoxia-inducible factor 1. *J Biol Chem.* 1994;269:23757-63.
173. Chen C, Pore N, Behrooz A, Ismail-Beigi F, Maity A. Regulation of glut1 mRNA by hypoxia-inducible factor-1. Interaction between H-ras and hypoxia. *J Biol Chem.* 2001;276:9519-25.
174. Kannel WB, Abbott RD, Savage DD, McNamara PM. Epidemiologic features of chronic atrial fibrillation: the Framingham study. *N Engl J Med.* 1982;306:1018-22.
175. Morillo CA, Klein GJ, Jones DL, Guiraudon CM. Chronic rapid atrial pacing. Structural, functional, and electrophysiological characteristics of a new model of sustained atrial fibrillation. *Circulation.* 1995;91:1588-95.
176. Farih S, Villemaire C, Nattel S. Importance of refractoriness heterogeneity in the enhanced vulnerability to atrial fibrillation induction caused by tachycardia-induced atrial electrical remodeling. *Circulation.* 1998;98:2202-9.
177. Todd D, AP W, Flynn S, Hobbs W, Garratt C. Repetitive one-month periods of atrial electrical remodeling promote stability of atrial fibrillation. *Circulation.* 2000;102:II-154.
178. Sparks PB, Jayaprakash S, Vohra JK, Kalman JM. Electrical remodeling of the atria associated with paroxysmal and chronic atrial flutter. *Circulation.* 2000;102:1807-13.
179. Tielemans RG, Crijns HJ. The 'second factor' of tachycardia-induced atrial remodeling. *Cardiovasc Res.* 2000;46:364-6.
180. Ausma J, Duytschaever M, Wijffels MC, Borgers M, Allessie MA. Loss of efficacy of cardioversion by class Ic drugs after long term atrial fibrillation in the goat. *Eur Heart J.* 2001;21:543.
181. Garratt CJ, Duytschaever M, Killian M, Dorland R, Mast F, Allessie MA. Repetitive electrical remodeling by paroxysms of atrial fibrillation in the goat: no cumulative effect on inducibility or stability of atrial fibrillation. *J Cardiovasc Electrophysiol.* 1999;10:1101-8.

182. Grammer JB, Zeng X, Bosch RF, Kuhlkamp V. Atrial L-type Ca<sup>2+</sup>-channel, beta-adrenoreceptor, and 5-hydroxytryptamine type 4 receptor mRNAs in human atrial fibrillation. *Basic Res Cardiol.* 2001;96:82-90.
183. Grammer JB, Bosch RF, Kuhlkamp V, Seipel L. Molecular remodeling of Kv4.3 potassium channels in human atrial fibrillation. *J Cardiovasc Electrophysiol.* 2000;11:626-33.
184. Elvan A, Huang XD, Pressler ML, Zipes DP. Radiofrequency catheter ablation of the atria eliminates pacing-induced sustained atrial fibrillation and reduces connexin 43 in dogs. *Circulation.* 1997;96:1675-85.
185. Barbez O, Pierre S, Duran MJ, Sennoune S, Levy S, Maixent JM. Specific up-regulation of mitochondrial F0F1-ATPase activity after short episodes of atrial fibrillation in sheep. *J Cardiovasc Electrophysiol.* 2000;11:432-8.
186. Fujii H, Ide M, Yasuda S, Takahashi W, Shohtsu A, Kubo A. Increased FDG uptake in the wall of the right atrium in people who participated in a cancer screening program with whole-body PET. *Ann Nucl Med.* 1999;13:55-9.
187. Warshaw JB, Terry ML. Cellular energy metabolism during fetal development. II. Fatty acid oxidation by the developing heart. *J Cell Biol.* 1970;44:354-60.
188. Warshaw JB. Cellular energy metabolism during fetal development. 3. Deficient acetyl-CoA synthetase, acetylcarnitine transferase and oxidation of acetate in the fetal bovine heart. *Biochim Biophys Acta.* 1970;223:409-15.
189. Warshaw JB. Cellular energy metabolism during fetal development. IV. Fatty acid activation, acyl transfer and fatty acid oxidation during development of the chick and rat. *Dev Biol.* 1972;28:537-44.
190. Warshaw JB, Kimura RE. Cellular energy metabolism during fetal development. V. Fatty acid synthesis by the developing heart. *Dev Biol.* 1973;33:224-8.
191. Kimura RE, Warshaw JB. Metabolic adaptations of the fetus and newborn. *J Pediatr Gastroenterol Nutr.* 1983;2:S12-5.
192. Webb JC, Patel DD, Jones MD, Knight BL, Soutar AK. Characterization and tissue-specific expression of the human 'very low density lipoprotein (VLDL) receptor' mRNA. *Hum Mol Genet.* 1994;3:531-7.
193. Oka K, Ishimura-Oka K, Chu MJ, Sullivan M, Krushkal J, Li WH, Chan L. Mouse very-low-density-lipoprotein receptor (VLDLR) cDNA cloning, tissue-specific expression and evolutionary relationship with the low-density-lipoprotein receptor. *Eur J Biochem.* 1994;224:975-82.
194. Kwok S, Singh-Bist A, Natu V, Kraemer FB. Dietary regulation of the very low density lipoprotein receptor in mouse heart and fat. *Horm Metab Res.* 1997;29:524-9.
195. Wang GL, Jiang BH, Rue EA, Semenza GL. Hypoxia-inducible factor 1 is a basic-helix-loop-helix-PAS heterodimer regulated by cellular O<sub>2</sub> tension. *PNAS.* 1995;92:5510-4.
196. Aasum E, Lathrop DA, Henden T, Sundset R, Larsen TS. The role of glycolysis in myocardial calcium control. *J Mol Cell Cardiol.* 1998;30:1703-12.
197. Clapham DE. Calcium signaling. *Cell.* 1995;80:259-68.
198. Daoud EG, Knight BP, Weiss R, Bahu M, Paladino W, Goyal R, Man KC, Strickberger SA, Morady F. Effect of verapamil and procainamide on atrial fibrillation-induced electrical remodeling in humans. *Circulation.* 1997;96:1542-50.
199. Zarse M, Stellbrink C, Athanatou E, Robert J, Schotten U, Hanrath P. Verapamil prevents stretch-induced shortening of atrial effective refractory period in Langendorff-perfused rabbit heart. *J Cardiovasc Electrophysiol.* 2001;12:85-92.
200. Lee SH, Yu WC, Cheng JJ, Hung CR, Ding YA, Chang MS, Chen SA. Effect of verapamil on long-term tachycardia-induced atrial electrical remodeling. *Circulation.* 2000;101:200-6.

# | *Stellingen* |

behorende bij het proefschrift

## Structural remodelling during atrial fibrillation

Victor L.J.L. Thijssen  
Maastricht, november 2002

- 1 | Cellular degeneration and apoptosis are not the end-stage of ongoing dedifferentiation, but result from other underlying factors (This thesis).
- 2 | Rather than a sign of cardiomyocyte dedifferentiation, the changes in TnI isoform expression appear to be a response to a decreased calcium sensitivity of the myofibrils. (This thesis)
- 3 | The transient increase in the expression of HIF1 $\alpha$  indicates that a certain amount of ischemic stress during the onset of AF cannot be ruled out. (This thesis)
- 4 | The observation that many of the structural changes occur during different cardiac diseases suggests an uniform primary response mechanism of cardiomyocytes in jeopardy (This thesis)
- 5 | Gezien de fluctuaties op de huizenmarkt lijkt het verstandiger de hypotheek te vervangen door de hypertheek.
- 6 | Het is niet te verwachten dat met de aankoop van de Joint strike fighter het gedoogbeleid met betrekking tot de softdrugs zal veranderen
- 7 | Voor veel AF patienten lijkt te gelden: oud van geest maar jong van hart.
- 8 | Nog even en op de markt is ook de Euro een Daalder waard.
- 9 | Het feit dat uit Engels onderzoek blijkt dat in de Nederlandse competitie het scoringspercentage van strafschoppen erg hoog is geeft aan dat ofwel de Nederlandse keepers nog slechter zijn dat de nemers van de strafschoppen ofwel dat de strafschoppen voornamelijk genomen worden door buitenlandse spelers.
- 10 | Het gebruik van micro-arrays heeft binnen de wetenschap geleid tot een verschuiving van het Rationalisme naar het Expressionisme.